SISSA - SCUOLA
INTERNAZIONALE
SUPERIORE
STUDI AVANZATI
TRIESTE
Strada Costiera 11

ISAS - INTERNATIONAL SCHOOL FOR ADVANCED STUDIES

T E S I

DIPLOMA DI PERFEZIONAMENTO

"MAGISTER PHILOSOPHIAE"

THE 1982-84 ECLIPSE OF THE PECULIAR BINARY STAR "EPSILON AURIGAE"

CANDIDATO:

dott. S. Ferluga

RELATORE:

Prof.ssa M. Hack

Anno Accademico 1982/1983

TRIESTE

THE 1982-84 ECLIPSE OF THE PECULIAR BINARY STAR "EPSILON AURIGAE"

by

STENO FERLUGA

Supervisor

MARGHERITA HACK

A thesis
submitted in conformity with
the requirements for the degree of
Magister Philosophiae

International School for Advanced Studies
Sector of Astrophysics
Trieste - 1982-83

C O N T E N T S

F O R E W O R D

"This star in one of the most interesting objects known to astronomers". So was defined Epsilon Aurigae, by Otto Struve and C.T.Elvey in 1930, in their basic paper first providing reliable orbital elements for this peculiar binary system. After half a century, many other more interesting objects have been discovered in Astronomy, but still the problem of ε Aur has not yet been definitely solved. The case of ε Aur may be interesting also if viewed in a hystorical perspective, since it can provide a good example of a restricted astrophysical problem, where one can realize how the advancement of knowledge takes place, by means of interaction between theory and observation.

The present work is a study, based on the author's observations, of the current 1982-84 eclipse of ε Aur.

Part 1) is a general review of the actual state of knowledge about ε Aur, providing the frame in which the new data, given in part 2 and concerning the eclipse, are to be interpreted. Particular relevance is given here (Chap.II) to a discussion of previous observations , so that, with the contribution of the writer's new ones, an

updated observational picture should be realized. This is going to be the basis, together with still to be collected end-eclipse data, of a future theoretical research, for working out a possibly conclusive model.

Part 2) presents original results; the foundamental ones (Chap.III) are now in press for "Astronomy and Astrophysics", some other (Chap.IV) were partly anticipated in a communication on the "International Bulletin of Variable Stars", while the last ones (Chap.V) are still unpublished. Finally the "Note", added at the end of Chap.III, is the argument of a "contributed paper" at the forthcoming 7th Regional Meeting of IAU in Florence.

Appendixes A), B), C) contain respectively: A) the plots of UV low-resolution spectra which were analyzed; B) a high-resolution atlas of UV lines, detected as peculiar in eclipse; C) a preliminary determination of the variable UV excess, still in progress.

PART 1

R E V I E W

Chapter I

HISTORICAL INTRODUCTION

A general overview of the matter is given in this Chapter. Arguments regarding physical interpretation, and more recent observations, will be further developed in Chapter II and in the following Part 2 which is entirely devoted to new observations.

I.1) The Discovery

Although Epsilon Aurigae is a star easily visible even to the naked eye (its usual apparent magnitude is 3.0), its pecularities have passed unnoticed to scientific research for long. As regards the spectral type and the luminosity class, ε Aur can be classified as a normal bright supergiant (class Ia), of intermediate spectral type (F Ø or F 2).

The story of its discovery as a variable star dates back to 1821, in Germany, when pastor J.H.Fritsch, an ama-

teur astronomer, realized that star Epsilon in the Auriga had diminished its brightness (Fritsch, 1924). The phenomenon of 1821 was actually the first eclipse of ε Aur to be observed, but the fact was not understood, and did not arouse any particular interest. No one suspected, in particular, that it could be an eclipsing binary.

The next eclipse occurred in 1848; the German astronomer Argelander, and others, observed it. At that time, in order to estimate the apparent brightness of the stars, the only methods, which were available, were those based on the sensibility of human eye. It had been Argelander himself who established the most famous of these methods, still bearing his name. Notwithstanding his perspicacity, as an observer of variable stars, Argelander did not notice anything strange in ε Aur, and he did not even understand that the loss of brightness was due to an eclipse. So, when the phenomenon was over, the star was completely forgotten by the scientific community, and the following eclipse even passed unnoticed.

The interest aroused only when the eclipse of 1902 occured. One year later, the German astronomer H.Ludendorff published the results of his discovery, indicating that ε Aur was an eclipsing binary, and with his fundamental work (Ludendorff, 1903) he gave way to the study of ε Aur. Later on, using spectroscopic measurements of radial velocities, he confirmed that the motion of the primary component (that is the visible star), rotating around an ideal barycentre, revealed the existence of a second body orbiting around it, which should be responsi-

ble for the observed eclipses. Therefore, ε Aur had to be a single-spectrum binary system, in which the secondary component was not directly observable, and appeared only when it eclipsed the primary.

Ludendorff, starting from all the visual observations which were then available, derived the first determination of the orbital elements, and of the period, which at that time was the longest known: 27.1 years. Moreover he noticed that during the whole eclipse, which lasted nearly two years, the brightness of the star was nearly constant, and was reduced by 0.8 magnitude. If normally interpreted, this flat minimum in the light curve (fig.I.1) should mean that the primary component was totally eclipsed, by a larger secondary. In this case, the light visible during the minimum phase, corresponding to a fourth magnitude star, should come out precisely from the secondary component. But, then, it seemed strange that such a bright star wasn't recognizable in any way, outside the eclipse, by means of spectroscopic observation.

Another, much more sophisticated interpretation, was the one supposing that the eclipse was only pseudo-total, in the following sense: the light, observed during the minimum phase, was still that of the primary, beeing eclipsed by an obscure body. In this case, in order to explain the flat minimum, it would have been necessary to use particular hypotheses about the geometry of the system, and the nature of the secondary obscure component. Anyway, a complex picture of this type finally prevailed and was accepted: in fact the more superficial idea, that

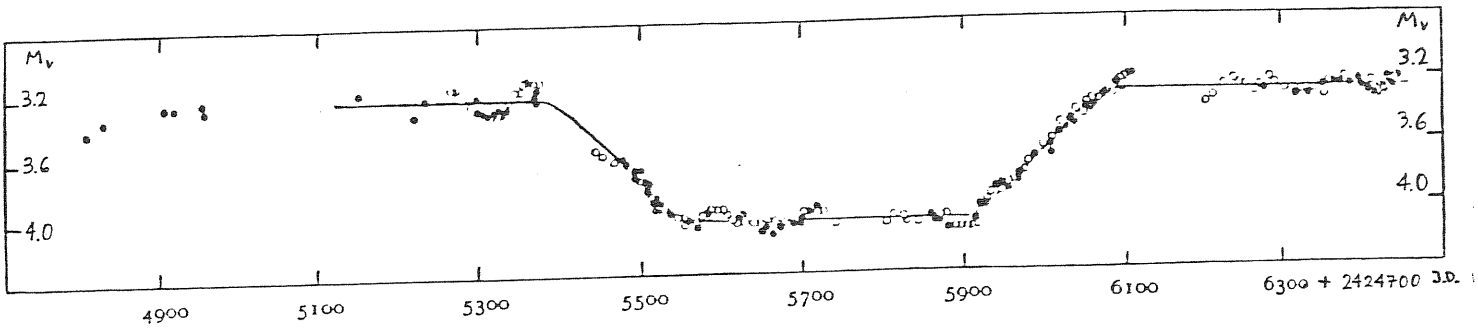

Fig. I.1) The light-curve of ε Aur. The graph shows the apparent visual magnitude M_V, versus time, during the eclipse of 1929. The various phases of the event are well visible; note the characteristic flat minimum, corresponding to the total eclipse, which lasts about 1 year.

both components were ordinary stars, was destined to meet ever increasing difficulties. Such a simple assumption, for instance, implied that the primary's eclipse was to be followed by the secondary's one. Ludendorff predicted that the secondary eclipse was to occur about 18 years after the principal eclipse; but the event, surprisingly, didn't occur.

The mystery got deeper, as soon as ε Aur became the object of more accurate observations, especially thank to new spectroscopic techniques, which were then introduced into astronomical reasearch. The eclipse of 1929, which lasting two years had began in 1928 and was over in 1930, was studied by Huffer (1932) and others: he obtained data from 98 nights' watching. He realized that during the total eclipse, but also outside the eclipse itself, the brightness was only approximately constant, due to slight aperiodical fluctuations of about 0.2 magnitude. Such nearly semiregular variability could be easily intrinsic in the primary component, considering the type of the star; in fact, the supergiants are subject to this sort of phenomena, but anyway the general picture of the variability of the system became more complicated.

Furthermore, Otto Struve and C.T. Elvey (1930) had compared more than 250 spectra of Epsilon Aurigae, collected during the eclipse of 1929. They noticed that the spectral absorption lines, normally symmetric, had instead strange asymmetric profiles during the partial phases of the eclipse. In the total phase, though, the lines were once again symmetric, and deeper. This fact could

find an explanation in the Doppler effect, relative to the rotational velocities of the two components, partially superimposed. But there were also, unexpectedly, some lines not participating in the phenomenon, which remained unchanged during the whole eclipse.

The most important problem, however, derived from the fact that the observations showed a "grey eclipse", that is, the depth of eclipse resulted independent from wavelength. Practically, during the total phase, the colour and the type of the spectrum remained unchanged, as if the eclipsing body was an opaque veil, instead of a star. In fact, if it was a star, it should have been identical to the eclipsed one, since the spectrum remained the same. Such hypothesis (primary and secondary supposed to be equal) didn't hold, since it was contradicted by observations: not only the secondary eclipse should have been visible, as foreseen by Ludendorff and never observed, but also the spectrum of the secondary outside eclipse should have been clearly visible, while it had never been observed.

Large incongruities became then evident, as soon as the researchers tried to obtain mathematically, from the observable data (by methods normally used for binary systems), the relationship between the radii of the two hypothetical components. The minimum of brightness, corresponding to the total eclipse, was too deep for so long a period. Finally the two stars, making up the ε Aur system, must really have been enormous. To the primary component, being an early F supergiant, a mass equal to

nearly 15 solar masses, and a radius of about 50 solar radii, could be reasonably assigned. From the parameters of the orbit, it resulted for the hypothetical secondary, a mass of 10 to 20 solar masses, and dimensions which could be of hundreds of solar radii. How was it possible that such a gigantic body could remain invisible?

Something very strange should therefore be hidden inside the system of ε Aur; perhaps the secondary component, that is the eclipsing body, could be a unique type of a star, or the first one of a still unknown kind. From the time of these puzzling discoveries in the 1930's, to this day, remarkable theoretical efforts have been made, in order to give an interpretation to the observed phenomena. For the present, there is no definite model, and this is to say, actually, that the real nature of this binary system remains still unknown.

I.2) The debate about Models

a) The first astronomer, who tried to give a hypothesis about the nature of the mysterious body which at intervals of 27 years eclipsed the visible component of ε Aur, was Ludendorff himself, in 1924. He suggested that the eclipsing body could be a swarm of meteorites (Ludendorff, 1924), but after he gave up developing further this idea, perhaps because he was not very sure of it. But today, after 60

years of researches, we can realize that probably Ludendorff was much nearer to the truth, than he himself and his contemporaries could imagine.

b) In 1937 Kuiper, Struve and Strömgren produced the first real model of Epsilon Aurigae (Kuiper et.al, 1937). They imagined that a huge fading "infrared super-star", of low temperature and density, existed. Such body, called "I Star", should rotate round the visible component of Epsilon Aurigae, and be much larger (2 800 solar radii). Passing in front of the visible companion, this body should completely eclipse the visible star, but still should let its light partly filter; in fact, the layers of I Star were supposed to be semi-opaque. Even if this model became soon popular, it showed some weak points, from the very beginning. For instance, during the eclipse, the thicker internal zones of I Star should have partly absorbed the light of the primary, and some characteristic spectral lines would have appeared; but these lines (or molecular bands) have never been observed. Furthermore, owing to the temperature that the "I Star" was supposed to have (little above 1,000°K), this huge body should have produced an intense infra-red emission. This radiation, in spite of repeated researches with more and more sensitive instruments, has never been revealed.

The 1956 eclipse (started in 1955 and finished in 1957), which at last was observed with modern methods, was supposed to give finally the answer to these problems. A large

campaign of spectrographic and photometric observations was organized, in order to obtain a good "covering" of the phenomenon. The large amount of collected data helped to make up in detail the observational picture of ε Aur; even if the new data didn't add much to the matter already known (on the contrary they gave rise to new problems), they were to supply the foundations for a new generation of improved models. A wide scientific discussion was to develop about a set of competing models, all of which could apparently explain the observations, but each one beeing based on a different picture of ε Aur (Fig. I.2).

c) In the meanwhile, Otto Struve had revised in 1955 the first model, drastically reducing the dimensions of cumber some "I Star", and embedding it in a very large system of gas clouds (Struve, 1956); these clouds were supposed to move, in a complicated shape of an "eight", wrapping up also the visible star. In spite of these argumentations, it remained the fact, already discovered by Kraft one year before (Kraft, 1954), that the gas could hardly be opaque

Fig. I.2) (see following page)-Proposed Models for ε Aur

a) Ludendorff, 1924
b) Kuiper, Struve and Strömgren, 1937
c) Struve, 1955
d) Hack, 1961
e) Huang, 1965
f) Kopal, 1971
g) Handbury and Williams, 1976
h) Plavec, 1981
i) Cameron, 1971
j) Wilson, 1971

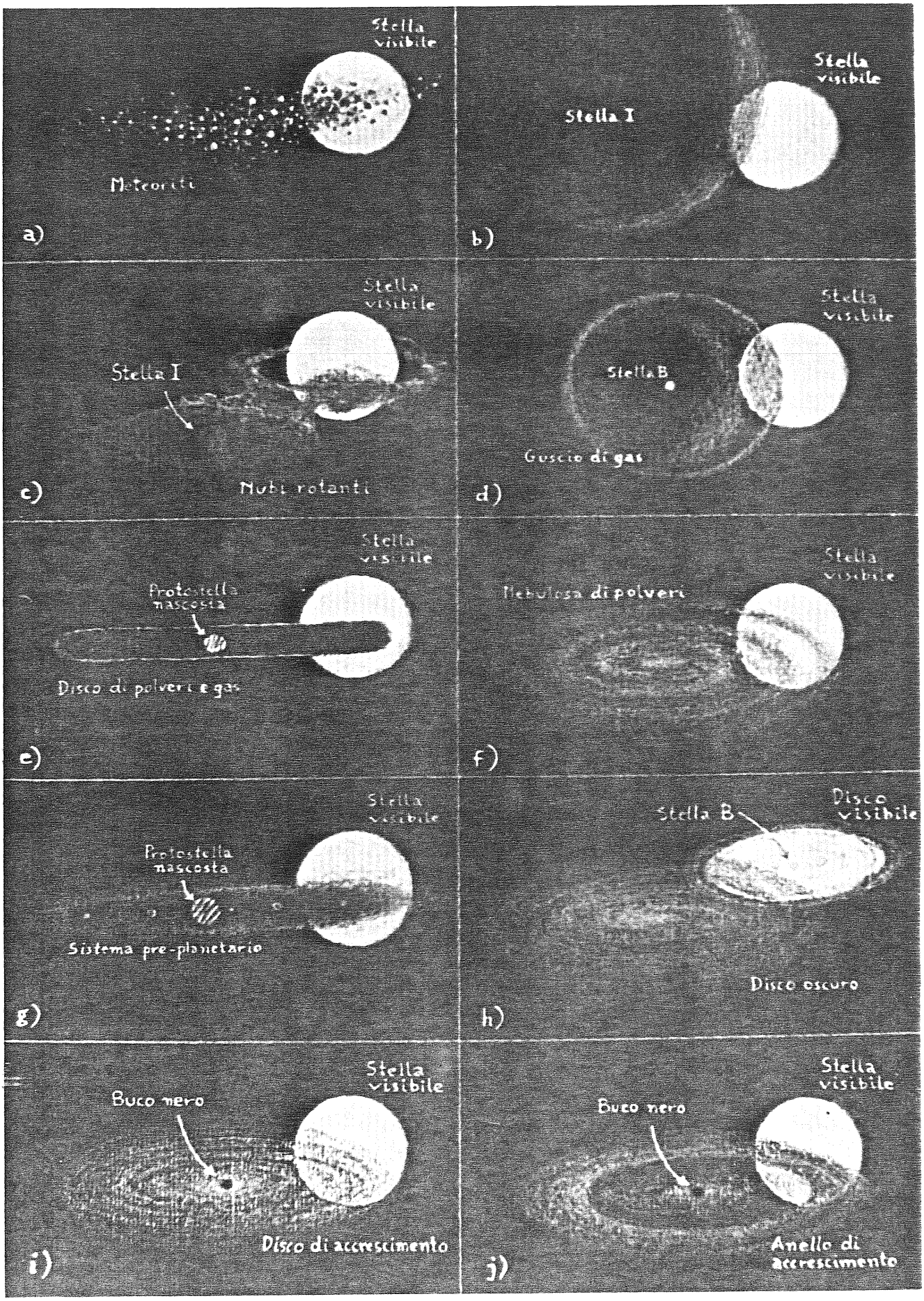
Stella visibile
Meteoriti
a)
Stella visibile
Stella I
b)
Stella visibile
Stella I
Nubi rotanti
c)
Stella visibile
Stella B
Guscio di gas
d)
Stella visibile
Protostella nascosta
Disco di polveri e gas
e)
Stella visibile
Nebulosa di polveri
f)
Stella visibile
Protostella nascosta
Sistema pre-planetario
g)
Stella B
Disco visibile
Disco oscuro
h)
Stella visibile
Buco nero
Disco di accrescimento
i)
Stella visibile
Buco nero
Anello di accrescimento
j)

enough, as to produce the observed eclipse.

d) Margherita Hack, after analysing (Hack, 1959) a sample of spectra, obtained during the 1955-57 eclipse, proposed in 1961 a completely new model (Hack, 1961). She suggested that the object, orbiting around the bright visible star, could be a hot dwarf presumably of type B (too weak, compared with the primary, to be observable), surrounded by a semi-transparent gas shell. This secondary component, with its gaseous envelope, eclipsed periodically its bright companion star, which remained anyway observable in transparence. Such a picture, in which the gaseous shell could maybe have an elliptic, discoidal or ring-like shape, reproduced naturally the characteristics of the observed eclipse. Moreover, it was very reasonable that a B star could possess a gaseous envelope, as this fact had already been observed in other cases. Also the semi-transparence of the gas found a convincing physical motivation, since the ultra-violet radiations emitted by the B Star were enough energetic to ionise the gas in the shell; as a consequence, the shell should become semi-opaque and grey, due to electron scattering (a mechanism that Struve had already suggested, although he didn't find the source which could ionise the gas. (Fig. I.3)

e) Su-Shu Huang suggested in 1965 another possible configuration of the system of Epsilon Aurigae, which could explain many of the pecularities observed, and had the merit of remarkable conceptual simplicity (Huang, 1965).

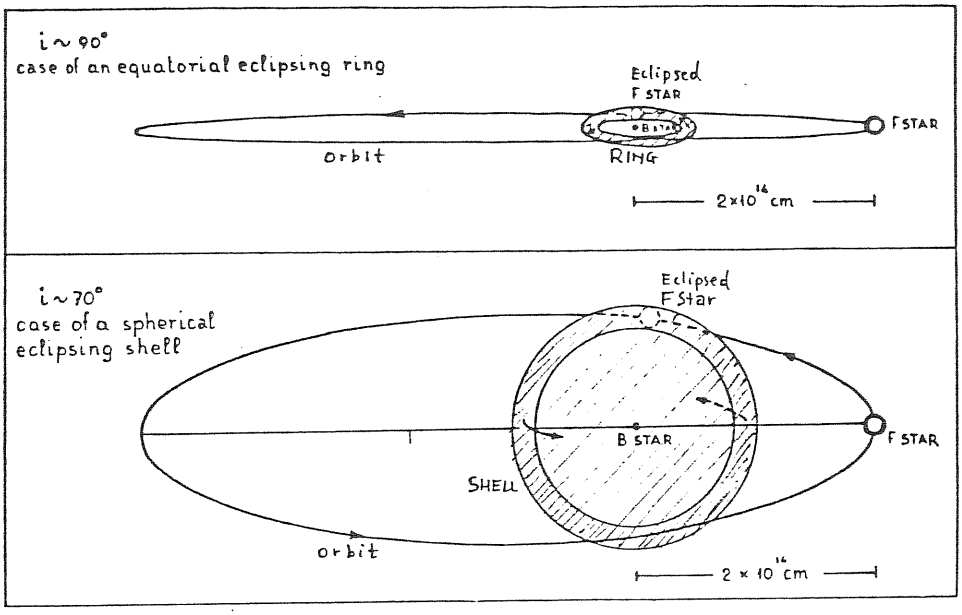

Fig I.3) – Geometry of Hack's model. The shell, or ring, is supposed to be semitransparent. (Hack, 1961).

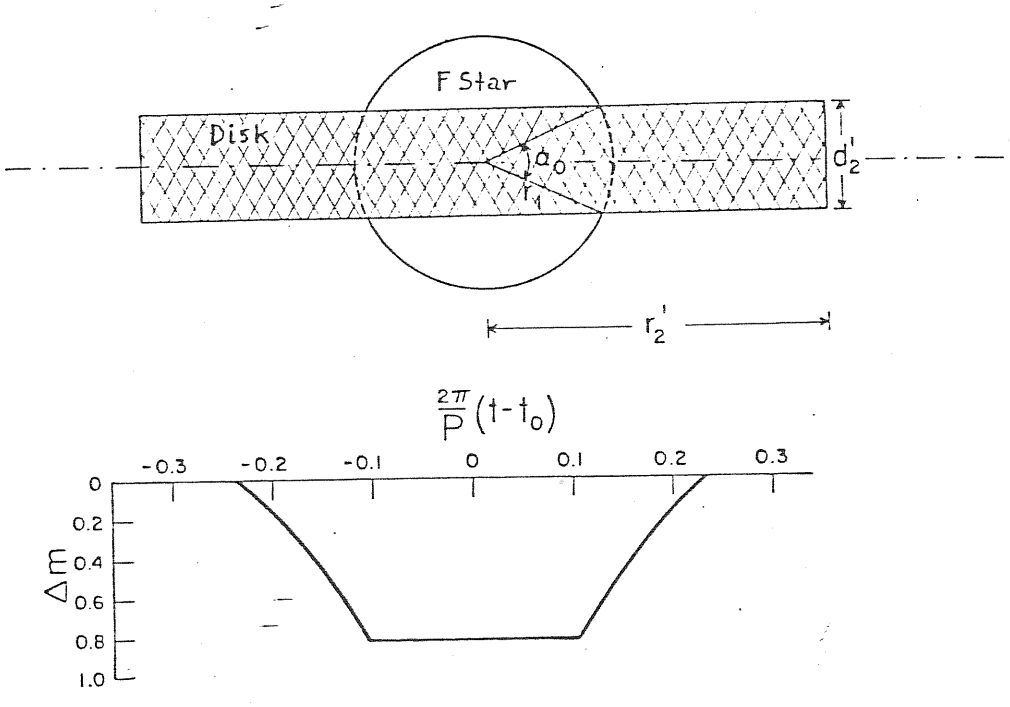

Fig I.4) – A schematic diagram of Huang's model for ε Aurigae, and its resulting light-curve during eclipse. It is assumed that we observe this system edge-on. Consequently, the rotating gaseous disk around the secondary component will appear to be a dark rectangle which obscures the primary component (Huang, 1965).

He imagined that, round the visible star, there was rotating a secondary companion embedded in a discoid nebula, supposed to be seen in section due to prospectic effect. This nebula, which Huang compared to the one originating the solar system, should anyway have resulted completely opaque, just owing to the fact that it appeared in section, that is in the direction of its maximum thickness. In this way, the problem of the invisibility of the secondary component was solved, since it could be well hidden in the center of the opaque disk. Then the eclipse must have occurred when, in front the visible star, the nebular disk had passed; such a disk, seen in section, must have appeared like a dark band, on the body of the primary star. During the transit, the light arriving on the Earth would then diminish by a constant factor, while the colour and the spectral characteristics should obviously remain unchanged. By this means, both the "flatness" and "greyness" of the eclipse were explained. Huang contested the electron scattering as a cause for the opacity of the disk, saying that it should have been accompanied by other effects, which had not been observed (such as light polarization). In turn, he proposed that the material which caused the nebula to be opaque consisted of dust particles, formed out of nebular gas itself. He went as far as to state that the nebula could contain also bigger conglomerates, solid bodies, or even bodies with planetary sizes. (Fig.I.4)

f) Zdenek Kopal, who already since the 1950's had maintained that the object causing the eclipse in the ε Aur system

was a dust cloud, presented in 1971 his improved model (Kopal, 1971). As to the geometry of the eclipse, Kopal's idea followed partially Hack's model: the eclipsing body was identified with a large nebular discoid, homogeneous and semi-transparent, seen obliquely. This nebula, when passing before the primary visible star, would cover it by putting itself in between like a veil (uniform and colourless), and would produce an eclipse like the observed one (flat and grey). The physical nature of the nebula, which was supposed to be formed by coarse circumstellar dust, and maybe by larger solid fragments, was more like the one imagined by Huang (or even by Ludendorff, half a century before). In particular Kopal was convinced that the nebular object was a real pre-planetary system, similar to the nebula which gave origin to the solar system; moreover he thought that the object was only in the very first stages of evolution, so that in the center of the nebula the star formation process was just to begin. Hence, according to Kopal, in the ϵ Aur system the secondary component didn't exist as a star yet, and simply this fact should have been the reason for the unobservability of the secondary.

g) Handbury and Williams tackled the problem in 1976, presenting a model which was somewhat more sophisticated than the previous ones (Handbury and Williams, 1976). Improving the idea that the eclipsing body was a nebular disk seen in section, they stated that it should appear like an opaque band, but semi-transparent at the edges, being presumably more rarefied in its outer parts. Without putting

special constraints on its composition, they suggested it might be a mixture of gas and dust. Then, from the presence of this nebular material, one could infer that the ε Aur system was of very recent formation. Therefore, the two researchers believed that the visible primary supergiant was in its first stages of evolution (pre-main sequence phases), instead of being in the final stages, like the ordinary supergiants are (and like it was thought in the other models). As to the eclipsing disk, also Handbury and Williams thought it was a pre-planetary nebula, in the middle of which a protostar should be hidden, ready to make itself visible as soon as it would become a real star. The two authors suggested we should expect this occurring, so that their model would be confirmed; it's a pity we'll need waiting perhaps some ten thousands years!

h) Mirek Plavec produced in 1981 an idea which, in time order, seems to be the latest about Epsilon Aurigae: two pseudostellar discoids seen obliquely, revolving the one around the other (Plavec, 1982). He presumed that the visible star, instead of being an ordinary supergiant, was actually a hot rotating disk which only simulated a stellar behaviour, and contained in its centre a B-type dwarf. Around this whole, a large ellipsoidal grey body, more or less flat should rotate, and be responsible for the eclipse (vaguely like Struve's "I Star"). This strange model overturned the classical image of the ε Aur system, by identifying the disk and the B Star with the primary component, and not with the secondary one. But, along with the inte-

rest of originality, Plavec's model had also the little attracting characteristic, of explaining the observed phenomena in the most complicated way. This does not mean, anyway, that such a model should be discarded "a priori".

i) A black hole? During the 1970's, it seemed that the solution for the ε Aur problem, a system containing a dark object of about ten solar masses, had been found at last: it could be a black hole of ten solar masses, not-luminous by definition, orbiting around the visible star. It was Cameron the first, who threw out the idea, that the secondary component of Epsilon Aurigae was a collapsed star at the stage of a black hole (Cameron, 1971). He also added that the eclipse of the visible companion-star should be produced by a disk of solid particles revolving around the black hole itself.

j) Almost at the same time Wilson improved the model, proposing that around the black hole an opaque ring of dust was rotating (Wilson, 1971). He supposed that this ring had in the middle a semi-transparent opening (similar in some way to Saturn's rings), in order to reproduce theoretically at best the characteristics of the observed eclipse. But the enthusiasm for this "exotic" idea of the black hole in ε Aur went out rapidly when, going on with the studies concerning black holes, it was understood that around these objects very violent phenomena must occur, while in ε Aur they were absolutely not observed. For instance the matter in the surroundings of the black

hole, one moment before being sucked-in, must disintegrate into powerful X-ray and Gamma-ray explosions. Instead Epsilon Aurigae, as far as we know, has never emitted either X-rays or Gamma-rays (as on the contrary other objects do, such as Cygnus X-1, which is now indicated as a probable black hole candidate).

As to the origin of the eclipsing body, the most acceptable hypothesis remains the one by Paczynski (1975), who suggested a mass loss from the outer atmosphere of the visible component, being this a normal phenomenon for supergiant stars. Instead of dispersing into space, in the case of ε Aur system this material should have fallen on the companion, simply because of a normal mass-transfer effect. A discoidal nebula should then have formed, hiding in its interior the secondary component, and producing the eclipse of the visible star. Hence, for Paczynski, the nebula was not a pre-stellar body but, on the contrary, it was an object produced by an advanced evolution of the system.

I.3) Recent Observations

After the eclipse in 1956, ε Aur became the object of more and more sophisticated telescopic observations, in order to test the various models. In the meanwhile spectroscopic studies (Morris, 1962), and astrometric measurements of great precision (van de Kamp, 1978a) had permitted to determine the orbit and the other parameters of the system

in a better way. The following indicative values have been reported by van de Kamp, in a review article (1978b). Distance from the Earth: 1,900 light-years. Separation between the components: 3.93×10^9 km. Mass of the primary: 15,5 solar masses. Mass of the dark companion: 13,7 solar masses.

Decisive information about the nature of ε Aur were to be collected, however, by observations taken outside the traditional domain of visible light, particularly studying the infrared and ultraviolet. The results of infrared observations by Low and Mitchell (1965) and later by Woolf (1973), not showing any remarkable infrared excess, ruled out finally the existence of the "I Star" proposed by Struve. On the other hand Hack and Selvelli (1979) evidenced, by means of observations made by the satellite I.U.E., an excess of brightness in the ultraviolet: this was the sign of the presence of a hot star, which confirmed the model proposed by Hack herself 18 years before (Hack, 1961). As to the nature of the eclipsing body, anyway, it remained still to decide upon its real structural parameters (dimensions, shape, and composition), and about its physical characteristics (temperature, density, and processes involved). Above all there was to clarify the position of this object, with respect to stellar evolution.

The 1982-1984 eclipse, which is on now, is beeing studied in order to get a definite solution for these questions. A world-wide campaign of observations is coordinated by means of the bulletin "ε Aur Newsletters", in order to inform the researchers - possibly in real time -

about the going on of the eclipse; also the author of this work is partecipating, in collaboration with Hack. Recently, studying ε Aur in the ultraviolet by satellite I.U.E., a surprising variability in the far ultraviolet has been revealed outside the eclipse, as well as during the total phase (Ferluga and Hack, 1983). It can be thus deduced that the eclipsing body displays an unexpected activity, which could be explained with the presence of the B Star, already hypothized by Hack (1961).

As to the rest, it seems that in general the present eclipse of ε Aur, observed with modern technologies, is going on since now almost like the preceding ones. It will took anyway several months, to carry out data processing, and before the results will be published. Finally, in 1985 a special conference is expected to take place in USA, in order to draw the conclusions of the whole research campaign.

Chapter II

THE OBSERVATIONAL PICTURE

Since the writer's new results are presented in Part 2, we shall review in this chapter only the observations performed by other researches before the present eclipse, considering in particular the best stated results. In more detail, will be described those observations which are related with the author's ones, because of convergence in methodology or in finalities.

II.1) The Parameters of the System

Although, as it will be seen, sometimes one can find some disagreement between different authors' results, most of the foundamental parameters of the system are well known. Since particular determinations, or controversial ones, will be discussed case by case in the following sections, here we shall list at the beginning the basic data concerning ε Aur, which are reported in the catalogues (Batten et.al., 1978; Hoffleit, 1982).

Tab. II.1	ε Aur = HD 31964	
Coordinates (1900):	$\alpha = 04^h54^m.8$ $(+7^m.2)$, $\delta = +43°40'$ $(+9')$	[*]
Apparent magnitude (out of eclipse):	$V = 2.99$, $B-V = +0.54$, $U-B = +0.33$	
Spectral type:	FØ I ap (+B?)	
Rotational velocity (km/sec):	$V_r \text{sen} i_r = 29$	[**]
Orbital period (days):	$P = 9890$	
Eccentricity of the orbit:	$\varepsilon = 0.20$	
Radial velocity of baricenter (km/sec):	$V_o = -1.4$	
Semi-amplitude of radial velocity curve (km/sec):	$K_1 = 15.0$, $(K_2 = 17.0$?)	[o]
Major semi-axis of the orbit (km):	$a_1 \text{sen} i = 2.00 \times 10^9$, $a_2 \text{sen} i = 2.27 \times 10^9$	[oo]
Masses of the components (solar masses):	$m_1 \text{sen}^3 i = 16.8$, $(m_2 \text{sen}^3 i = 14.8$?)	

---

[*] The value in parentheses is the variation in 100 years.

[**] Here, i_r is the inclination of the rotation axis, with respect to the line of sight.

[o] Indexes (1) and (2) stay respectively for the primary and secondary component.

[oo] As usual, i is the inclination of the orbital plane, with respect to the "plane of the sky".

As concerns the quality of these determinations, the orbit is anyway classified "d" by Batten et al.(1978), that is "poorly determined"; this is, obviously, because of the well known peculiarities of the system (Chap. I).

Besides that, there is also a remarkable disagreement between the surprisingly large value of the parallax reported in the catalogue by Hoffleit (1982), that is $\pi = 0.''007$, and the one given by van de Kamp, who finds $\pi = 0.''0017$. This last result, which appears to be very precise, is to be discussed in the following section.

II.2) Astrometry

Using the diameter of earth's orbit around the sun as a baseline, one can determine annual parallaxes of stars, taking photographs with long-focus telescopes, and using precision plate-measuring machines. By this means, employing a large number of plates, stellar parallaxes have been determined directly, with an accuracy of about .005", or little better. In the case of ϵ Aur a comparison between the observed apparent magnitude, and the expected absolute luminosity for an FØ I a star, leads us to predict a distance corresponding to a parallax, which should be about of the same order than the above accuracy. It is then evident that, for ϵ Aur, the direct method for measuring parallax is unadequated.

For ε Aur (as for some other spectrophotometric binaries), this difficulty may be overcome, by measuring the parallax in an indirect way, as follows. From spectroscopic and photometric observations, one can get the linear dimension of the binary's orbit; for instance Wright (1970) gives a value of 13.2 a.u., for the visible component of ε Aur. However, the orbital motion of this star has also to be seen, by a terrestrial observer, as an angular motion over the celestial sphere. This motion can be measured astrometrically, following the apparent orbit of the star on the plain of the sky. Since the orbit of our star is about ten times larger than the earth's orbit, it means that such a measure has to be about ten times easier than a measure of the annual parallax (which is nothing but a measure of earth's orbit, placed at the distance of the star). Then, dividing angular dimensions of star's orbit, by corresponding assumed linear dimensions in a.u., one finally gets by definition the value of the parallax.

This indirect method has been followed by van de Kamp (1978 a), who measured the apparent motion of ε Aur, during the years 1939-1977. The solution derived for the astrometric orbit, assumed to be circular, gives geometric orientational elements for the orbital plane:

(II.1) $$i = 89° \pm 3° \quad , \quad \Omega = 92° \pm 3°,$$

where (as usual) i is the inclination of the orbital plain with respect to the "plain of the sky", and Ω is the position-angle of the line of nodes (intersection between the two plains); the results obtained by van de Kamp are

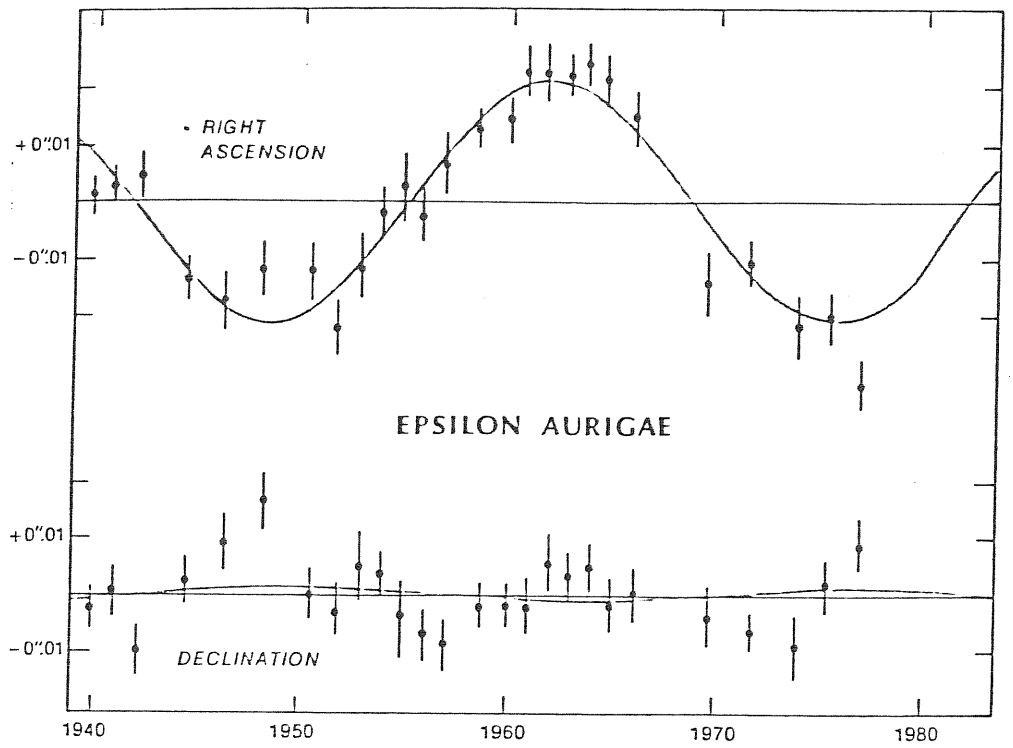

Fig II.1) The orbital motion of Epsilon Aurigae is displayed separately in right ascension and declination. Each point is the seasonal mean of measures on many Sproul Observatory plates, and the length of each vertical bar is twice the probable error. The extreme refinement of the observations is indicated by the vertical scale, in hundredths of a second of arc. (van de Kamp, 1978 a).

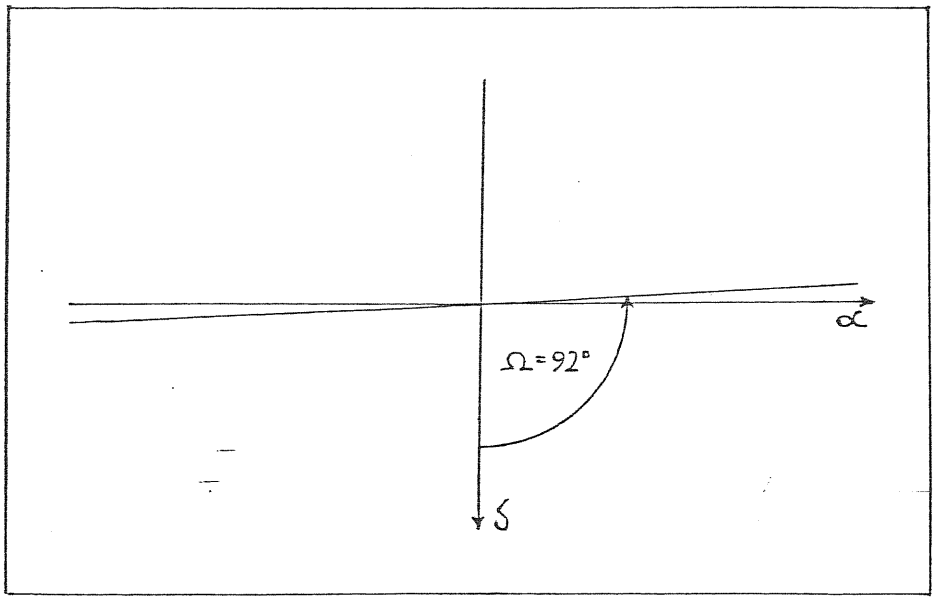

Fig II.2) The apparent orbit, considered by van de Kamp (1978 a), for ε Aur.

shown in figs. II.1) and II.2). Moreover, his solution gives a value of 0".0227 (±.0010) for the apparent radius, which combined with the value of 13.2 a.u. for the corresponding linear dimensions (Wright, 1970), provides the following result for the parallax of ε Aur:

(II.2) $$\pi = 0".00172\ (\pm.00008),$$

where the error shown is only the astrometric one. Anyway, also if one has to remember that this result is based on some assumptions, regarding the linear dimensions and the circularity of the orbit, a final determination for the parallax of the order of 1.7 milli-arcsec appears to be reliable.

The value II.2), which has been found for the parallax, corresponds to the distance

(II.3) $$\Delta = 580 \text{ pc} .$$

This leads to an absolute visual magnitude of -5.9 (±.1), affected by interstellar extinction. Adopting a visual interstellar correction of 0.8 mag., (Morris, 1963), one then may obtain for ε Aur the absolute visual magnitude

(II.4) $$M_V = -6.7 \pm .1 ,$$

where error shown is only the astrometric one, not including a larger uncertainity due to the interstellar correction factor. Anyway, the astrometric result (II.4) can be usefully compared with other, more indirect, determinations of the absolute magnitude and related parameters, as radii and equivalent temperatures.

Such an emphasis has been given to astrometric investi

gations, since they can provide results, that cannot absolutely be obtained in any other way. Besides obviously parallax π, also the value of Ω given in (II.1) couldn't be found elseway, but astrometrically. Values of π and Ω become of foundamental importance, in case of ground-based interferometrical observations. Such observations, if performed in phase of totality, should be able to discriminate experimentally between alternative models; the writer is now preparing these observations, with the Michelson infrared interferometer of CERGA Observatory, in France.

II.3) Photometry

The most complete investigation of the light curve of ε Aur may be considered the one of the 1955-57 eclipse, presented by Gyldenkerne (1970). These observations cover the various phases of the eclipse almost continously, except two restricted gaps during totality and in the post-eclipse phase, due to the difficulty of observing this star in summer (when it undergoes lower culmination at night). Gyldenkerne's light-curve for the visual magnitude V is shown as a solid line in fig. II.3), superimposed to the dotted light-curve of the preceding 1928-30 eclipse (Güssow, 1936); as one can see, second-order fluctuations appear to be superimposed over the primary light curve.

This second-order variability has been analysed in de-

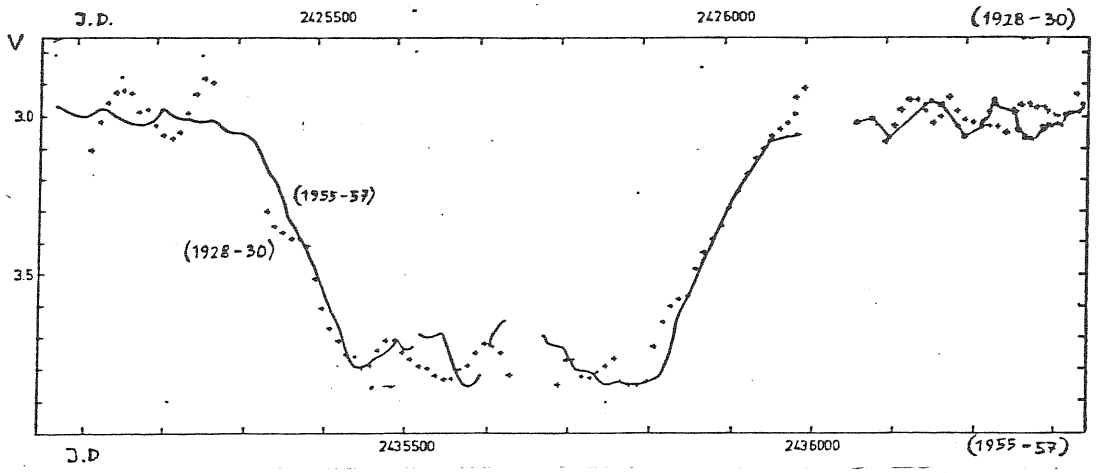

Fig. II.3) The 1955-57 light curve (solid line, lower abscissa), together with the 1928-30 light-curve (dots, upper abscissa), from Gyldenkerne (1970). Second-order variability appears to be superimposed upon the primary minimum.

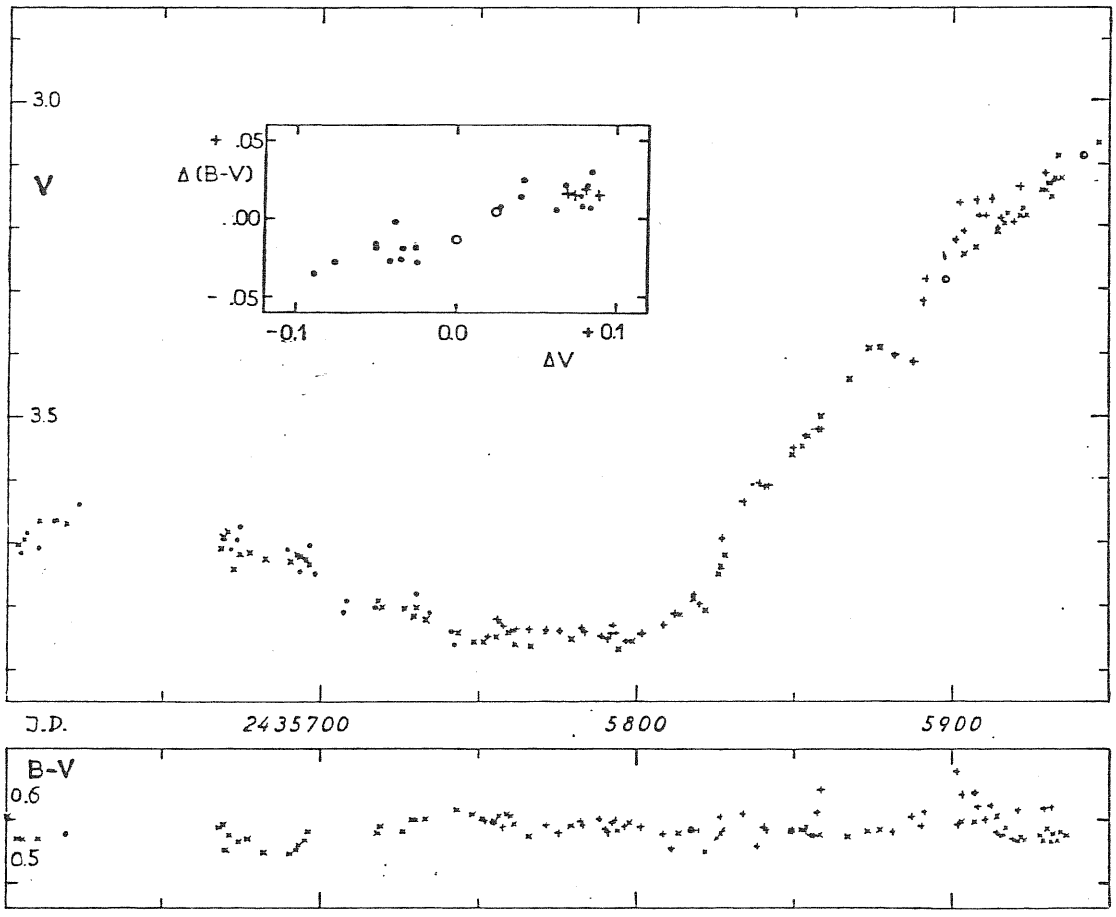

Fig. II.4) The V and B-V light-curves, for the 1955-57 eclipse, during the last part of totality and the egress phase. B-V is almost constant, indicating that the eclipse remains grey at all phases. Detailed analysis shows that small deviations $\Delta(B-V)$ from the mean $\overline{B-V}$, are related with second order variability ΔV from the mean valve $\overline{V}$ of totality (see Inset).

Inset: The deviations $\Delta(B-V)$ from the mean colour index plotted against the deviations ΔV from the mean magnitude for totality. The open circles correspond to the phases at the second contact, the plus-signs to the phases at the third contact (Gyldenkerne, 1970)

tail; fig. II.4) shows an enlarged portion of the 1955-57 light-curve for the V, together with the corresponding (B-V) values. Notwithstanding (B-V) is approximately constant, since greyness of the eclipse is preserved over the phase, small fluctuations are present; these can be related with the second-order variability of V, as shown in the inset of fig. 4). By a linear regression, Gyldenkerne finds for second-order fluctuations

(II.5) $$\Delta(B-V) = 0.320\,\Delta V - 0.005.$$

The physical interpretation of this variability is still not clear. Since there is a similarity, between this $\Delta V/\Delta(B-V)$ ratio, and a corresponding one found for Cepheids (Larsson-Leander, 1958), it has been suggested that second-order variability in ε Aur may be due to intrinsic cepheid-like pulsations of the primary component. On the other hand it seems, also from data of 1928-30 eclipse, that the amplitude of fluctuations is larger during totality, than out of eclipse; this should mean that second-order fluctuations are not intrinsic, but somehow coupled with the primary variation. In this case, an explanation could be found, for instance, on the basis of a hypotetical ring-like structure of the eclipsing body (Wilson, 1971).

An important contribution to the solution of the problem should come by comparing the second-order photometric variability, with high-dispersion spectroscopic measurements of radial velocities; in case of cepheid-like nature of the pulsations, a characteristic correlation should come out. Since data from past eclipses are not enough significant,

Tab. II.2) The 1955–57 Eclipse
(Gyldenkerne, 1970)

1. Contact	J.D.	2,435,295	=	1955 July 6
2. Contact		2,435,430	=	1955 November 18
3. Contact		2,435,824	=	1956 December 16
4. Contact		2,435,965	=	1957 May 6
Mid-eclipse (symmetrical minimum)		2,435,624	=	1956 May 30

Duration of phases	1955–57 eclipse	Mean of previous eclipses
Duration of eclipse	670 days	714 days
Duration of totality	394 days	330 days
Duration of first partial phase	135 days	182 days
Duration of second partial phase	141 days	203 days
Period	9885 days	9888 days
Amplitude	$0^m.75$	$0^m.80$

Interval in Julian date	Average magnitude V	
Pre-eclipse 2,434,760–2,435,250	$2^m.998$	50
Post-eclipse 2,436,050–2,436,488	3 .006	31
Totality 2,435,436–2,435,800	3 .767	117

Tab. II.3) Predictions for the 1982–84 Eclipse, by Gyldenkerne (1970).

1. Contact	1982 July 29
2. Contact	1982 December 11
3. Contact	1984 January 9
4. Contact	1984 May 29

Note to tab II.3). Predictions for the ingress phase have been confermed by actual observations. (ε Aur. Newsletters, n° 8).

the collection of high-dispersion spectrograms, contemporary with UBV photometric observations, is part of the observational program of spectrophotometry, for the current eclipse, in which the author is involved.

II.4) Spectroscopy

Most of the investigations concerning ε Aur have been made in this field, on both sides of observation and interpretation. Since the amount of published material in considerable, a detailed review of single researches would bring us too far. Moreover, a complete spectroscopical reanalysis of the ε Aur system is in preparation in Trieste, with the author's collaboration, on the basis of a new large set of high-dispersion spectra. Plates were obtained in the period preceding and during the actual eclipse, and now are in the stage of digitization and processing by computer; so this will be the subject of a future work. In this section, we shall then limit ourselves to summarize the most important spectroscopical results in the visible, concerning the orbit and the masses (a), the F component (b), the eclipse (c), and the H_α line (d). The behaviour in the IR and UV, will be treated in the next section II.5).

a) The orbit and the masses. After the first determination

Table II.4) - Spectroscopic Elements of ε Aur

Orbital Elements		ε Aurigae
Period, P	days	9890
Eccentricity, e	—	0.200 ± 0.034
Longitude of periastron, ω^0	—	346.4 ±11.0
Periastron passage, T J.D. 2,430,000+	days	3346 ±278
Mid eclipse predicted	"	5543
J.D. 2,430,000+ observed	"	5638
Systemic velocity km/sec	$V_{0,1}$	−1.37 ± 0.39
Semi-amplitude, km/sec	K_1	15.00 ± 0.58
	K_2	(17.0: ?)
Semi-major axis, km	$a_1 \sin i$	20.0 × 10^6
	$a_2 \sin i$	22.6 × 10^6

Absolute Elements	ε Aurigae	
	Primary	Secondary
Spectrum	F0 Iap	B:
Luminosity, M_v		
Spectroscopic	−8.7	−3:
Eclipse data	−8.6	
Temperature T_{eff}, °K	7800	30,000
Bolometric correction	0.11	−3:
Diameter, R/R⊙		
Spectroscopic	277	5
Eclipse data	295	(1000)
Mass, $\mathcal{M} \sin i$ ($\mathcal{M} = M/M\odot$)	15·5	13·7

Source : Wright (1970), Castelli (1978).

of the orbital elements by Ludendorff (1924), Kuiper Struve and Stromgren (1937) calculated a new orbit, which changed slightly the period but leaved almost unchanged the other elements. Morris (1963) then combined these data with more recent ones, deriving the radial velocity curve shown in fig. II.5). As one can see, there remains a considerable scatter of the experimental points about the mean curve; it seems probable that the scatter is real, resulting from random motions in the atmosphere of the F star(*). Wright (1970) revised Morris' solution, by means of an iterative computer programme; the final orbital parameters, together with the derived absolute elements of the system, are given in tab. II.4). Spectroscopic luminosities and diameters of the F star, reported in the table for comparison with the eclipse data, are the updated ones by Castelli (1978), for which a very good agreement is achieved.

Problems arose , as soon as one considers the masses of the two components, which can be inferred from the observed spectroscopic orbit of the primary. Since we know that the secondary spectrum is not observable out of eclipse, only the primary mass function is available

$$f(m) \equiv \frac{(m_2 \sin i)^3}{(m_1+m_2)^2} = 3.34\ m_\odot \ , \qquad \text{(II.6)}$$

where the experimental value 3.34 was derived by Kuiper et al. (1937). Such a high value of the mass function leads, as it is well known, to a puzzling high value for the mass of the non-luminous secondary; this happens, since the primary is supposed to be a normal F supergiant, having there

---

(*) Such motions are normal in supergiants.

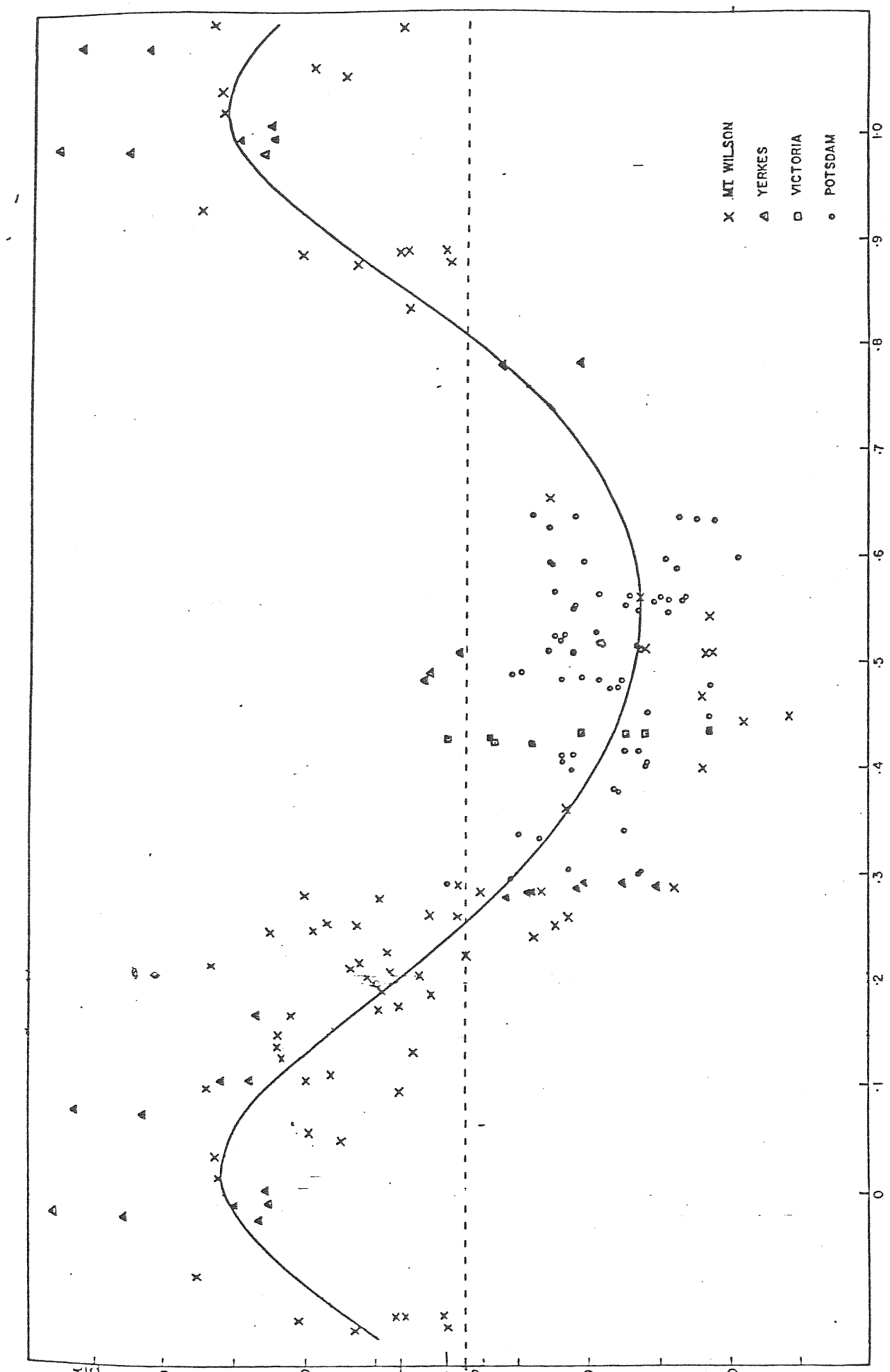

RADIAL VELOCITIES OF EPSILON AURIGAE (Morris, 1963)
Fig. II.5)

fore not less than 10 solar masses.

Let us here examine closer the problem. In the following tab. II.5), different values of the mass ratio (m_1/m_2) have been assumed, and the corresponding possible masses m_1 and m_2 of the components are listed, together with their separation a; the observed value (II.6) of the mass function was used in the computation, assuming two possible values of the inclination angle i=90° and i=70°.

Tab. II.5) Possible values of masses

assumed m_1/m_2	for i=90° m_1	m_2	for i=70° m_1	m_2	for i=90° a	for i=70° a (in A.U.)
2	30	15	36	18	40	42.5
1	13.4	13.4	16	16	26.5	28
1/2	3.8	7.5	4.5	9	20	21
1/4	1.3	5.2	1.6	6.3	16.5	17.5
1/10	0.4	4.0	0.49	4.9	14.5	15.5

The separation a comes from the relation $a=a_1(m_1+m_2)/m_2$, where the primary's orbit semiaxis a_1 is known spectroscopically, $a_1 \sin i = 13.3$ A.U.

The classical solution that has been usually adopted for ε Aur (tab. II.4) considers m_1/m_2 of the order of unity, implying (tab. II.5) a normally massive primary, and a high mass for the non-luminous companion, difficult to be explained. But let us now hypotize a strongly undermassive primary (for its luminosity), because of mass loss in the post-main-sequence evolution; let for instance the primary have a mass

between 1 and 5 solar masses, which corresponds (tab. II.5) to a ratio m_1/m_2 of about 1/4 or 1/2. In this case, one finds that the mass of the secondary component lies between 5 and 9 solar masses, and such values could be consistent with the presence of a late B dwarf, suggested by the UV observations (Hack and Selvelli, 1978) described in the next section II.5).

Supposing the primary had an initial mass (on the m.s.) of about $10 \div 15$ solar masses, the required final stage of less than 5 solar masses could have been reached, after a post-main-sequence evolution during 10^6 years, with a mass loss of about 10^{-5} solar masses/year; these values are high, but still possible. In this case, the origin of the extended eclipsing body, embedding the secondary, comes straightforward from the primary's mass loss. In fact the mass of the eclipsing object, estimated on the basis of its dimensions and of its electron density (deduced from opacity), appears to be not greater than 10^{-5} solar masses. Then, it is enough that only a very small part (10^{-6}) of the mass lost by the primary, could have been captured by the companion, in order to provide the eclipsing body to be formed.

b) The spectrum of the F component. It has been studied extensively first by Hack (1959), who provided identifications and equivalent widths. She also evidenced spectroscopic intrinsic variability, as an effect of variable turbulence: slight variations in profiles and equivalent widths of the lines are found out of eclipse, and some times certain close pairs of lines (such as the Fe I lines

at λ 4250) are blended, while at other times they are resolved.

Later, the out-of-eclipse spectrum of ε Aur has been revisited by Castelli (1977), who measured radial velocities for all ions in different spectra. Analyzing intrinsic out-of-eclipse variability, she drived the following conclusions: (i) a fast variation of the equivalent widths and profiles, with time intervals even of 15^m, while there is no corresponding variation of radial velocity; it seemes this can be due to macroturbulence; (ii) a different behaviour of the radial velocity of the Balmer lines, with a time interval of two months, which indicates a variation in the characteristics of the external layers of the atmosphere. Moreover, she evidenced an asymmetry in almost all the strongest line profiles, with a red sharp edge and a violet wing.

Spectral analysis, of F component's atmosphere, was finally improved by Castelli herself (1978). A radiative-equilibrium, plane-parallel, LTE model atmosphere was computed, and fitted with observational data. By this procedure abundances were derived, which resulted not significantly different from solar ones. Asymmetry of line profiles out of eclipse was interpreted as due to negative acceleration in the outer atmospheric layers. The final parameters, got by Castelli for the F star, are the following.

Table II.6) - Castelli's atmospheric model

Effective temperature	$T_e \simeq 7800$ °K
Gravitational acceleration	$\log g = 1$
Bolometric correction	B.C. = 0.11
Electron pressure at optical depth $\bar{\tau} = 1$	$\log P_e = 0.79$
Gas pressure at optical depth $\bar{\tau} = 1$	$\log P_g = 1.21$
Microturbulence	from 2 to 20 km s^{-1}, increasing with optical depth
Luminosity	$L/L_\odot = 256000$
Radius	$R/R_\odot = 277$
Mass	$M/M_\odot = 28$

The value of Radius is in very good agreement with the one derived from the orbit (tab. II.4), but the value for $M = 28\ M_\odot$ leads again (tab. II.5) to a conseguent high mass for the obscure secondary. Figure II.6) shows how a comparison, between observed and computed spectrum, puts in evidence significant peculiarities.

In particular, the H_α line of hydrogen (fig. II.6a) exhibits an interesting structure. A central core with a total half-width of the order of one Ångström is flanked on each side by an emission feature extending from two to three Ångströms from the line centre. Beyond the emission there extends a shallow absorption wing, to at least eight Ångströms on either side of the line centre. Such extended wings are a normal feature of the hydrogen lines. The cen-

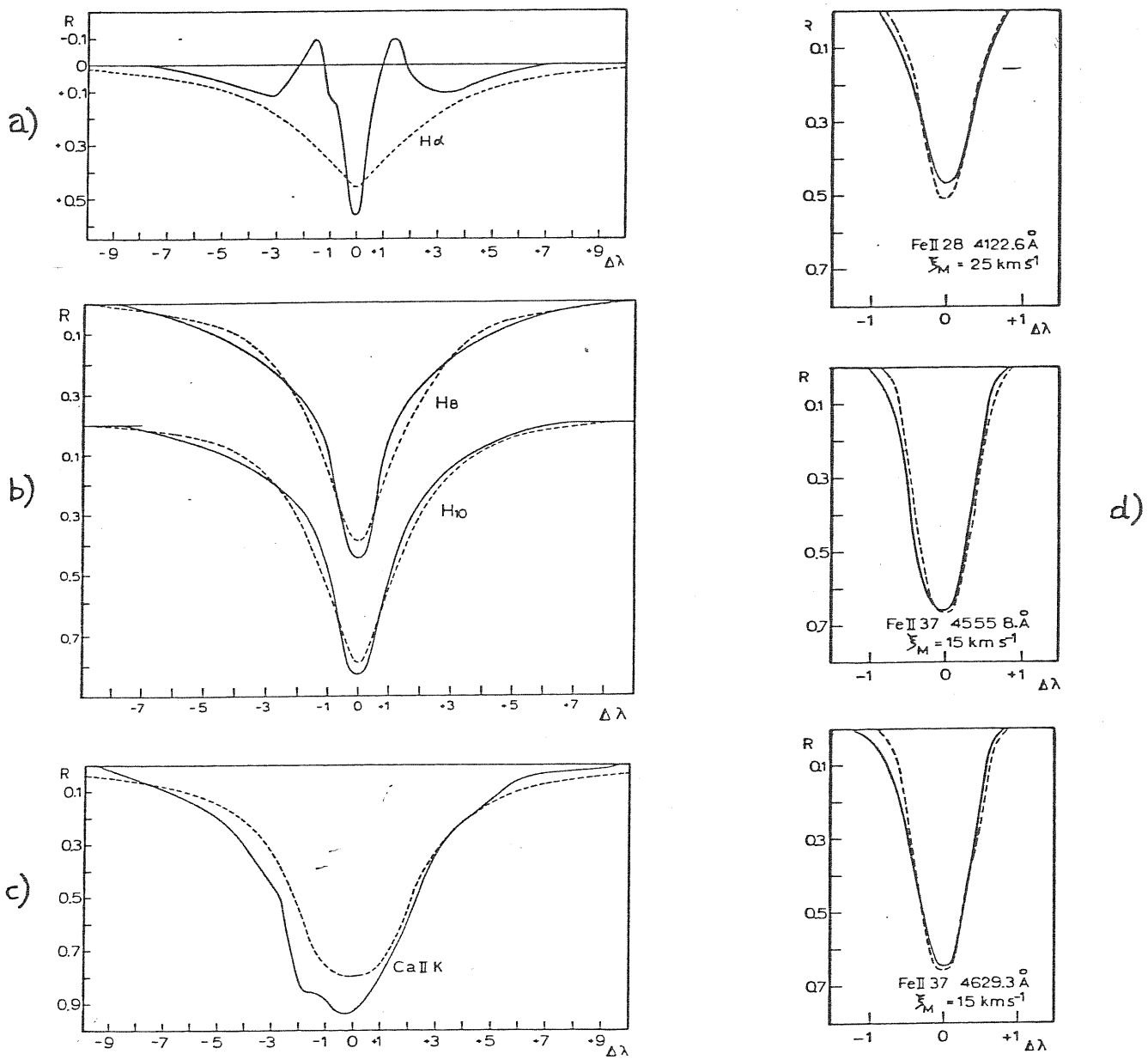

Fig. II.6) Out-of-eclipse line profiles: a comparison between observed (——) and computed (- - - -) profiles is shown (Castelli, 1978). L.T.E. standard model was used. The following features can be recognized.

a) Additional emission component in H_α is evident. Emission peaks are displaced by −72.4 km/sec to the violet, and by 61.4 km/sec to the red.

b) Good fitting is obtained for high Balmer members.

c) Additional, violet-displaced, absorption component is present in CaII K line. This absorption seems also to be variable.

a) Asymmetry in metallic lines (sharp red edge + violet wing), which is interpreted as a sign of deceleration in outer layers.

tral absorption feature has a fairly high central intensity, around 40 ÷ 50%, and the emission features rise to around 20 ÷ 30% above the continuum. The broad absorption wings have a depth of about 10% below the continuum, and are clearly seen only on tracings. The whole H_α structure as seen outside of eclipse is roughly symmetrical, but changes do occur, most noticeably in the emission features, which exhibit marked variations in total and relative strengths (Castelli, 1977). During the eclipse, the H_α feature displays a complex behaviour, which is described at point d).

c) The eclipse. The outstanding feature of the eclipsed spectrum is a doubling of most of the lines in the spectrum, first observed by Adams and Sanford (1930). Shortly before first contact, a new set of lines, generally referred to as "shell lines", appears in the spectrum, shifted to the red of the corresponding stellar lines. These lines, at first sharp and weak, strengthen through first contact and into the first partial phase; as second contact is approached most shell lines become broader and weaker, and cease to be visible shortly after second contact. About two months before third contact the same lines become visible again; at this time they are to the violet of the stellar lines, and broad again, having roughly the same width as the stellar lines. The lines become sharper and stronger during the second partial phase, then weaker again as fourth contact is approached. After fourth contact, the lines continue to weaken, but remain visible for at least four months after

fourth contact.

The foregoing description applies specially to the shell lines of neutral and ionized atoms, while the shell lines of hydrogen persist throughout the eclipse, and are fairly broad most of the time. In particular, they appear to increase in strength until mid-eclipse, and to decrease after. Anyway, also for metallic shell-lines, it is difficult to state unequivocally whether actually disappear near mid-totality, since a weak shell line usually manifests it self as an asymmetry of the corresponding stellar line and, unless the asymmetry is pronounced, it is indistinguishable from a normal variation of the stellar line profile, such as those seen out of eclipse. Certainly, however, the metallic shell lines become too weak to be measured during the total phase except at the beginning and the end.

The profiles of metallic and hydrogen lines during the eclipse are shown in fig. II.7), as they were first illustrated by Struve and Elvey (1930), and by Hack (1959). As often happens, in fig. II.7) metallic shell lines cannot be individually distincted from the corresponding broader atmospheric components, but they appear as asymmetrical, red-shifted or violet-shifted cores.

The observed behaviour of the shell spectrum has been interpreted by Struve et al. (1937), assuming that shell lines are formed in the outer layers of the eclipsing body; the absorption spectrum of these regions has to reproduce the spectrum of the primary, since these layers are supposed to be excited by the primary's radiation. The shift toward the red before totality, and toward the violet

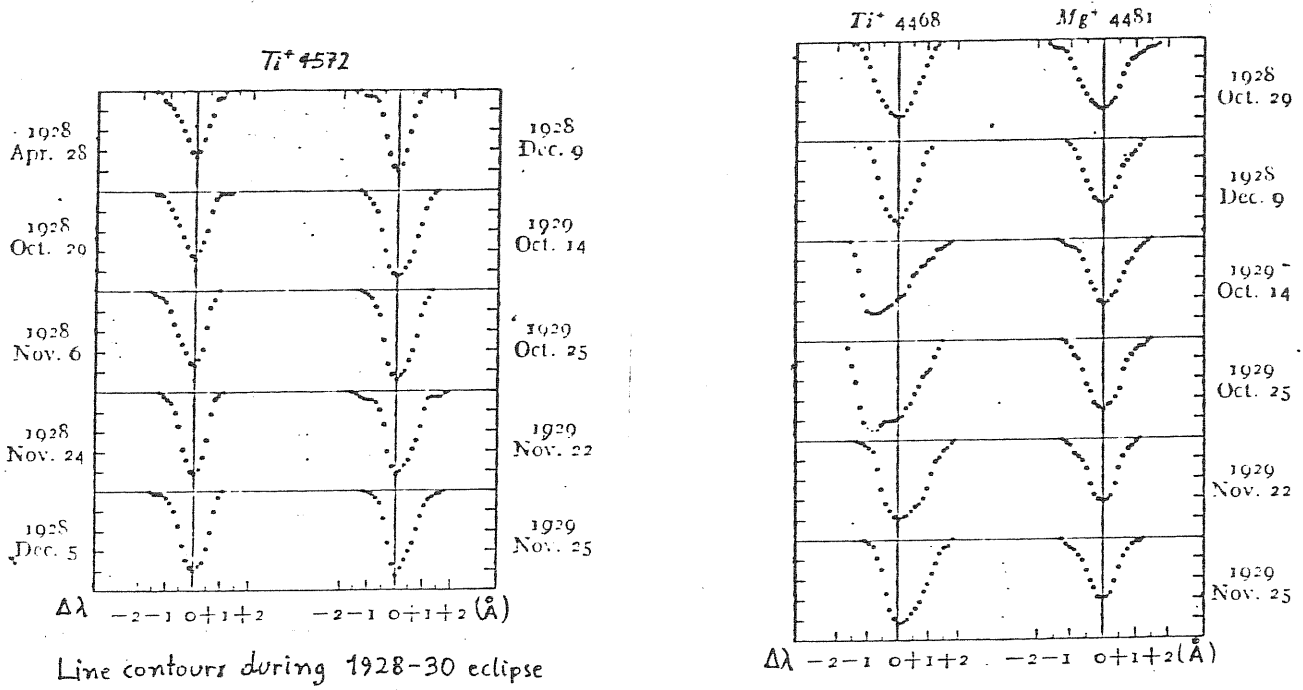

Line contours during 1928-30 eclipse
(Struve and Elvey, 1930)

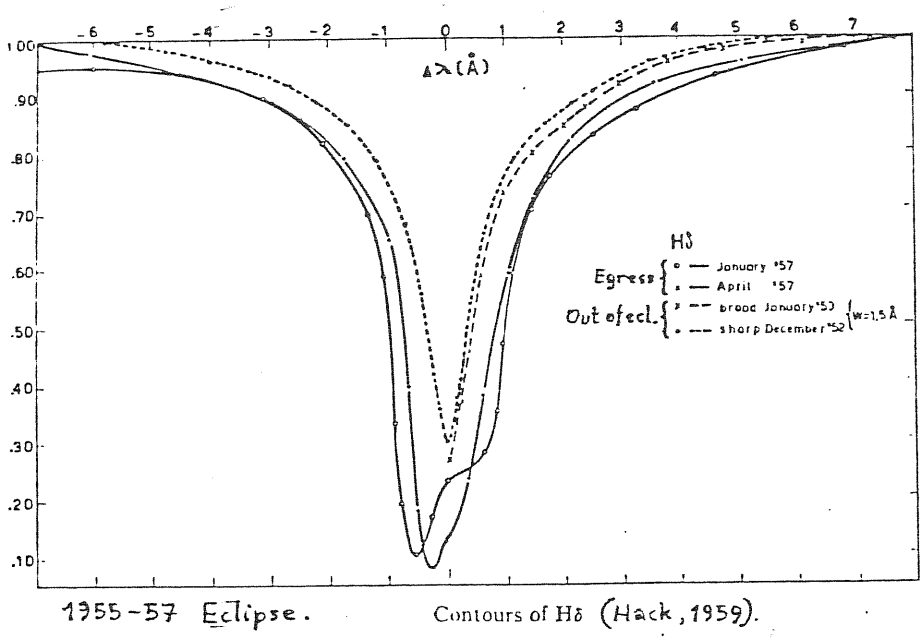

1955-57 Eclipse. Contours of Hδ (Hack, 1959).

Fig. II.7) Variations of line profiles with the eclipse phase.
(normalized absorption)

after it, can then be attributed to a rotation of the eclipsing body itself, the sense of rotation beeing the same as that of the orbital motion. Similar considerations may also explain the behaviour of the broader shell components of hydrogen lines, e.g. see next point d) for H_α.

The physics of the shell spectrum has been first discussed by Kraft (1954), and then extensively analyzed by Hack (1959, 1961) on the basis of the curve of growth method. The physical problem concerns the presence of diluted exciting radiation in the shell region. From the geometry of the system one finds that the F star, seen from the companion, covers a fraction of celestial sphere equal about to 10^{-4}; that is to say, by definition, that the geometrical dilution factor is 10^{-4}, for the primary's radiation in the shell region. If no other effects are present, this geometrical factor 10^{-4} should also represent the effective physical dilution factor; that is, in the shell region one should have the normal (non-metastable) atomic levels depopulated by a factor of 10^4. With such a strong depopulation, Kraft (1954) showed that the eclipsing body had to be about 10^3 less opaque, than observed during the eclipse.

The problem could be overcome, by directly measuring the effective physical dilution factor, in the shell region. Hack (1961), examining high-dispersion spectrograms of the 1955-57 eclipse, found in the shell spectrum evidence of diluted radiation by a factor of 10^{-1}, since normal levels of Ca I, Mg I and Fe I were depopulated by a factor of 10, with respect to metastable ones. The difference, between the physical and geometrical dilution factors in the eclip

sing body, was interpreted as indicating the presence of a source of additional UV radiation; this radiation could be able of populating the non-metastable levels with more efficency, than the geometrically diluted radiation of the F star.

Anyway, it was rather difficult to explain how an F supergiant could be the source of a strong UV excess, such as the one required for the above mechanism. To solve this last problem, it was proposed by Hack that the UV ionizating source could be a hot dwarf star, embedded in the central region of the eclipsing body itself. This model of ϵ Aur has received recently strong experimental confirmations, first by the discovery of UV excess (Hack and Selvelli, 1979) described in the next section II.5), and finally by the writer's observations, proving that far UV is not affected by the eclipse, as reported in part 2).

d) The H_α feature. Observations of the H_α line show that this feature, during eclipse, undergoes a sequence of changes unlike those observed for the other lines. These changes have been described in detail by Wright and Kushwaha (1957), and are here illustrated in fig. II.8). It is evident that the overall intensity of the emission changes considerably, as well as the ratio of the intensities of the two emission wings.

An examination of the sequence of spectra taken through the 1955-57 eclipse, and shown in fig. II.8), provides that the reduction in intensity of the H_α emission is not uniform. It can be seen that the red wing decreases faster

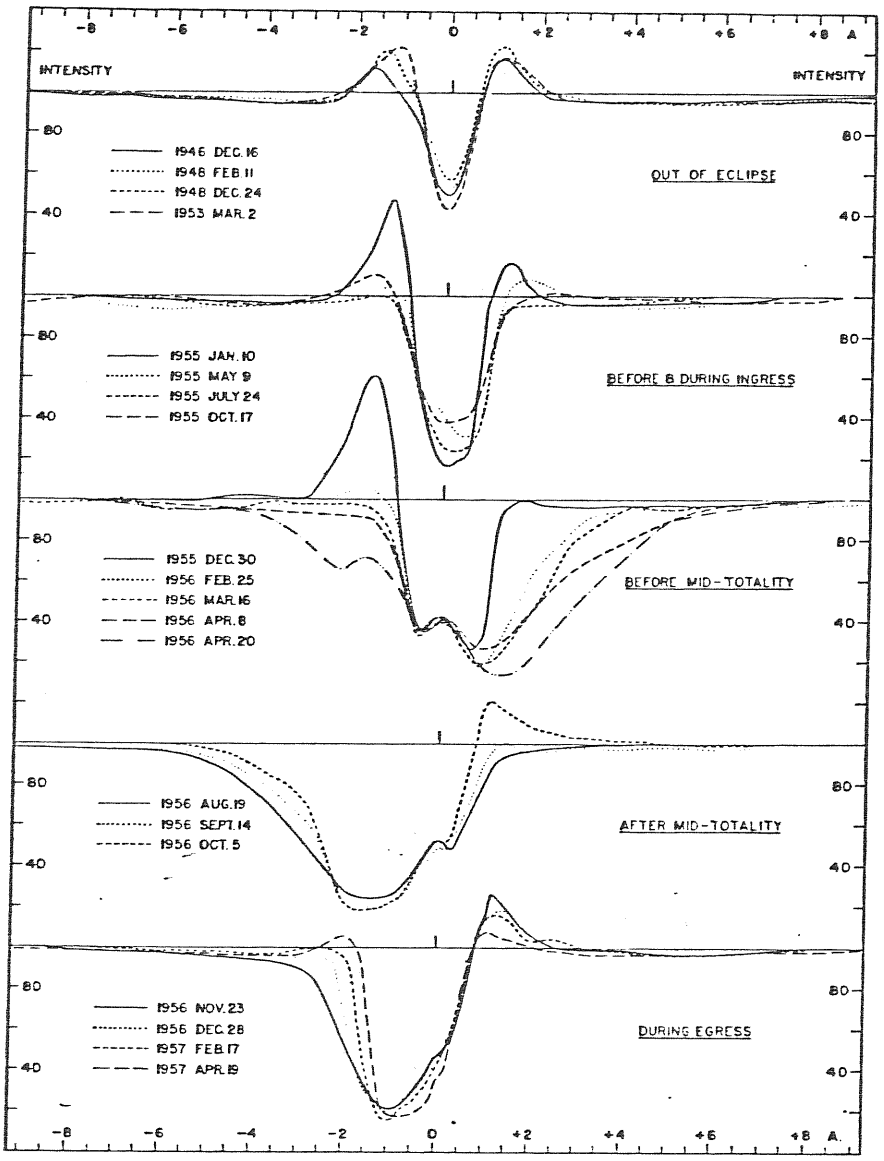

Fig. II.8) - Observed intensity profiles of Hα in the spectrum of ε *Aurigae*. The continuum at intensity 100 is relative to the F star determined at wave-lengths more than 10 A from Hα. The terrestrial absorption lines have been eliminated from the intensity tracings. (Wright, Kushwaha, 1957)

than the violet wing during ingress, and recovers its original strength sooner than the violet wing during egress.

New observation of H_α, both spectroscopic and photometric, have been performed by the author, during the current 1982-84 eclipse. Preliminary results show that H_α, during the present eclipse, is repeating phase-by-phase the same behaviour, that was here described for the past 1955-57 event. These new data, together with a general interpretation of the phenomenon, will be analyzed more in detail in part 2).

Let us now discuss briefly the physical processes, by which the H_α feature may be originated. Figure II.6a) shows clearly that the out-of-eclipse H_α line may be regarded as being the resultant of two components: a "normal" stellar absorption line, similar in profile to the higher members of the Balmer series but somewhat broader and deeper, and a superimposed line. Measured relative to the stellar continuum, the equivalent width of the out-of-eclipse emission component results of the order of 1.5 A.

The mechanism, by which the H_α emission is excited, is not immediately apparent. One may consider radiation, by the surface of the F star, as a possible excitating mechanism; but computations by Morris (1963) show that, for a reasonable F-star surface temperature of 7300 °K, the effect is too small by a factor of about 600 to account for the observed emission. The problem is similar to the one already described at point c), concerning formation of the shell spectrum, in presence of diluted radiation from the F star. Therefore it remains the possibility, that the

hypothized central hot star of the secondary component (Hack, 1961), radiates enough ultraviolet light, to produce the necessary excitation.

A further clue, to the nature of the excitation mechanism, is the fact that no emission is seen at Hβ (with the possible exception of a very weak, sharp line reported by Frost et al., in 1932). There is thus an indication that the Balmer decrement is very steep, which is a characteristic of collisional excitation (Aller 1956); this fact could suggest that the H_α emission is excited not by recombination, but rather by collision.

II.5) Infrared and Ultraviolet

a) The Infrared. Observations of ε Aur in the infrared are rather poor; no IR spectroscopy has been performed still now, and no IR data have been collected in past eclipses. The only data available concern large-band photometry, in Morgan's bands.

First reliable data were given by Low and Mitchell (1965), in a half-page milestone paper: as it is known, these observations show no strong IR excess, and therefore the presence of any large I star, as the one proposed by Struve et al. (1937), is excluded. Low and Mitchell's measurements are given in column (2) of tab. II.7), together with the more recent and complete data by Woolf

(1973) in column (3); values are not corrected for interstellar absorption.

Table II.7) - Infrared Data

(1) λ (μm)	(2) $m_v - m_\lambda$	(3) m_λ
2.2		1.9 ±.1
3.5	1.74 ±.03	
3.6		1.4 ±.1
4.8	2.3 ±.3	1.3 ±.1
8.6		0.7 ±.1
9.2	1.9 ±.2	
11.3		0.6 ±.1
18.0		0.5 ±.3

Woolf's results are also shown in fig. II.9). The shape of the spectral energy distribution from the visual to 5μ is appropriate for a late A or early F star suffering about 1.3 mag of visual extinction. Longward of 5μ an increasing IR excess is revealed, and after 10μ the energy distribution is elevated of about a factor of 2; but still the observation at 18μ sets a strong limit on the presence of any large cool star in the system.

The dimensions of the system imply anyway, because of heating by the F star, a temperature of several hundreds of degrees for any companion. Such an object, is then beeing

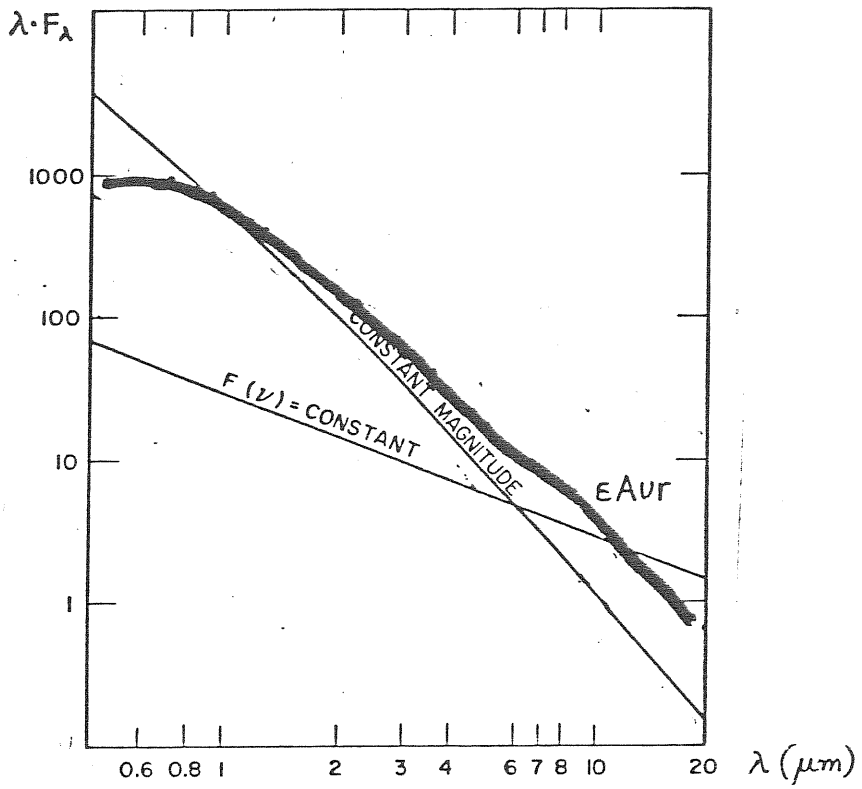

Fig II.9) – The Infrared Spectrum of ε Aur (Woolf, 1973)
An IR excess is evident longward 5μm.

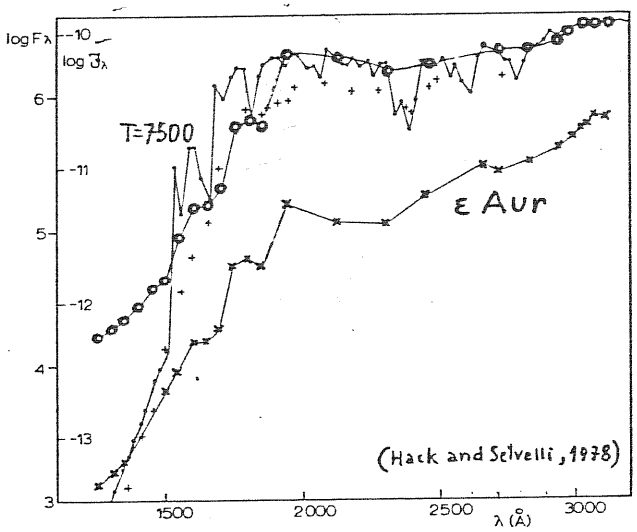

Fig. II.10) — The UV spectrum, flux at the earth $\mathcal{F}_\lambda$ (in erg cm^{-2} s^{-1} A^{-1}), observed for Epsilon Aur (×, non-corrected for interstellar extinction, and ⊙ corrected for interstellar extinction with E_{B-V} = 0.30) and that observed for Alpha Car (S2/68 observations) divided by 30 (+) in order to make it comparable with that expected for Epsilon Aur which is 3.7 mag less bright than Alpha Car. F_λ is the flux (erg cm^{-2} s^{-1} A^{-1}) computed for an atmosphere with parameters T_e = 7500 K and log g = 1 (•).
An UV excess is evident shortward 1650Å.

predicted not to show up, at wavelengths longer than 20μ. In conclusion, it should be precisely the 5-18μ excess, to be interpreted as the very radiation from the companion of ε Aur.

Substracting the expected contribution of the F star, one finds that the radiation of this companion behaves as follows. The spectral flux F (ν) is approximately constant, at a level of about 10 flux units, between 5 and 10μ. Then, at longer wavelengths it falls off like a blackbody, with a total radiation in this tail slightly larger than that produced by the A star. This radiation could be similar to the radiation observed from the envelopes around Be stars (Woolf, Stein, and Strittmatter 1970).

We can then note that this IR behaviour of the eclipsing body in ε Aur is consistent with models both by Hack (1961) and by Huang (1965). Shell temperature and electron density ($\sim 10^{11}$ cm^{-3}), derived from IR observations, are found by Woolf in good agreement with those predicted by Hack's model. On the other side, the observed equality of 10-18μ emission by the two components of the system, is consistent with Huang's picture, in which the projected area of the disk is about equal to the surface area of the F star; in this case, the disk should have a temperature similar to that of the star.

Woolf finally predicts that, near 10μ, there will be a long secondary eclipse, and its depth is expected to be of the order of 0.2 mag.

The importance of new observations, to be performed during the present 1982-84 eclipse, is now clear: if the

15-18 μ excess comes really from the eclipsing body, it should be enhanced during eclipse, because the primary contribution is attenuated. In wiew of this, IR spectrophotometry of ε Aur will be done, at national TIRGO infrared 1.5m telescope, about at the end of totality; unluckyly, a corresponding shift of observations at early totality was completely lost, because of seasonal adverse-weather conditions.

b) The Ultraviolet. The first Ultraviolet observation of ε Aur was performed by Hack and Selvelli (1979), with the "International Ultraviolet Explorer" satellite (IUE); an outstanding far-UV excess, shortward 1650 Å, was detected. The observed UV spectrum is represented in fig. II.10) by the lower line, while the upper line with circles is the same spectrum, corrected for interstellar extinction; a comparison with the other upper line, representing the expected spectrum for the F star, shows the existence of an increasing UV excess towards the shorter wavelengths.

Interpreting the excess, as due to the emission by a hot secondary component embedded in the eclipsing body, a radius and an effective temperature were derived for this secondary, by a best-fit method assuming different radii and temperatures for the primary. Estimated values for the secondary resulted

(II.7) $R_B = (1.0 \pm .5) \times 10^{11}$ cm , $T_B = 15.000 \pm 3.000$ °K ;

the radius and the temperature of the primary were consistent, within the fitting range, with those predicted by Castelli (1978) and given here in tab. II.6). Corresponding

values, for the secondary's apparent and absolute visual magnitudes, were found to be respectively

(II.8) $\qquad v_B = +9.2 \quad , \quad V_B \approx -1 \quad ;$

such a high value of v_B could explain the difficulty of detecting the secondary in the visible.

Since the secondary is embedded in an extended envelope, responsible for the primary's grey eclipse, the secondary itself should be permanently auto-eclipsed, by such envelope. Supposing this eclipse had the same grey depth as the primary's one, Hack and Selvelli suggested that secondary's "intrinsic" values of magnitudes should be obtained by subtracting 0.8 mag from (II.7), while "intrinsic" radius should be about $\sqrt{2}$ times larger than R_B in (II.8). Such values lead, finally, to conclude that the secondary must be a late-B main sequence star. Spectral low-resolution analysis in the far UV was also performed, providing identifications for strongest lines; moreover, a complex structure of the Mg II λ 2800 resonance doublet was revealed.

Later, a high-resolution analysis of the mid-UV spectrum of ε Aur was performed by Castelli et al.(1982), on the basis of IUE data, and of older balloon-borne BUSS observations. The method of LTE theoretical spectrum was employed, adapting a previous atmospheric model, already used by Castelli (1978) for the visible, and here described in section II.4b). Moreover, the theoretical spectrum was convoluted with the IUE instrumental profile, in order to make possible the comparison with observed spectrum.

Complete identification was given from about 2450 Å to

3230 Å; abundances were found to be almost solar, with an overabundance of iron-group elements, but not of Fe itself. Several peculiarities were found: (a) a variability of some lines with time; (b) the presence of emission components, besides in MgII λ 2800, also in some other strong lines as those of FeII multiplets UV 1, 62 and 63; (c) the presence in many lines of a blue-shifted variable absorption component.

These out-of-eclipse peculiar lines can be explained, supposing they are formed at various heights in an expanding region, over the photosphere of the F star; expansion velocity of this "shell" is then found to be 37 ± 15 km/sec. The problem is where does this expanding medium extend in the system of ε Aur, since it could extend from the cromosphere, to a circumstellar envelope, or even to a surrounding interstellar region.

Ultraviolet observations have then proved to be foundamental, in unveiling the nature of ε Aur system, since: (i) the far-UV spectrum permits us to observe directly the secondary; (ii) the mid-UV shows us the behaviour of primary's envelope. The 1982-84 eclipse was hence expected to offer, for UV observers, an occasion of obtaining otherwise inaccessible informations, such as: (i) a possible discrimination of the two components' emission, (ii) a test for the primary's envelope extension.

As we shall see in the next chapter, devoted to the writer's UV observations of the actual eclipse, results have been even superior to these hopes.

PART 2

OBSERVATIONS

Chapter III

THE ECLIPSE IN THE ULTRAVIOLET

In this Chapter, and in the following ones, separate new contributions are presented. The first research (Chap.III), which is also the most substantial one, consists in a study of the ultraviolet emission of ε Aur, before and during the actual eclipse phase. Observations were made with the "International Ultraviolet Explorer" satellite (IUE). Data analysis was performed under the supervision of M.Hack, and with the technical aid of C. Boehm. Results given in this chapter are referred to an article in press for "Astronomy and Astrophysics" (Ferluga, Hack and Boehm, 1983), and to a "contributed paper" at the 7th IAU Regional Meeting (Ferluga and Hack, 1983).

III.1) Observations and Data Processing.

The low-resolution IUE spectra that have been considered are listed in tab. III.1). Observations, concerning the last spectrum (9) were performed by the writer, at

TABLE III.1)-Observations, Low Resolution.

1 No. of Spectrum	2 IUE Image & Apert.	3 Exposure (s)	4 Date Observer			5 Spectral Range λ min, λ max (Å)
(1)	LWR 6005, L	120	1979, Nov. 1; Gilra	9^h	23^m	1900, 2500
(2)	SWP 14647, L	1800	1981, Aug. 4;	9	22	1200, 1700
	LWR 11238, L	50	Plavec	9	42	1900, 3200
(3)	SWP 14654, L	1200	1981, Aug. 5;	0	51	1200, 1690
	SWP 14654, S	300	Stickland	0	51	1690, 1910
	LWR 11246, L	120		0	9	1910, 2415
	LWR 11246, S	60		0	9	2415, 3200
(4)	SWP 16522, L	35	1982, Mar. 12;	19	54	1500, 1950
	LWR 12776, L	9	Chapman	19	59	2400, 3200
(5)	SWP 16628, L	1200	1982, Mar. 26;	7	33	1200, 1570
	SWP 16628, S	420	Stickland	7	33	1570, 1940
	LWR 12864, L	30		7	7	1940, 2420
	LWR 12864, S	30		7	7	2420, 3200
(6)	SWP 18137, L	1500	1982, Sep. 27; Stickland	18	24	1200, 1700
(7)	SWP 18570, L	2400	1982, Nov. 16;	15	35	1200, 1695
	SWP 18570, S	600	Molaro	15	35	1695, 1950
(8)	SWP 19492, L	1800	1983, Mar. 20;	5	12	1200, 1725
	SWP 19492, S	600	Morossi	5	12	1725, 1900
	LWR 15523, L	300		6	9	1900, 2425
	LWR 15524, L	20		6	9	2425, 3200
(9)	SWP 20643, L	1980	1983, Aug. 8;	21	11	1200, 1700
	SWP 20644, L	270	Ferluga	22	39	1700, 1900
	LWR 16552, L	270		21	34	1900, 2400
	LWR 16551, L	27		20	51	2400, 3200

the VILSPA Satellite Tracking Station of the European Space Agency (ESA), in Spain. Spectra (7) and (8) were obtained also at VILSPA by colleagues of Trieste Observatory, P.Molaro and C.Morossi. In addition, the observational material concerning the less recent spectra from (1) to (6) is from different authors, and has been made available by the VILSPA Data Bank.

The dates of observations, given in the third column of Tab. III.1), show that the first spectra, from (1) to (5), were all taken out of eclipse; spectrum (6) corresponds roughly to mid-ingress, while spectra (7) and (8) represent the end of partial phase and early totality respectively. The last spectrum (9) corresponds about to mid-totality. Symbols L and S in column 2 stand for large (10"x20") and small (3") aperture. Only the best exposed part of each image, indicated in the last column, has been utilized. Plots of the single images are shown in Appendix A .

The procedure of deconvolution and calibration, for all the spectra considered, has been performed with VILSPA software, in the updated version. The way in which the spectra are extracted, from IUE rough data, cannot be described here in detail; the effects of deconvolution and calibration procedures are illustrated in fig. III.1), where a section of spectrum (9) is shown.

In order to be sure in excluding possible spurious effects of variability, due to evolving IUE data-processing technology, particular controls were performed. Self-consistency of the VILSPA software, applied to low-resolution

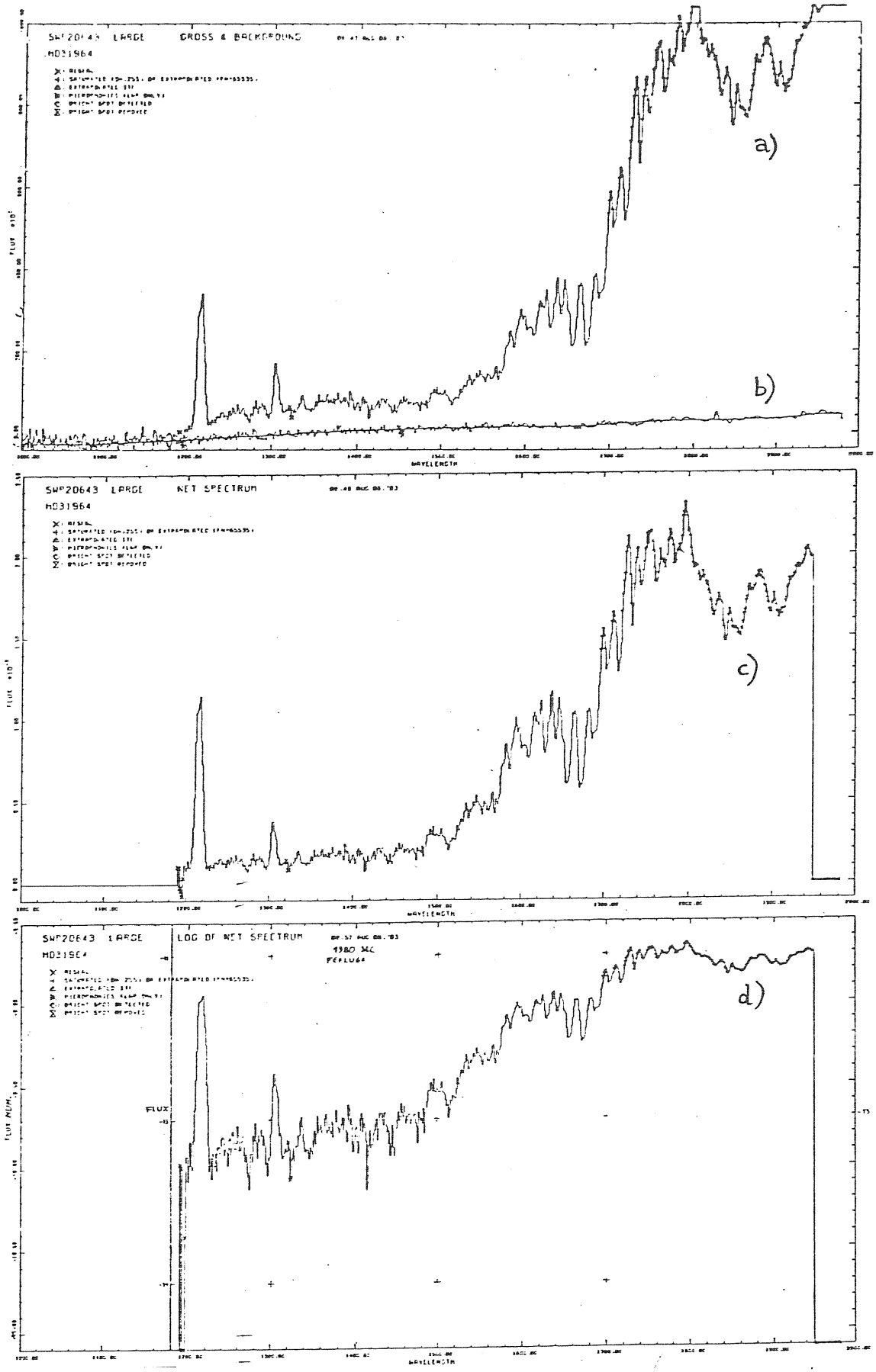

Fig. III.1) – Extraction of the spectrum: deconvolution and calibration procedure for IUE; Image SWP 20643 (Large Aperture), Spectrum (9).

a) Gross spectrum
b) Background of SWP Camera
c) Net spectrum
d) Final calibrated net spectrum, in logarithmic scale.

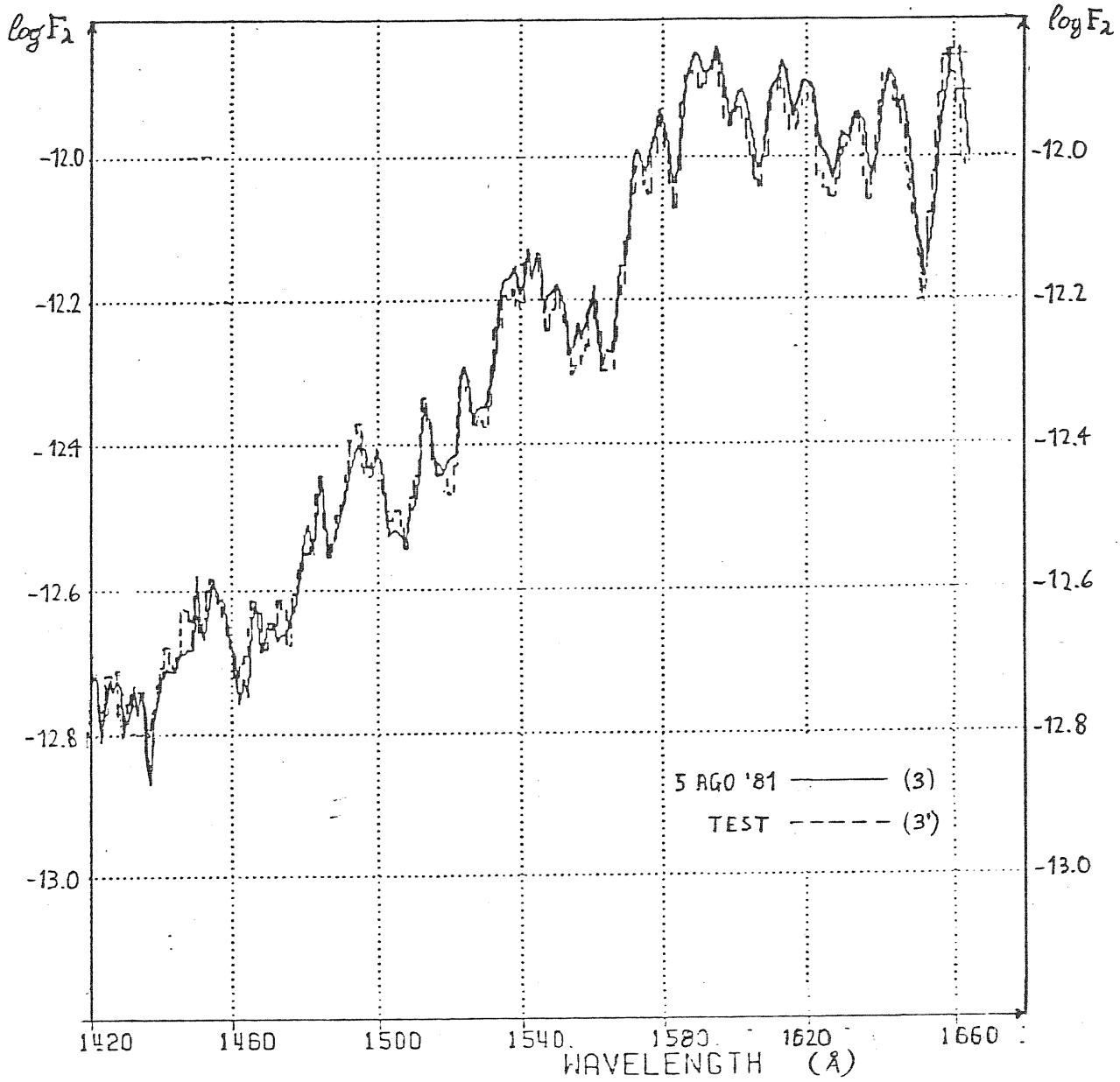

Fig. III.2) Software test, for spectrum (3). An enlarged portion is shown. Solid line: VILSPA Software Dashed line: IUEARM precision procedure. Differences are very small, consisting mainly in a slight sharpening of the features in IUEARM, because of a better noise-remotion procedure.

data taken in considerably different epochs, was tested. The reliability of the software is fully confirmed, by a check (fig.III.2) with the high-precision deconvolution procedure IUEARM, at the Computing Center of the Trieste Astronomical Observatory.

Moreover, since the small aperture does not gather all the light of the star, it allows no absolute flux calibration. Therefore, small-aperture images have been considered only when they partially overlap with a large-aperture image, taken nearly at the same time, which can provide its own flux calibration. Anyway, the flux derived by the small-aperture images is affected by a systematic error, estimated on of the order of 5%, caused by the uncertainty in the vertical shift necessary to fit the spectra obtained with the large and small apertures.

III.2) The UV Continuum

A comparison between eclipsed and uneclipsed spectra is shown in Figure III.3). Four selected spectra are plotted, providing significant indications. It should be noted that the following results are here derived, only on the basis of data concerning out-of-eclipse, ingress and early-totality phases; successively, after spectrum (9) was taken, they have been fully confirmed by mid-totality observations (see "Updating" hereafter).

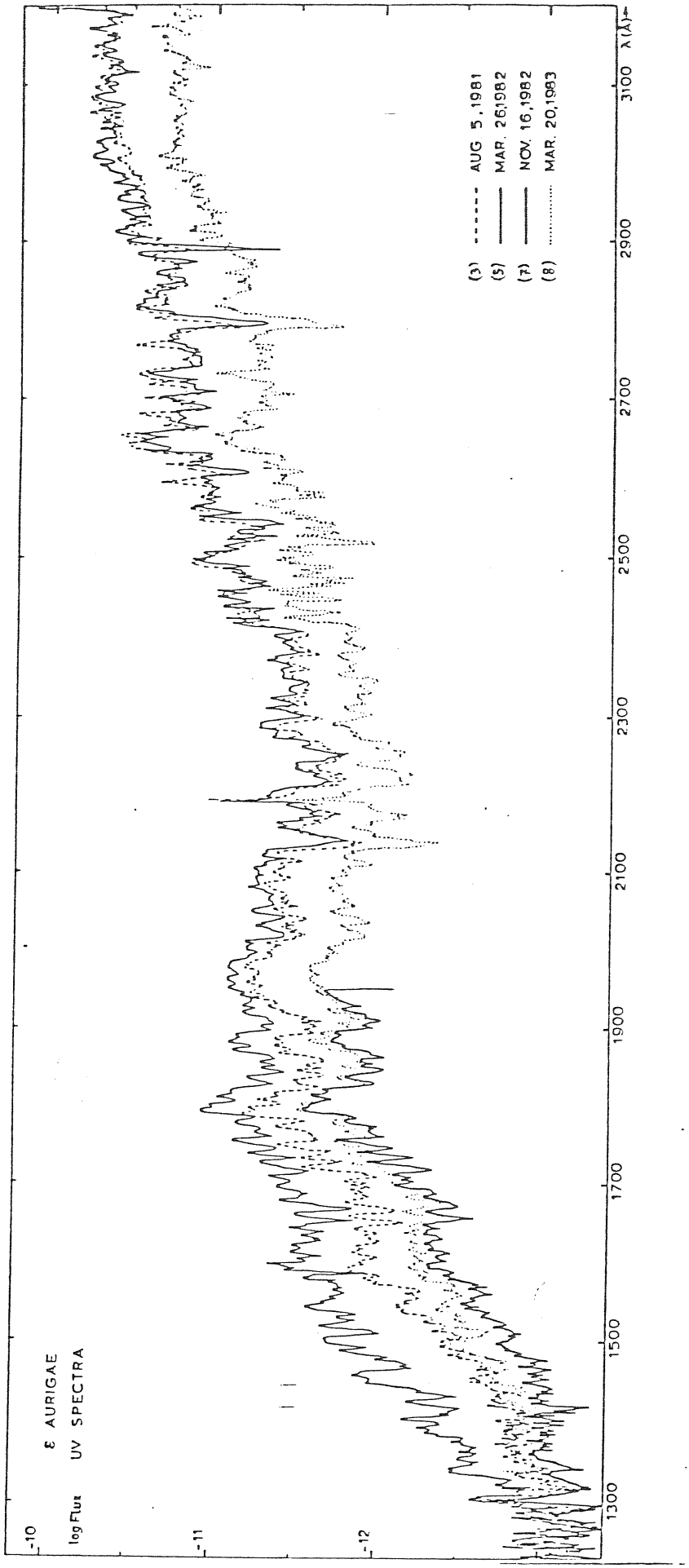

Fig. III.3) Four significant spectra of ε Aur, taken before and during the eclipse, are plotted together; Fluxes are in erg cm^{-2} s^{-1} $Å^{-1}$. A detailed comparison is described in the text (section 'Results', a) to e)). The spectrum taken in totality (dotted line) is higher than the one taken in the partial phase (lower solid line).

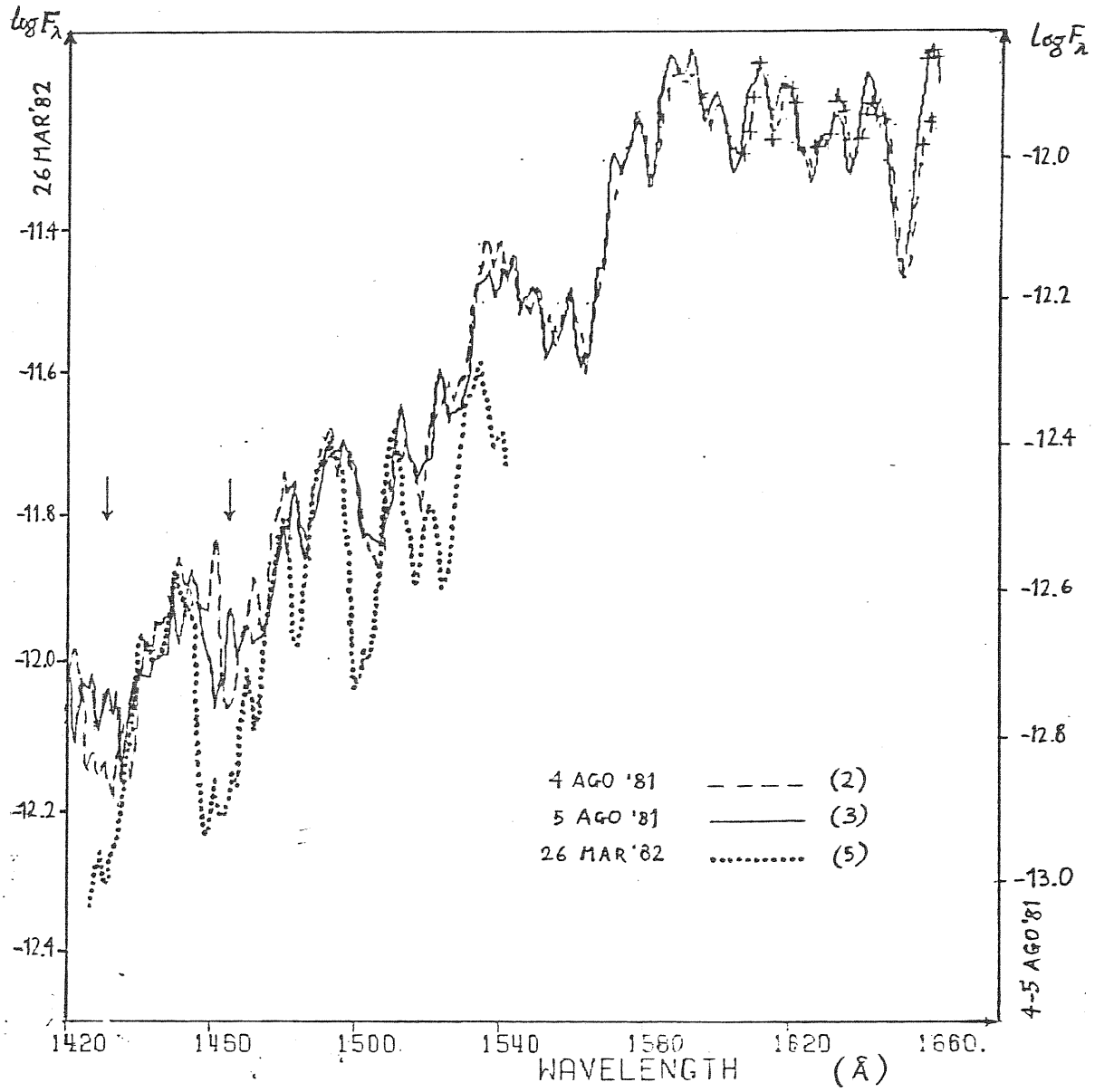

Fig III.3') - Line variability in far UV; see text at point III.2b) for detailed description. In the figure, the "active" spectrum (5) has been shifted downwards (left-side ordinate), with respect to the other two "quiescent" spectra (2) and (3) (right-side ordinate), in order to make direct comparison possible. Short-time variabity (3)-(2) is clearly above the noise (cfr. fig III.2), in the regions showed by the arrows.

a) Out-of eclipse flux variability. Spectra (3) and (5), both taken out of eclipse, show remarkable variations of the flux in the spectral range 1300-2150 Å. The flux on March 26, 1982 (5) is higher than the flux on August 5, 1981 (3); the difference increases towards shorter wavelengths, while at $\lambda \gtrsim 2150$ Å there are practically no flux variations.

b) Out-of-eclipse line variability. In the range 1400-1600 Å, the spectral absorption lines are systematically deeper in the "active" phase (5), than at all other epochs. Moreover, in the same spectral range, a detailed comparison between spectra (3) and (2), reported in Figure III.3') shows variations of the line profiles, on a time-scale of 15 hours.

c) Greyness of the eclipse. In the wavelength range 2150-3200 Å the totally eclipsed spectrum (8) on March 20, 1983 differs from the nearly identical out-of-eclipse spectra, (3) and (5), only by a shift in the logarithmic flux scale. This means that the UV depth of the eclipse is almost constant with wavelength (as it is in the visible).

d) Invariance of the λ 2200 absorption feature. Comparing spectrum (8), with spectra (3) and (5), no remarkable deepening of the wide absorption feature at $\lambda \simeq$ 2200 Å appears, in correspondance with the eclipse phase.

e) Eclipse vanishing at short wavelengths. Complex behaviour is displayed in the range 1300-1700 Å. The flux during the partial phase on Nov. 16, 1982 (7) is

lower than during totality (8); the effect of the variability described in a) is thus evident. Moreover, by comparing eclipsed spectra (7) and (8) with non-eclipsed ones (3) and (5), it appears that the depth of the eclipse decreases, and gradually vanishes, towards the shortest wavelengths.

Quantitative measurements of the continuum fluxes, for all the 8 spectra considered, are given in the left part of Table III.2). Values of monochromatic fluxes are tabulated for selected wavelengths, representing "windows" over the continuum, which is supposed to be matched by a curve passing through the highest points of the spectrum (Castelli et al., 1982); adopted continuum is shown, by a dashed line, on the plots of Appendix A). On the last line the corresponding visual magnitudes, obtained from IUE Fine Error Sensor (FES), are reported; values from (1) to (6) are taken from Chapman et al. (1983), while (7) and (8) are derived from our observations, using the same calibration (Holm and Rice, 1981).

Flux variations, for significant couples of spectra, were computed; they are given, in terms of differences of monochromatic magnitudes, on the right part of Table III. 2), and are plotted in Fig. III.4). In particular, "(5)-(3)" is the amplitude of the "activity" observed out of eclipse, reaching a maximum of 1.75 mag. at 1500 Å. Then, "(8)-(3)" represents the depth of total eclipse, which is about 1 mag. in the mid UV (slightly larger than the 0.85 mag. observed in the visible), but under 1500 Å

TABLE III.2) Continuum fluxes.

Sp. / Date / λ(Å)	− log F_λ (erg cm^{-2} s^{-1} Å^{-1})								Δm (mag)			
	(1) 1.11.79	(2) 4.8.81	(3) 5.8.81	(4) 12.3.82	(5) 26.3.82	(6) 27.9.82	(7) 16.11.82	(8) 20.3.83	(5)−(3) Δm_{out}	(5)−(4) Δm_{bur}	(8)−(3) Δm_{tot}	(8)−(7) Δm_{in}
3200	–	10.37	10.30[a]	10.34	10.30[a]	–	–	10.74	.00	–	1.10	–
3110	–	10.44[b]	10.27[ab]	10.31	10.31[a]	–	–	10.72	.10	–	1.12	–
3005	–	–	10.38[ab]	10.22	10.24[ab]	–	–	10.63	−.35	–	.70	–
2905	–	–	10.45[ab]	10.46[b]	10.45[ab]	–	–	10.88	.00	–	1.07	–
2820	–	–	10.50[ab]	10.50	10.51[a]	–	–	10.97	.00	–	1.17	–
2735	–	–	10.53[ab]	10.61[b]	10.58[a]	–	–	10.98	.12	–	1.12	–
2615	–	–	10.81[ab]	10.95	10.81[a]	–	–	11.26	.00	–	1.12	–
2495	11.11[b]	10.95[b]	10.84[a]	10.83	10.86[a]	–	–	11.35	.05	–	1.27	–
2405	11.38	11.31	11.43	11.21[c]	11.33	–	–	11.78	−.25	–	.87	–
2295	11.29	11.32	11.33	–	11.26	–	–	11.70	−.32	–	1.07	–
2205	11.40	11.35	11.46	–	11.34	–	–	11.76	−.30	–	.75	–
2120	11.36	11.35	11.38	–	11.28	–	–	11.78	−.25	–	1.00	–
2035	11.31	11.33	11.42	–	11.26	–	–	11.76	−.40	–	.85	–
1950	11.20	11.21	11.22	11.09	11.10	–	11.66[a]	11.62	−.30	.02	1.00	−.10
1795	–	–	11.18[a]	11.05	10.94[ab]	–	11.55[a]	11.51[a]	−.60	−.11	.82	−.10
1685	–	11.91[b]	11.82[b]	11.57	11.43	12.22	12.30	12.17	−.97	−.35	.87	−.32
1595	–	11.87[b]	11.84	11.59[c]	11.36	12.26	12.31	12.20	−1.20	−.57	.90	−.27
1500	–	12.38	12.41	11.91[c]	11.71	12.71	12.74	12.43	−1.75	−.50	.05	−.77
1405	–	12.72	12.73	–	12.17	12.96	12.97	12.82	−1.40	–	.22	−.37
1335	–	12.92[c]	12.86[c]	–	12.47	13.04[c]	13.03[c]	12.89[c]	−.97	–	.07	−.35
1304	–	12.62	12.66	–	12.59	12.72	12.74	12.71	−.17	–	.12	−.07
1240	–	12.90[c]	12.89[c]	–	12.80[c]	13.04[c]	13.03[c]	12.98[c]	−.22	–	.22	−.12
m_{FES}	–	3.25	3.25	3.20	3.22	3.69	3.98	4.10	−.03	.03	.85	.12

Notes to Table III.2)

a) Small aperture
b) Over-exposed
c) Under-exposed

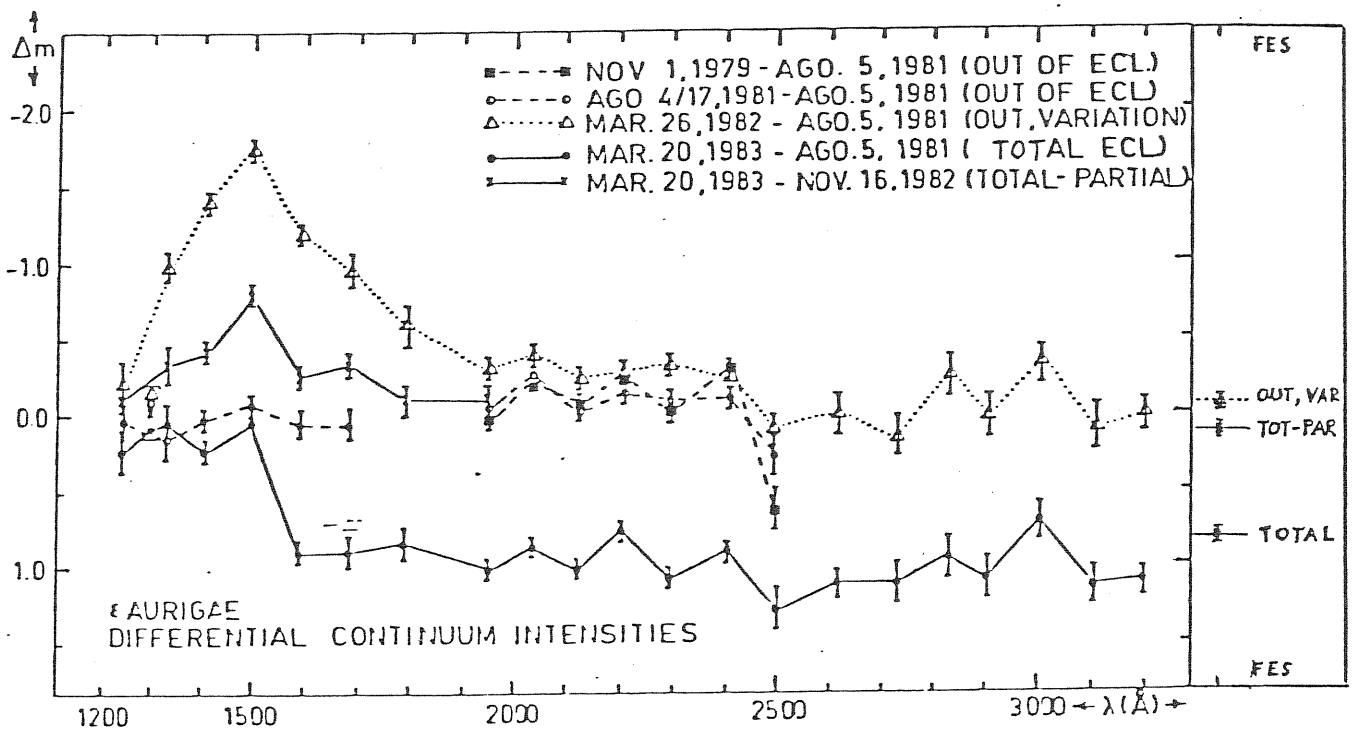

Fig. III.4) UV variability. The differences in magnitude between various phases, vs. wavelength, are given. The lower solid line represents the depth of total eclipse, while the dotted line shows out-of-eclipse activity.

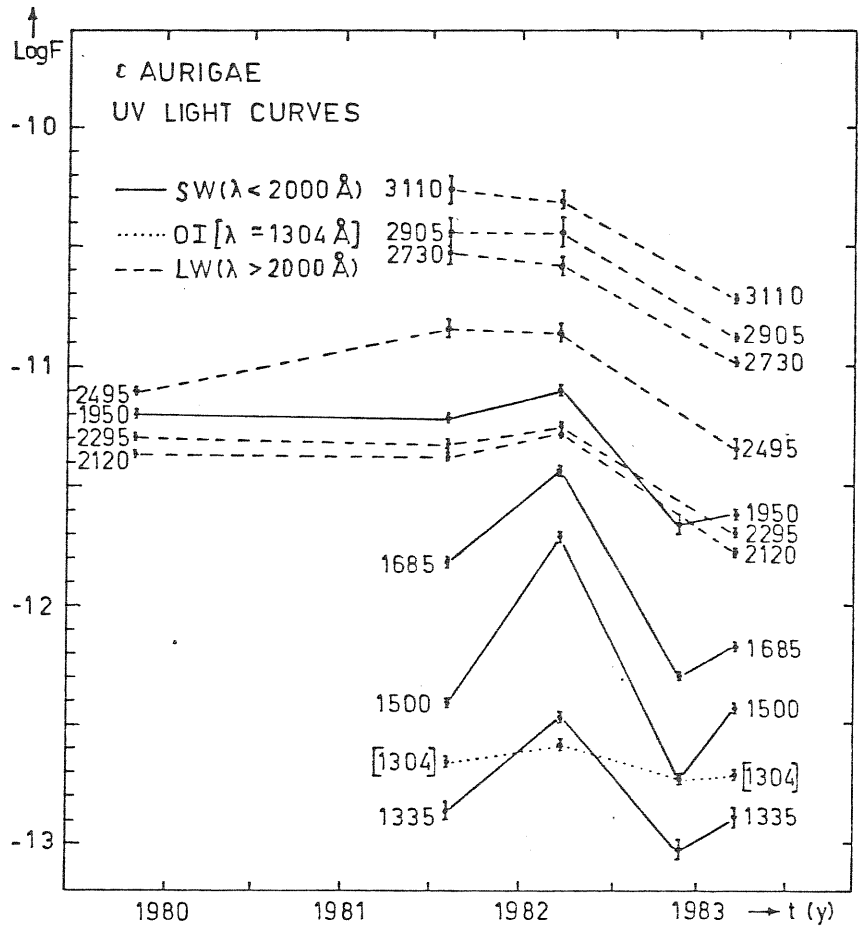

Fig. III.5) Monochromatic UV light curves; fluxes are in erg cm^{-2} s^{-1} $Å^{-1}$. The OI λ1304 curve (dotted line) seems to be unaffected both by the eclipse and by intrinsic activity.

is masked by intrinsic variability, prevaling in the far UV. For instance, "(8)-(7)" shows that at 1500 Å the flux measured during totality is surprisingly 0.8 mag. larger than the flux in the partial phase.

Monochromatic light-curves, derived from table III.2), are shown in Fig. III.5). At long wavelengths the drop due to the eclipse is evident, while at short wavelengths the behaviour is complicated because of intrinsic activity. The light-curve at λ 1304, corresponding to the OI lines, shows little or no evidence of the eclipse; moreover, it is practically insensitive to the out-of-eclipse activity.

Error bars, in Figures III.4) and III.5) are estimated taking into account the uncertainty due to the small-aperture fitting procedure, and the effects of over-exposure or under-exposure.

Updating. Let us now examine the last spectrum (9), taken in phase of mid-totality, which corresponds in fig. III.6) to the lower solid line. For comparison, three already known spectra are shown together: out-of-eclipse spectra (3) and (5) are given by the upper lines (solid and dashed respectively), while the early-totality spectrum (8) is given by the other (dashed) lower line.

One can see that the couple of eclipsed spectra, (8) and (9), display exactly the same kind of far-UV variability, which was previously detected, out of eclipse, in the couple (3) and (5). Moreover, in the rest of the spectrum, the couple of totally eclipsed continua (8) and

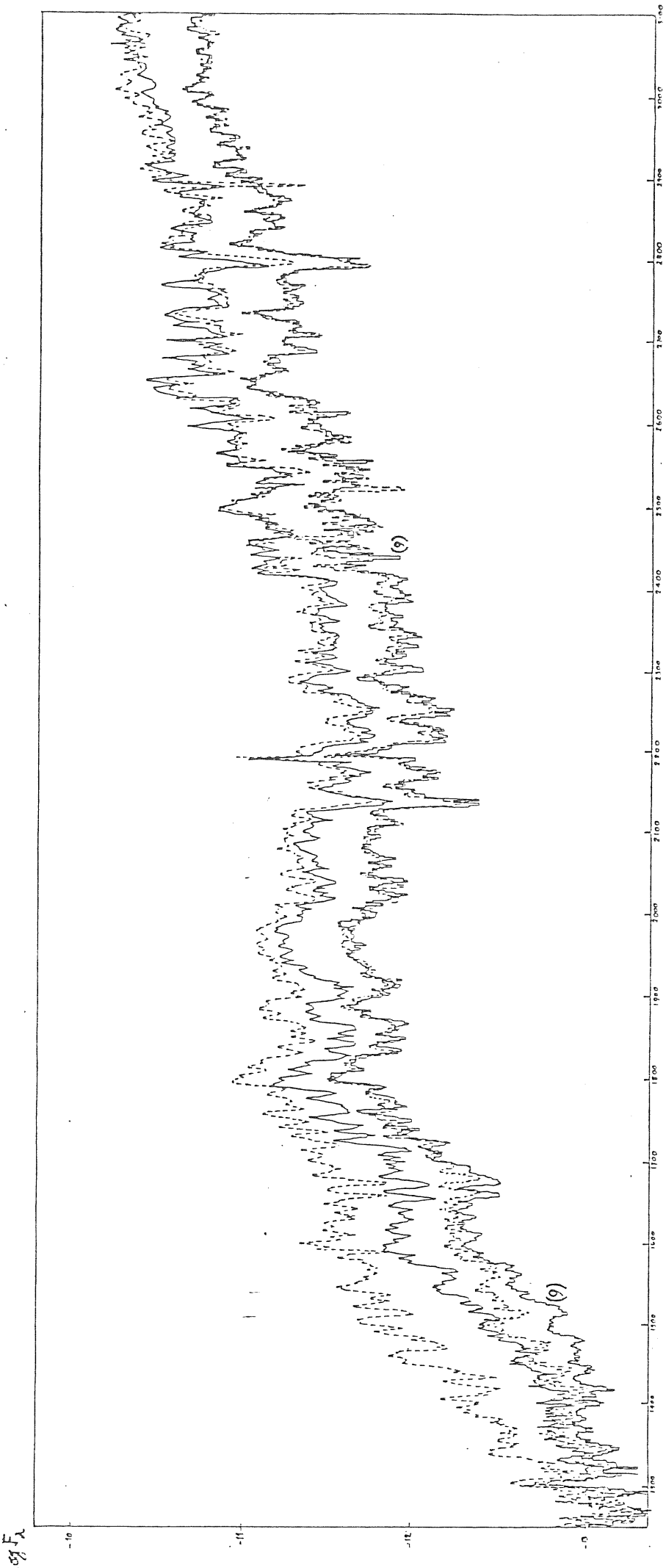

Fig. III.6) The updated mid-totality spectrum (9), compared with spectra (3), (5), (8) already given in fig III.3).

Upper lines (out-of-eclipse) { ----(5) active (1982, Mar 26); ——(3) quiescent (1981, Aug 5)

Lower lines (total eclipse) { ----(8) active (1983, Mar 20); ——(9) quiescent (1983, Aug 8)

(9) are coincident; this shows that, from early totality (8) to mid totality (9), the eclipse remained of constant depth in time. Greyness of the eclipse is outstanding, in mid and near UV, from the overall parallelism of the couple (8), (9) with respect to the couple (3), (5).

Finally, from these updated observations, one can conclude that all the results announced at points a)...e), which were first achieved only analyzing the ingress phase, are now strongly confirmed on the basis of mid-totality data.

III.3) Discussion

From the set of eclipsed and uneclipsed spectra, one derives the basic result, that the amplitude of the eclipse of ε Aur is reduced at $\lambda \lesssim 1400$ Å. Probably, the contradiction with the data reported by Chapman et al. (1983), who found an opposite trend in the wavelength dependance of the eclipse, is only apparent. In fact, Chapman et al. consider a spectrum taken out of eclipse on April 13, 1982, during an "active" period (near spectrum (5)), and compare it with a partially eclipsed spectrum taken on Sept. 21, 1982, during a "quiescent" period (near spectrum (6)). This causes an apparent deepening of the eclipse in the short wavelength range, which is dominated by intrinsic variability.

Eclipse depth, decreasing at short wavelengths, gives strong support to those models of ε Aur that predict the existence of a hot secondary component dominant in the far UV, and not affected by the eclipse because it passes in front of the primary. For the same reason, Plavec's model (Plavec, 1982), which locates the hot object inside the primary component (supposed to be a disk simulating an F supergiant), seems to be contradicted by observation.

Let us come to the source of far UV variability. Continuum fluctuations could be simply an intrinsic property of the hot secondary, but we need a mechanism also for line variations. Probably, variability could come from a presumed non-homogeneous structure of the extended body surrounding the secondary (and already responsible for the eclipse of the primary); in this case, according to the degree of clumpiness, the light of the secondary should be more or less attenuated, so that its spectral lines could be more or less filled by continuous emission of the extended body. Another possibility is the intrinsic variability of the extended body itself; an increase in its opacity may explain both the increase in the flux emitted (getting closer to black body conditions), and the deepening of the absorption lines (supposing they are formed in the body itself). An attempt for analyzing the variability of the UV excess is made in Appendix C .

Since there is no remarkable deepening of the λ 2200 absorption feature, associated with the eclipse, this fact puts serious constraints on the nature of the eclipsing body, ruling out its being made of standard-composition dust.

Therefore, if dust is present, it can be found only in small quantities around the secondary; otherwise it may be located in an external envelope surrounding the whole system. The existence of this extended structure is suggested by the emission line OI λ 1304, which is practically independent of the eclipse and of UV variability; a similar behaviour is also shown by the emission wings of the chromospheric lines of MgII λλ 2800, which are observable on IUE high-resolution spectra.

Finally, let us examine the greyness of the eclipse. There are indications that, in the near and mid UV, the eclipse is deeper than in the visible (Ake and Simon, IAU Circ. 3763); also the values given in our Table 2 confirm this trend, but the observed disagreement between optical and UV depths may be reduced to about 0.1 mag if only well exposed regions of the large aperture-spectra are considered. Anyway, in addition to electron scattering, which may provide the grey component of the eclipse (as suggested by Hack, 1959), another contribution to the opacity of the eclipsing body must be present the ultraviolet. This could be produced by strong blended absorption lines from the eclipsing body, affecting the position of the continuum (particularly on low-resolution spectra).

NOTE. The Mid-UV lines

High resolution spectroscopic IUE observations are used here, in order to study the effects of the eclipse over the lines, in the mid UV. It is pointed out how "normal" and "peculiar" lines can be recognized with respect to the eclipse, since the first ones display a phase-dependent behaviour while the others ones appear to be eclipse-independent.

Table III.3) - High Resolution Observations

Spectrum	IUE Image	Exposure (sec)	Date	Observer
(o)	LWR 11247.L	-	1981,Aug.5	Stickland
(i)	LWR 14645.L	900	1928,Nov.16	Molaro
(ii)	LWR 15522.L	3600	1983,Mar.20	Morossi
(iii)	LWR 16553.L	900	1983,Aug.8	Ferluga

Spectra listed in Tab.III.3) were taken at pre-eclipse (o), end ingress (i), early totality (ii), and mid totality (iii) phases; since usually, at short wavelengths, high resolution spectra of ε Aur are underexposed, here only the region from 2400 Å to 3200 Å is considered. Spectra (i) and (iii) are plotted together extensively (in Appendix B, at the bottom), in order to provide a direct visual comparison; together (in Appendix B, at the top) also Castelli's (1982) theoretical model, and an out-of-

eclipse spectrum, are plotted.

a) Normal Lines. By comparing spectra taken in different phases, as a first result one obtains that, except a few peculiar lines examined later in b), almost all the lines display a standard phase-dependant behaviour; this (shown schematically in fig. III.7) can be described as follows.

(i) At end ingress, a widening of the profile on the red side appears, suggesting the presence of an additional unresolved absorption component, with a redshift corresponding to a velocity of about +30 km/sec.

(ii) In early totality the effect is even more evident, presumably because of a corresponding enhancement of the red-shifted component. Although generally the two components are unresolved, giving the global appearence of a single larger and red-shifted line, there are also some cases in which a double-core structure can be directly observed.

(iii) At mid-totality, the lines remain deeper and larger with respect to out-of-eclipse ones, but no apparent redshift is present, as if the two absorption components were superimposed. Sometimes, a complex structure seems to be convoluted with the instrumental profile.

We note that similar phenomena have already been recognized on the visible spectra, in occasion of past eclipses

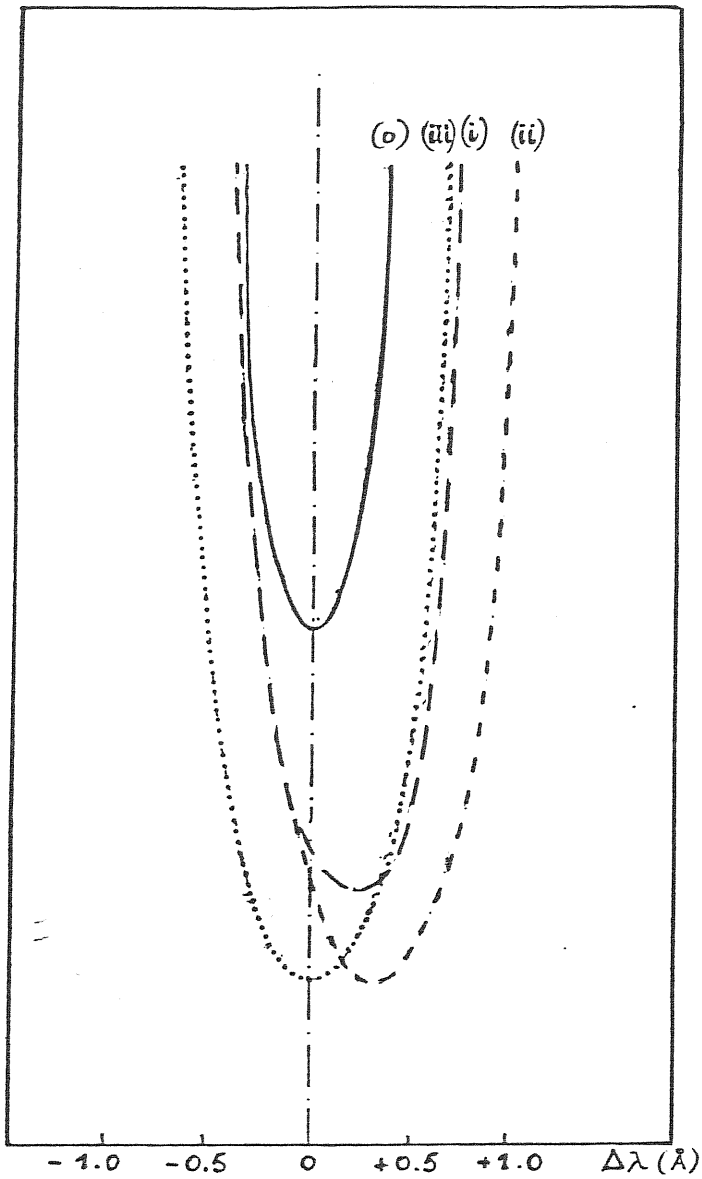

Fig III.7) - The "standard" phase-dependence of mid-UV line profiles (schematic).

o) Pre-eclipse;

i) mid ingress;

ii) early totality;

iii) mid totality.

of ε Aur, and have been interpreted as due to the shell spectrum (section II.4c); this should be then the first time, that it has been possible to detect the shell spectrum in the UV.

b) Peculiar lines. Some isolated lines in the mid-UV, such as resonance lines of MgI, MgII and FeII, do not participate to the general redward "oscillation" during ingress and early totality. Among these "steady lines", there are some features, which moreover seem not to participate in the general lowering of the continuum, corresponding to the depth of the grey eclipse; as an effect, these features "come out" in the eclipsed spectra, appearing as emission components of P Cygni-like profiles. Therefore we can classify the lines, which display a peculiar behaviour in eclipse, in the following way.

1) "Steady lines", with pure absorption profile. They are rare to be found; the best example is the strong MgI resonance line at λ 2852 Å, shown in fig. III.8c). Intermediate cases, displaying a more or less reduced redward oscillation during ingress, are more common; an example can be MnII λ 2576 and λ 2594 resonance lines.

2) "Steady lines", with outcoming emission component. They can be represented by the striking case of MgII λ 2800 resonance doublet (fig. III. 8d), where the existence of an eclipse-enhanced emission feature (fig. III.9) was already detect

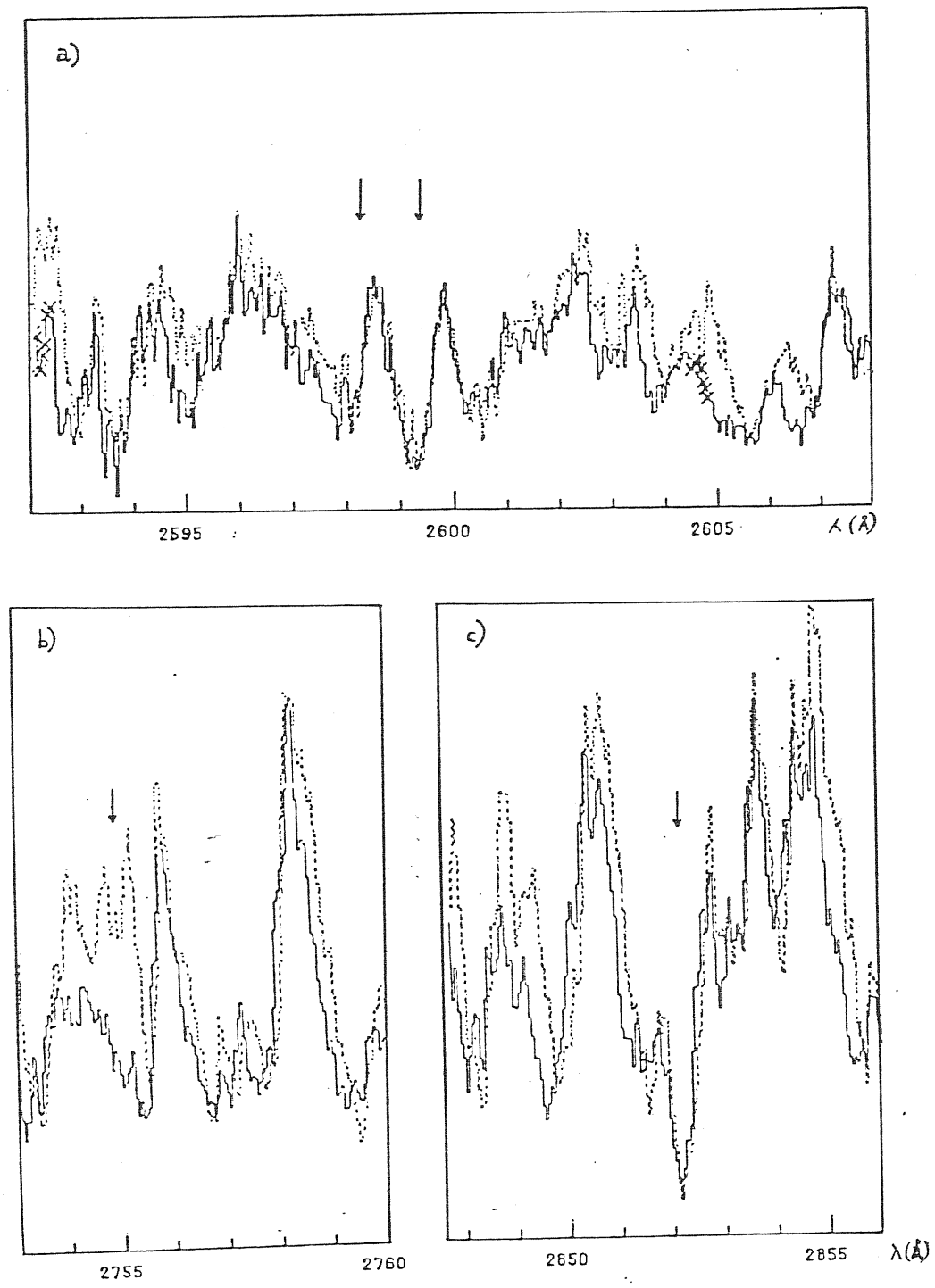

Fig. III.8) Peculiar UV lines during eclipse, in phases of end ingress (dotted line), and mid totality (solid line). Vertical scale is linear.

a) "Steady lines", with emission : Fe II λ2598, and λ2599 resonance

b) "Shell absorptions", at λ2755 Å.

c) "Steady line", with pure absorption : Mg I λ2852 resonance.

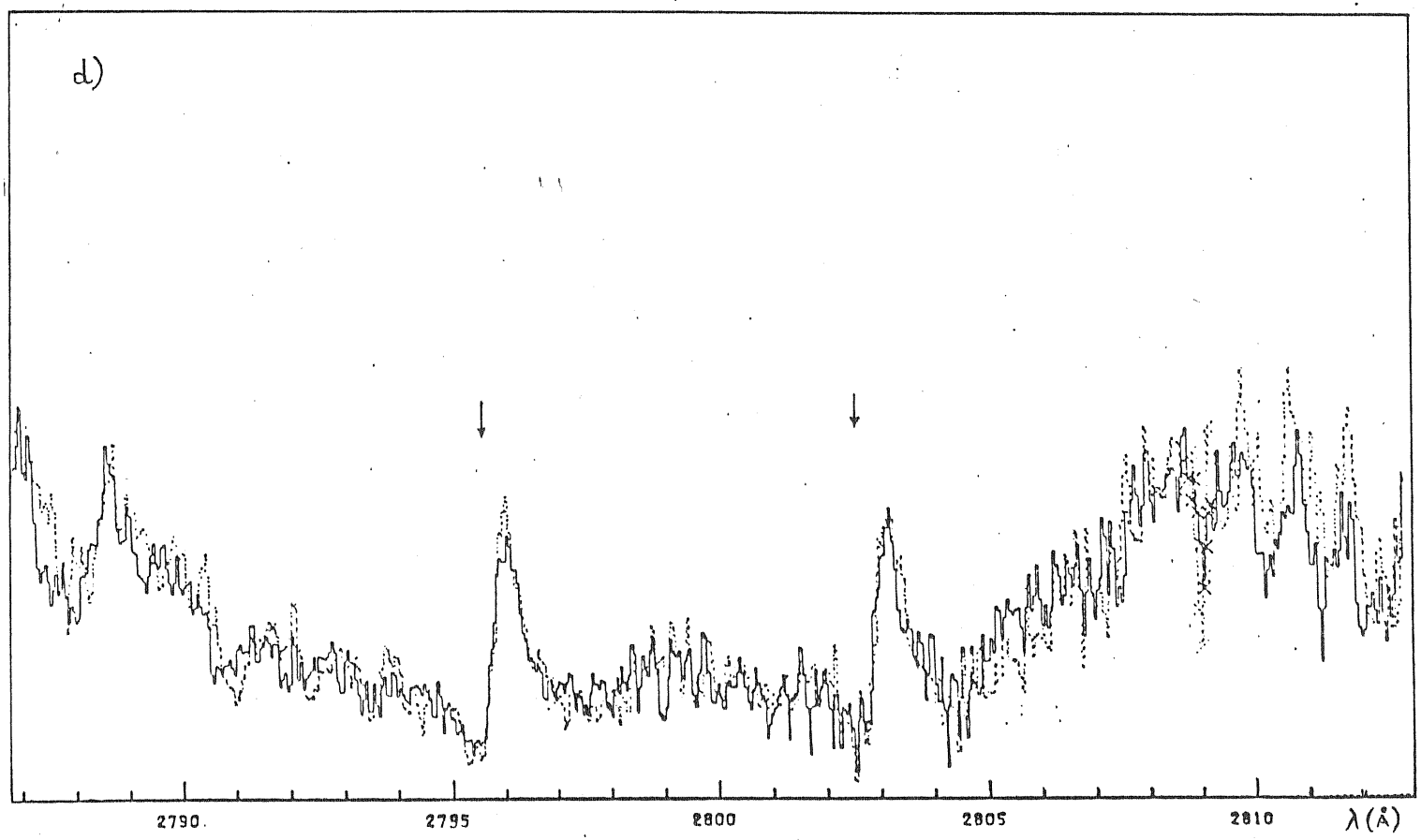

Fig III.8 d) – The Mg II doublet (resonance λ2800): The whole P Cygni-like profile is unaffected, in wavelength, by the eclipse phase (cfr fig III.8 a).

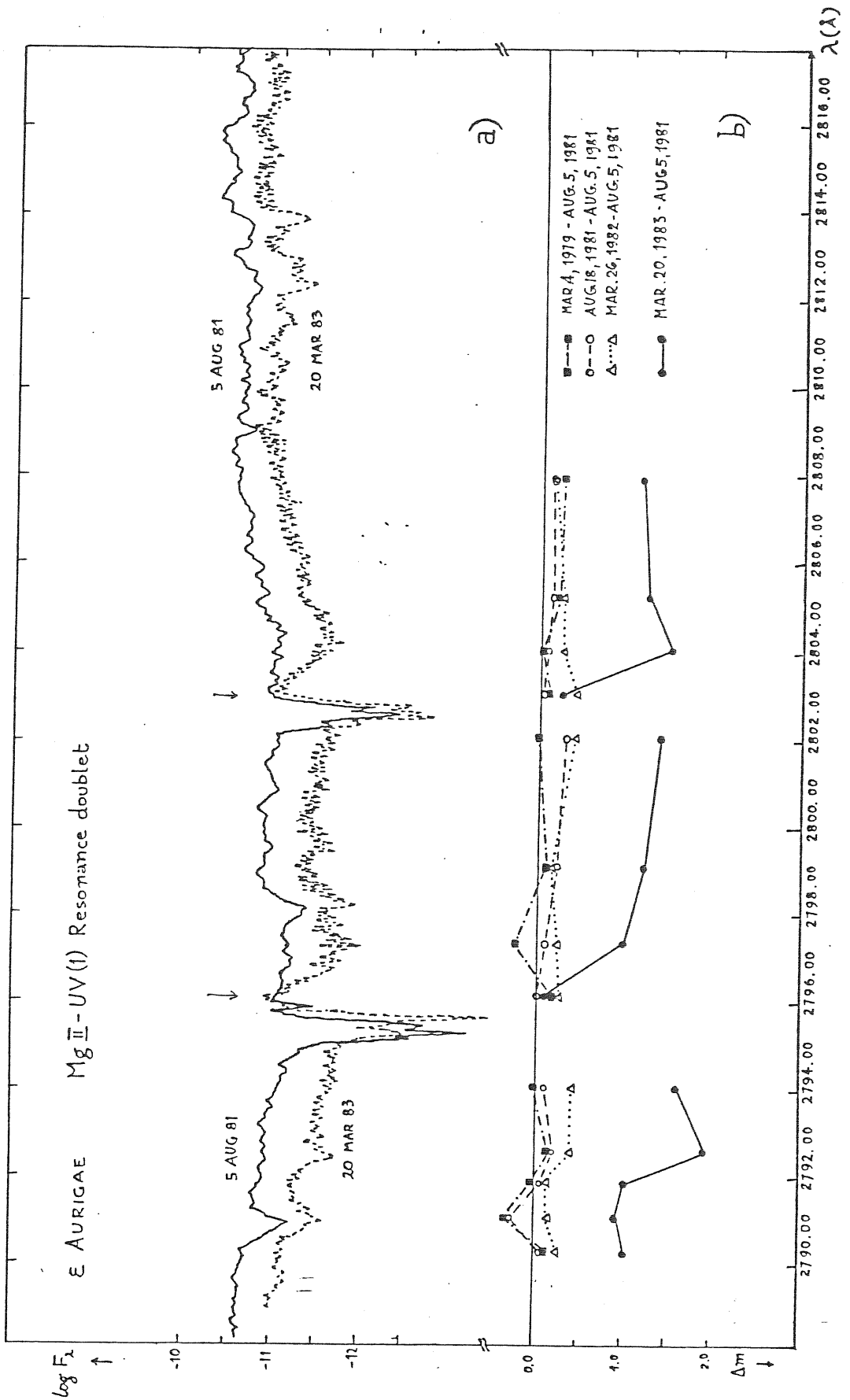

Fig III.9) - The outcoming of the emission component, during eclipse, for Mg II λ 2800.

a) Solid line; out of eclipse; Dashed line, totality. Features not partecipating to the general lowering of the continuum during eclipse, give origin to P Cygni-like profiles (arrows).

b) Continuum variability; Δm is given with respect to a comparison out-of-eclipe spectrum (Aug 5, 1981). Solid line, totality; broken lines; out of eclipse.

ed by Chapman et al.(1983). More generally, we find that the presence of an emission component is an extensive property of the stronger lines of FeII UV multiplets, especially (6), (62) and (63); the effect is more evident in the strongest lines, such as FeII λ 2598 and λ 2599 resonance (fig. III.8a).(*)

3) "Shell absorptions",which display an exceptional enhancement during totality (fig. III.8b). Their identification, together with the complete classification of eclipse-dependent and independent features, is a work still in progress.

c) Interpretation. In order to give an explanation to these observed phenomena, a key should be the following foundamental coincidence: all the lines, displaying the eclipse-independent behaviour (b) described at points 1) and 2), were classified as "peculiar" out of eclipse, by Castelli et al. (1982). The reason was that the profile didn't fit the synthetic spectrum, because of variable blue shift or because a possible emission contribution, which were attributed to an F star's expanding envelope (section II.4b).

On the other hand, there is also a group of lines, classified "peculiar" out of eclipse and hence "F envelope lines", which show a normal phase dependance (a) in eclipse. This group represents about 50% of "F envelope lines"; among them we find for instance TiII (5), CrII (5) (6),

---

(*) The outcoming of the emission feature can be recognized,comparing eclipsed and uneclipsed spectra (Appendix B , fig B1).

and MnII (5) UV multiplets.

Hence, the simplest interpretation that could be suggested is the following: "F envelope lines" behave as normal (a) or peculiar (b) with respect to the eclipse, according to where is their formation region, respectively internal or external to the secondary's orbit. But, in principle, behaviour (a) or (b) of "F envelope lines" could also be determined, respectively, by the presence or absence of a shell component in those lines. Since also more complex configurations are possible, a detailed spectral analysis is required, also on the basis of future observations, during the egress phase.

Chapter IV

THE BEHAVIOUR OF H-ALPHA DURING INGRESS AND EARLY TOTALITY

This study should be considered as a preliminary output of a more extensive research, based on a program of parallel photometrical and spectroscopical observations, "monitoring" all the phases of the 1982-84 eclipse. The program is carried out by the writer, at the Trieste Observatory for photometry, and at the "Observatoire de Haute Provence" (OHP) in France for spectroscopy; contemporary Trieste-OHP observations are performed with the collaboration of C.Böhm. Results shown in this chapter are very preliminar; they are based on analogic plots of a restricted set of spectra, since extensive work of plate digitization, and computer data processing, is still in progress. The following section IV.1) reproduces the text of the comunication given to the "International Bulletin of Variable Stars" (IBVS), n° 2326.

IV.1) Observations and Results

a) Narrow-band Photometry. At the Trieste Observatory, εAur has been observed with a photoelectric photometer equipped with two interferometric filters of 30 Å half-width. One of them is centered on the H_α 6653 Å line of neutral hydrogen, the other being centered on a nearby continuum region, say 6620 Å. The comparison star, λAur, is a solar type dwarf (GØV). Table IV .1) shows the magnitude of the line, minus the magnitude of the red continuum, together with the differences between ε and the comparison. Every value is an average of several particular measurements, made with a time resolution of, typically, 1 minute.

The first fact that these measurements seem to reveal is an evident decrease in the relative flux emitted by the line. It may be important to note that this drop happened only well after the beginning of totality, which probably occurred at the end of last year (Stencel, 1983). Figure IV .1) shows one complete run of observations; since the behaviour was similar on all the other observing nights, this seems exclude the occurrence of systematic short-time-scale variations in the red flux.

b) High-resolution Spectroscopy. In addition, some high-dispersion spectra have been obtained with the 152 cm coudé telescope of the Observatory of Haute Provence. One of the most noticeable variations, in the spectral

Table IV.1)-Photometry

Date	$\Delta m\,(H\alpha - 6620\text{Å})$	$\Delta m_{6620}\,(\varepsilon-\lambda)$
Nov. 19, 1982	- 0.05 ± 0.01	- 1.02 ± 0.01
Jan. 11, 1983	- 0.06 ± 0.02	- 0.98 ± 0.01
Jan. 17, 1983	- 0.04 ± 0.01	- 0.98 ± 0.01
Jan. 23, 1983	- 0.05 ± 0.01	- 0.92 ± 0.01
Mar. 17, 1983	+ 0.13 ± 0.02	- -
Mar. 18, 1983	+ 0.09 ± 0.01	- 0.94 ± 0.01

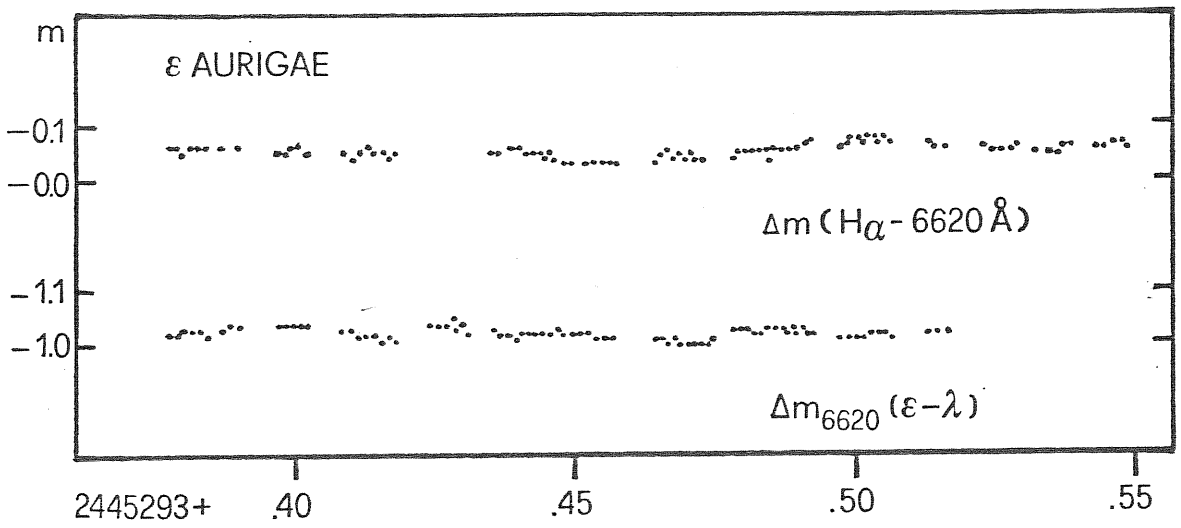

Figure IV.1)-Photoelectric measurements of ε Aurigae during one night, Nov. 19, 1982. The methods used are described in the text.

features, is the change in the profile of the H_α line. In figure IV.2), we have plotted the profiles at various epochs. In particular, we can see that the blueward emission wing seemed to remain unperturbed, while the redward one was gradually reduced until it disappeared during last March. In its place, a corresponding broadening of the absorption towards the red can be noted. This observational evidence explains and confirms the analogous decrease observed photoelectrically in the H_α band (30 Å wide).

A similar phenomenon was detected by Wright and Kushwaha (1957) during the corresponding phase of the 1955-'57 eclipse (fig. II.8), superimposed on strong variations in the blueward emission (occurring at that time on the occasion of the first and second contacts). Since significant variations in the H_α profile were seen also out of eclipse (Castelli, 1977), one is led to view the observed H_α behaviour in terms of a composite phenomenon. An eclipse effect, generated by combined rotations of the supergiant and of the eclipsing body can produce the H_α inverse PCygni-like profile, that we observed in March, before mid totality. Irregular variations, probably due to inhomogeneities, both of the primary shell and of the eclipsing object, may then be superimposed.

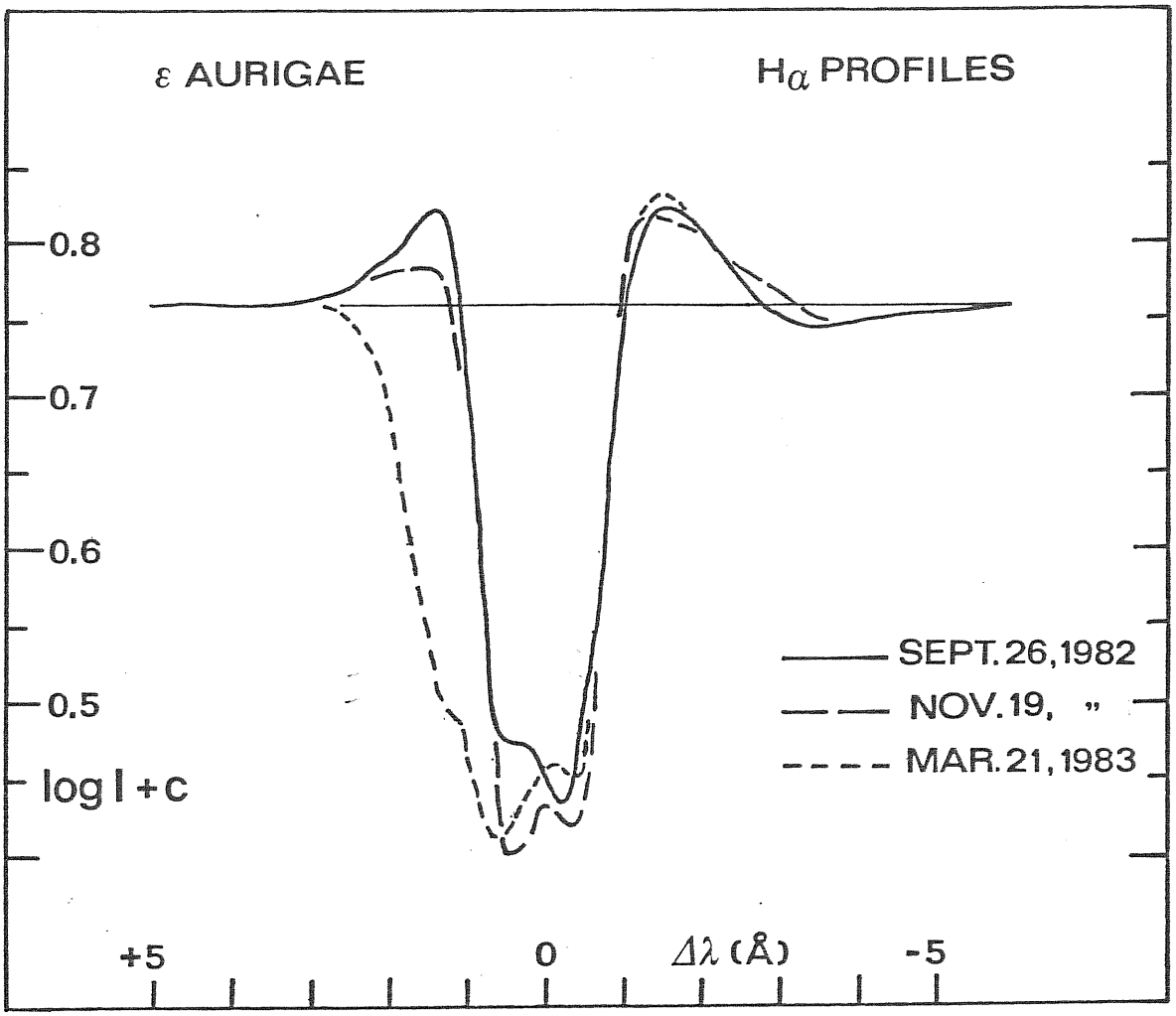

Figure IV.2). Comparison between H-alpha profiles at mid ingress, end ingress, and early totality phases, plotted in logarithmic scale of intensity.

IV.2) Discussion

Let us further examine the effect of the eclipse on H_α profile, with the aid also of Wright and Kushwaha's data concerning past 1955-57 eclipse, and already presented in chapter II.d). In view of the large intrinsic changes in the H_α feature, present also out of eclipse, it is evident that any mechanism proposed to explain the changes observed during eclipse cannot be expected to reproduce these changes exactly.

Anyway, two alternate hypotheses present themselves:
(a) The width of the emission is caused by rotation of the emitting region, and the changes of emission intensity are caused by the passage of an opaque body (the secondary component) in front of this region, occulting regions with different radial velocities at different times.
(b) The width of the emission is caused by turbulent motion in the emitting region, and the intensity changes are caused by the light passing through a rotating absorbing body (the outer layers of the secondary component), which produces a strong H_α absorption line changing in position as the line of sight passes through regions with different radial velocities. A simple consideration of the geometry of the system, indicates that hypothesis (a) requires the emitting region to be rotating in a retrograde direction, which is hardly admissible; hence one favours hypothesis (b), which is also consistent with the explanation given for the metallic shell spectrum in II.4c).

It should further be noted, that the eclipse of the emission component appears to begin some months before the eclipse of the star, and to finish some months after it; this can be seen in fig. II.8), taking into account that first and last contacts occurred on 1955 July 6, and on 1955 May 6 respectively (Tab. II.2). Hence the H_α emission must be produced in some region between the F star and the secondary component, and it seems reasonable to identify this zone with the critical region of the inner Lagrangian Point.

Moreover the broad absorption feature, which appears at H_α during totality (fig. IV.2), presumably originates in the outer regions of the secondary component, and not in the region responsible for the continuous opacity; in fact, the depth of the eclipse is approximately constant, whereas the H_α absorption changes greatly during minimum light. The great breadth of the absorption line seems to be caused more probably by turbulent motion, than by Stark broadening, since Stark broadening would require a high density in the secondary component, of the same order of magnitude as the density found in the atmosphere of the F star. Turbulent broadening instead demands high turbulent velocities of the order of 300 km/sec. in the outer regions of the secondary component, and a similar situation is already known to exist in the shell stars.

Chapter V

RADIAL VELOCITIES

DURING INGRESS PHASES

This is a preliminary report, concerning unpublished material, actually under processing at Trieste Observatory, by the writer and by C.Böhm.

V.1) The Method

Among the rather large series of optical spectra concerning ε Aur, and now stored for processing at the Trieste Observatory, a representative sample has been selected; these spectra were taken with the Coudè large spectrograph, at 152 cm telescope of the "Observatoire de Haute Provence" (OHP), getting high-dispersion plates (7 Å mm^{-1}). Upon this sample, a limited program of radial velocity measurements has been carried out, in order to obtain some preliminary indications about Doppler shifts of lines, during the first phases of the eclipse.

The spectra, which have been studied, are listed in Table V.1); they cover the spectral zone from 3800 to 5000 Å. Since the plates were obtained under the same instrumental conditions, and with the same emulsion (IIaO baked), our sample can be considered homogeneous. The period analyzed starts with the late pre-eclipse phase, and stops short before the 2nd contact.

Table V.1) - Spectra analyzed with the Abbe comparator

Spectrum	Date	Observer (s)
GC 1231	16.3.1981	Ramella, Stalio
GB 7313	31.7.1982	Boehm, Franco
GC 1354	26.9.1982	Boehm, Ferluga, Vladilo
GC 1357	30.9.1982	"
GC 1358	18.11.1982	Ferluga
GC 1362	20.11.1982	"

The instrument which has been used for these measurements is an Abbe comparator, electronically assisted, both for visualizing densitometric line profiles and for reading the reference micrometric scale. Although the measuring procedure remains the classic one, by these means results are considerably less influenced by the operator's subjective perception; the system accuracy can be considered of about $\pm 2\mu$, that is well below the photographic resolution limits.

Measurements are based on readings of the micrometric scale, in correspondence to visually identified character-

istic points of the stellar spectrum, and of the comparison lines. Data are then processed by a computer program, performing the following chain of operations.

i) Construction of an n-order polynomial, approximating the real instrumental dispersion function, on the basis of the readings of the comparison spectrum.

ii) Determination of the observed wavelengths, corresponding to the identified points of the spectrum.

iii) Comparison with a set of laboratory wavelengths, corresponding to identified spectral lines.

iv) Computation of radial velocities, taking into account the eliocentric correction.

V.2) Results

From a first examination of the measured radial velocities, one finds immediately that, in general, they don't agree with the (small) values predicted by the primary's radial velocity curve (Morris, 1963) for the observed early-eclipse phases. Figure V.1) shows some indicative results for the end-ingress phase: values of v_{rad} are found to be spread in an interval (vertical scale in figure), about from 0 km/sec to +30 km/sec toward the red, while the orbital expected value should be near to the baricentric velocity $v_o = -1.4$ km/sec. Taking into account the spectral be-

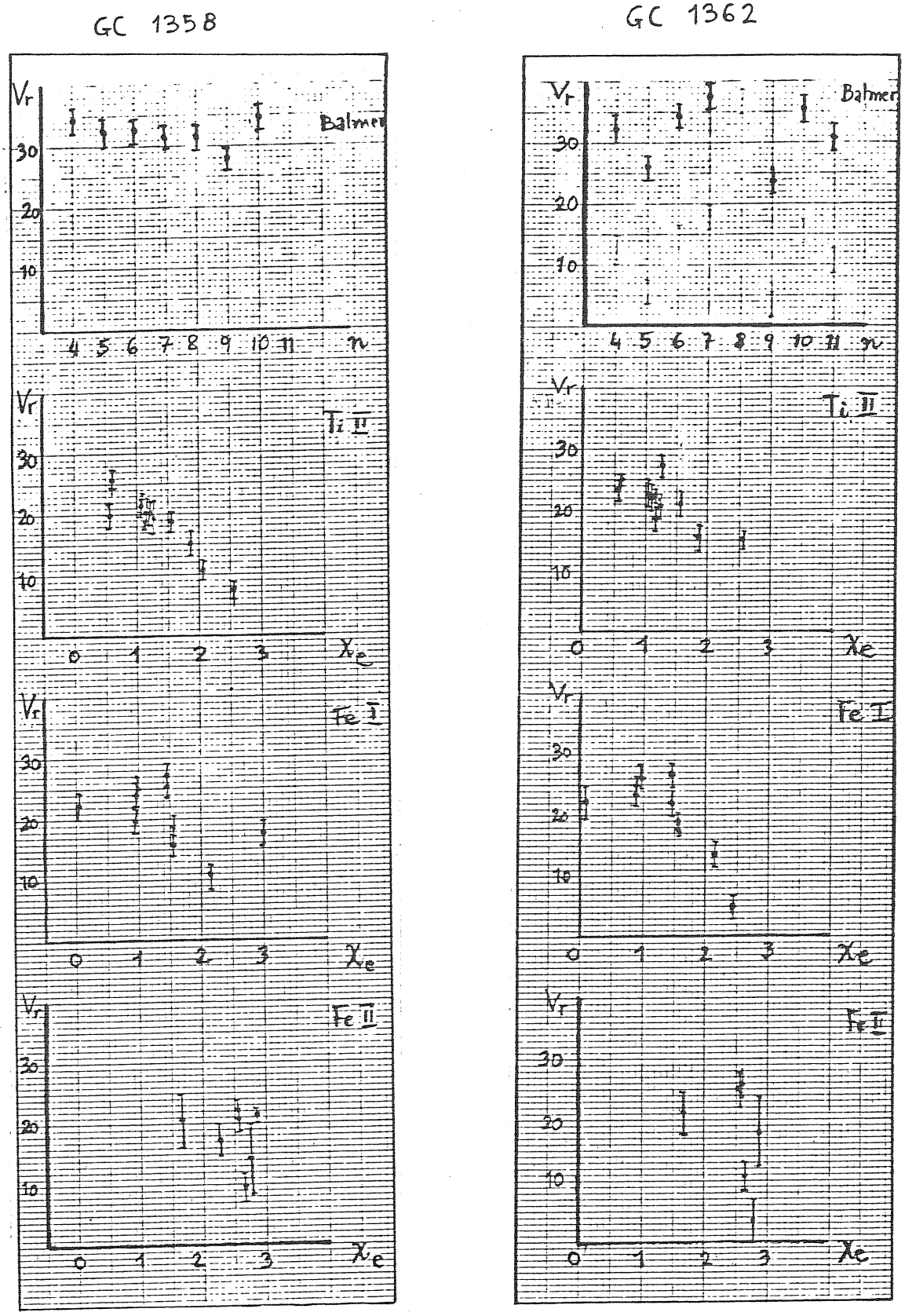

Fig V.1) – Radial velocities at end ingress are plotted (V_r in km/sec), in function of the excitation potential (χ_e, in eV) of the lower level of the transition; in case of Balmer lines, progressive nb. is given.

In both spectra GC 1358, 1362 metallic lines (Fe I and Ti II) show a decrement in V_r, which is about proportional to χ_e. Balmer lines on the contrary have always the same, high, V_r.

haviour of the eclipse (section II.4c), one is brought to explain this redward displacement of the line cores during the early eclipse, in therms of shell-spectrum components.

Most of the measured lines (that in total are about 120) are due to metallic elements, in neutral or single-ionized states, which are common in the spectrum of ε Aur. In particular FeI II and TiII are present with a large number of multiplets; this permits to measure radial velocities v_{rad} of those lines, which correspond to transitions starting from different values of the excitation potential χ_e. A closer look to fig. V.1) shows that a relation between v_{rad} and χ_e is well established, in particular for FeI and for TiII, in terms of a decrement of v_{rad} for increasing χ_e.

The other metallic lines (AlI, MgI, YI, SrII, VaII, BaII, CrII, NiII) are situated at intermediate velocities; a remarkable exception is the one of MgII ($\chi_e > 8$ eV), having a radial velocity consistent with the orbital (baricentric) one. Lines of the Balmer series (which often are not easy to be measured) do not show any clear dependance on progressive number n (Fig V.1, upper graphs), but have always rather high values of v_{rad} (about +30 km/sec). Finally the couple of H and K lines of CaII can be separated at least in two components; one beeing consistent with the orbital (baricentric) value, while the other is displaced for about 40 km/sec.

APPENDIX A)

IUE LOW RESOLUTION OBSERVATIONS

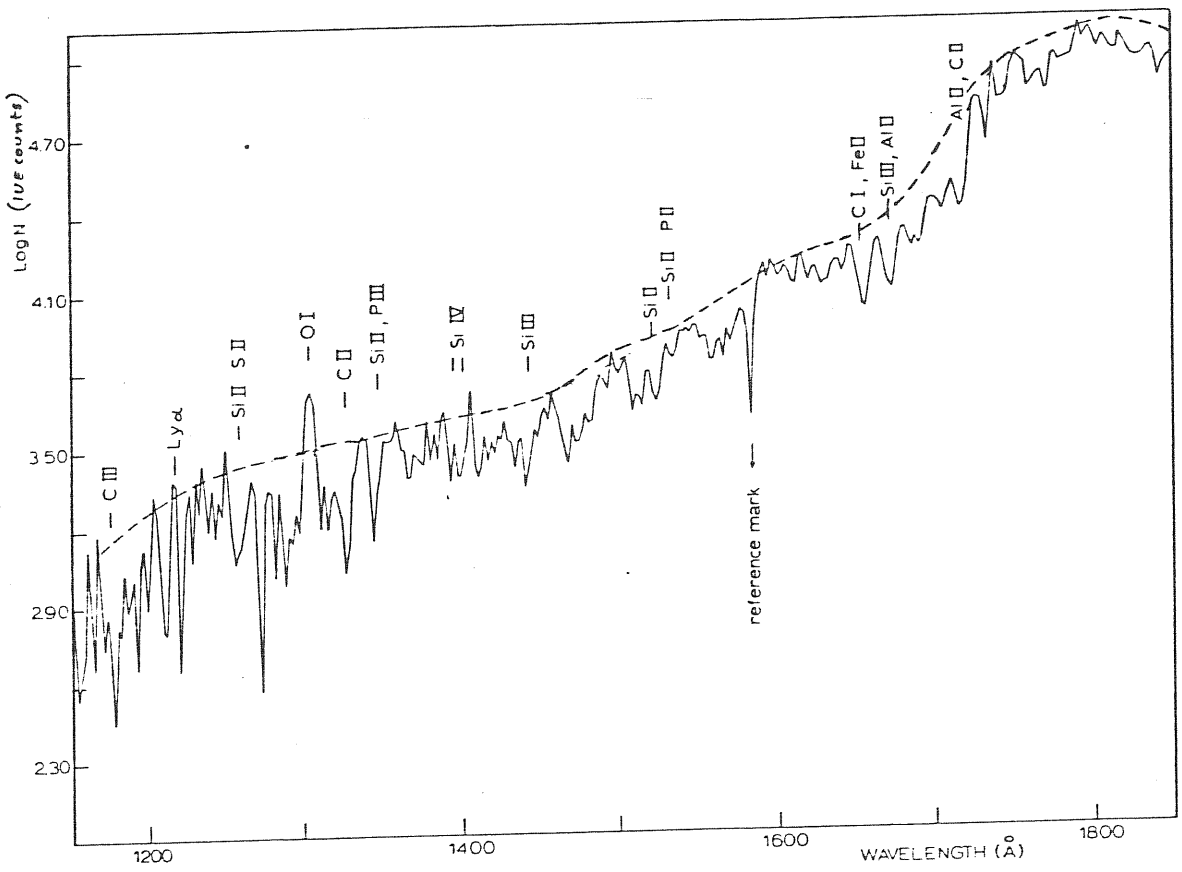

Fig. Aϕ – Comparison spectrum (Hack and Selvelli, 1979).
The adopted continuum is indicated by the dashed line.

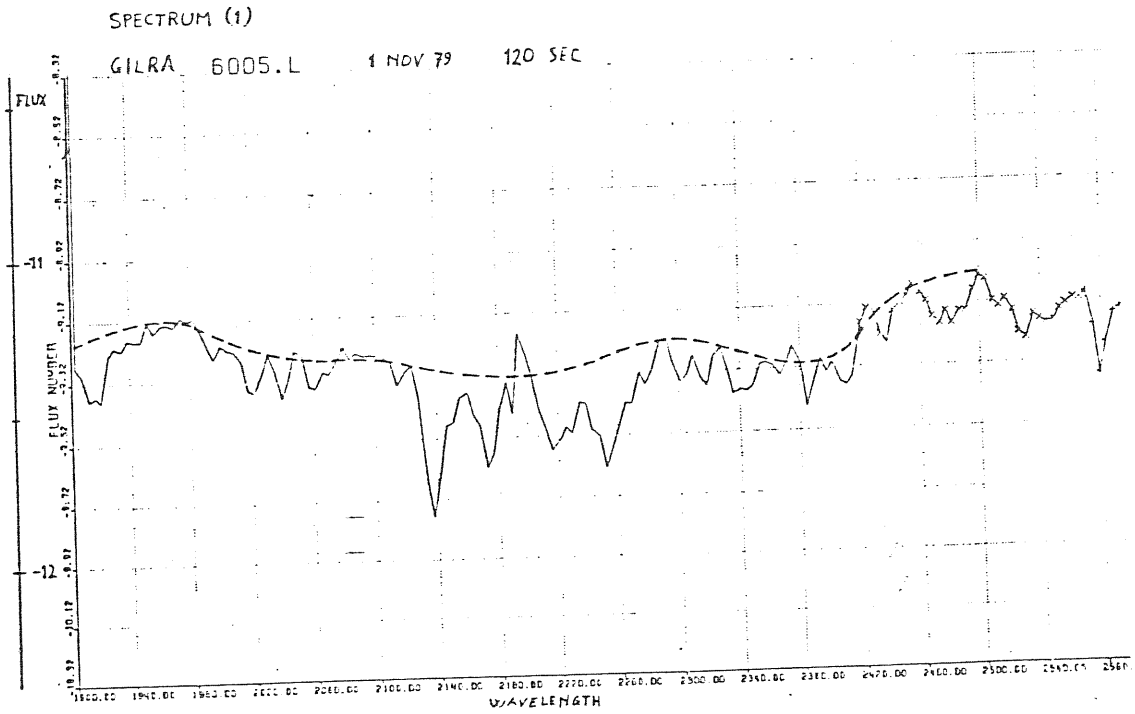

Fig. A1 – Spectrum (1), taken from IUE data bank of VILSPA.

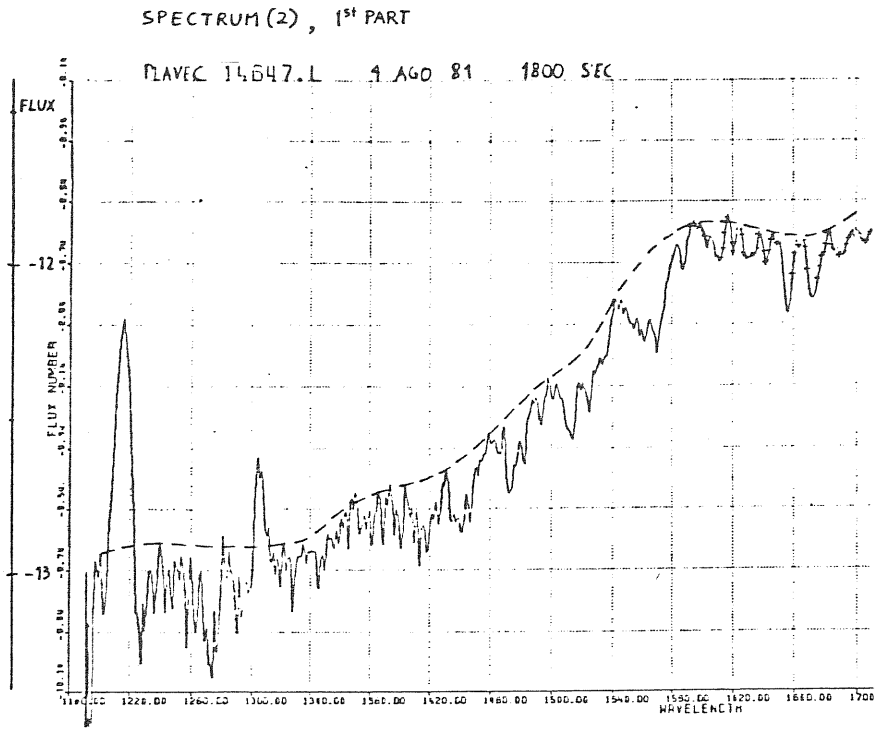

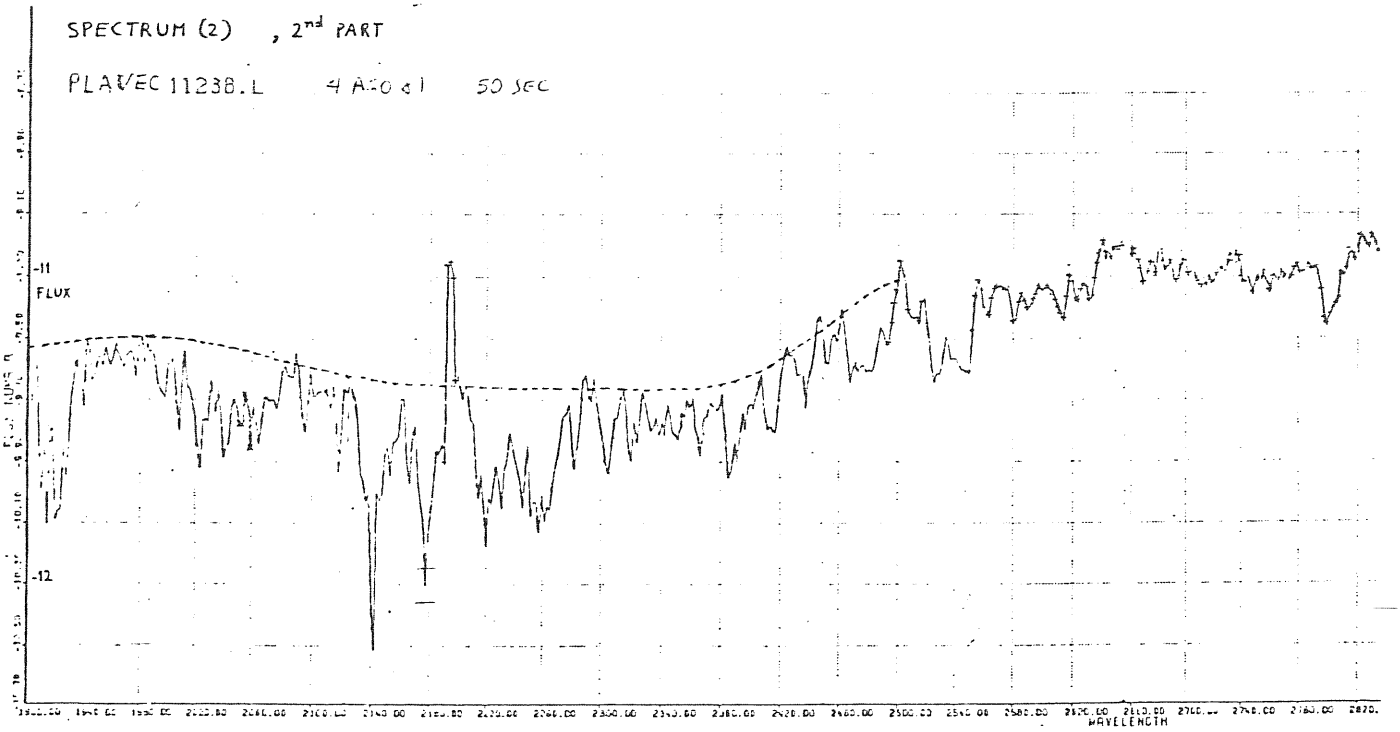

Fig. A2 – Spectrum (2), taken from IUE data bank of VILSPA.

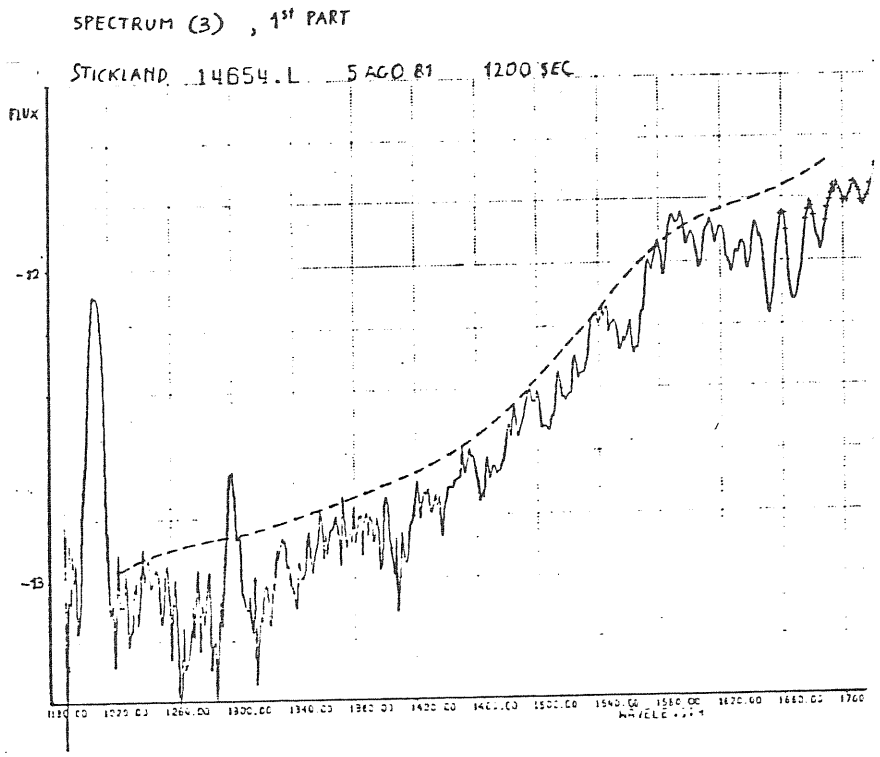

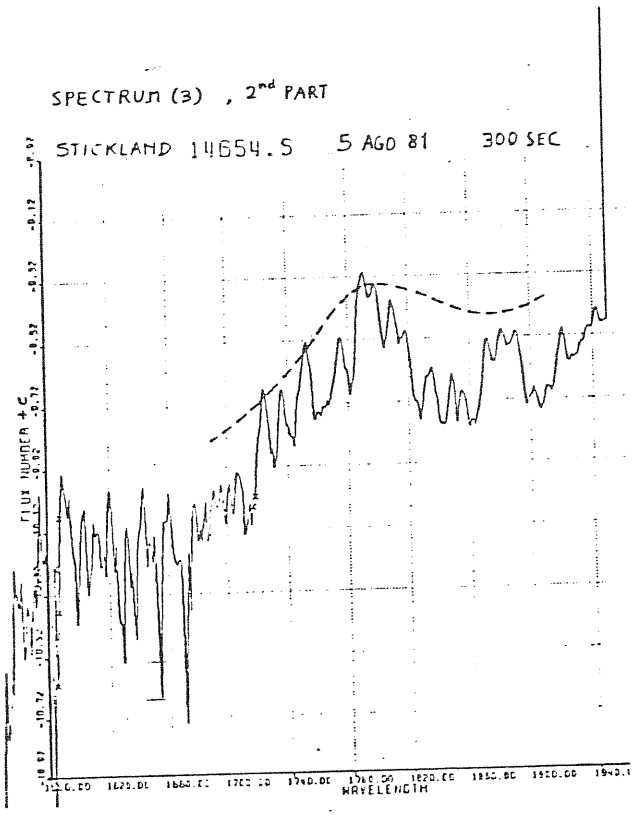

Fig. A3 - Spectrum (3), taken from IUE data bank of VILSPA.

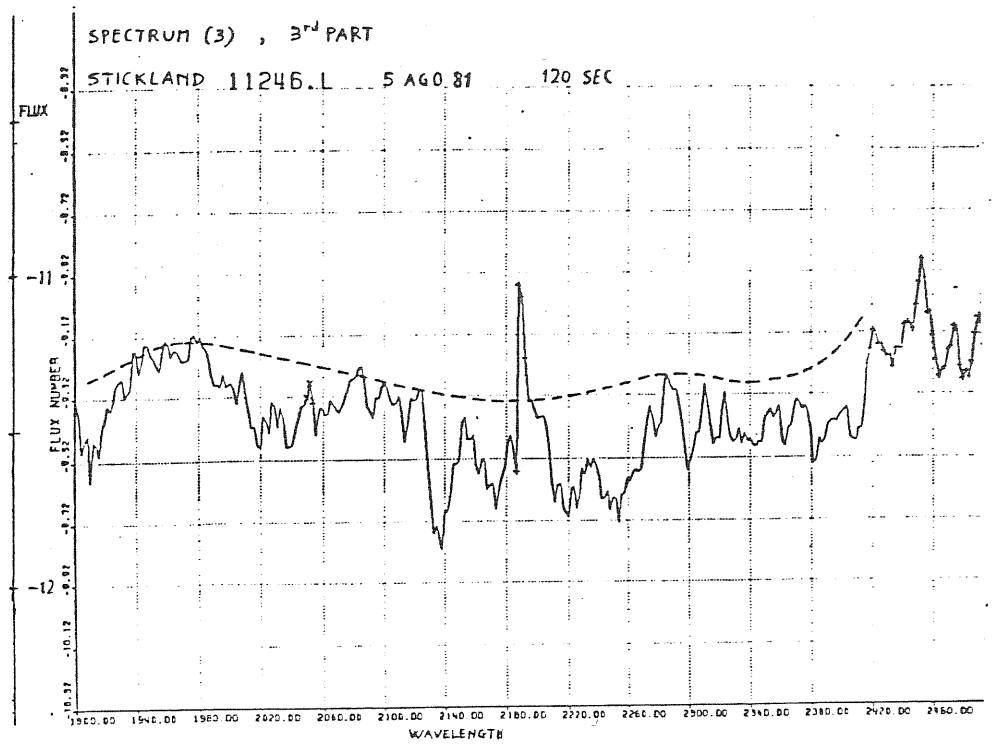

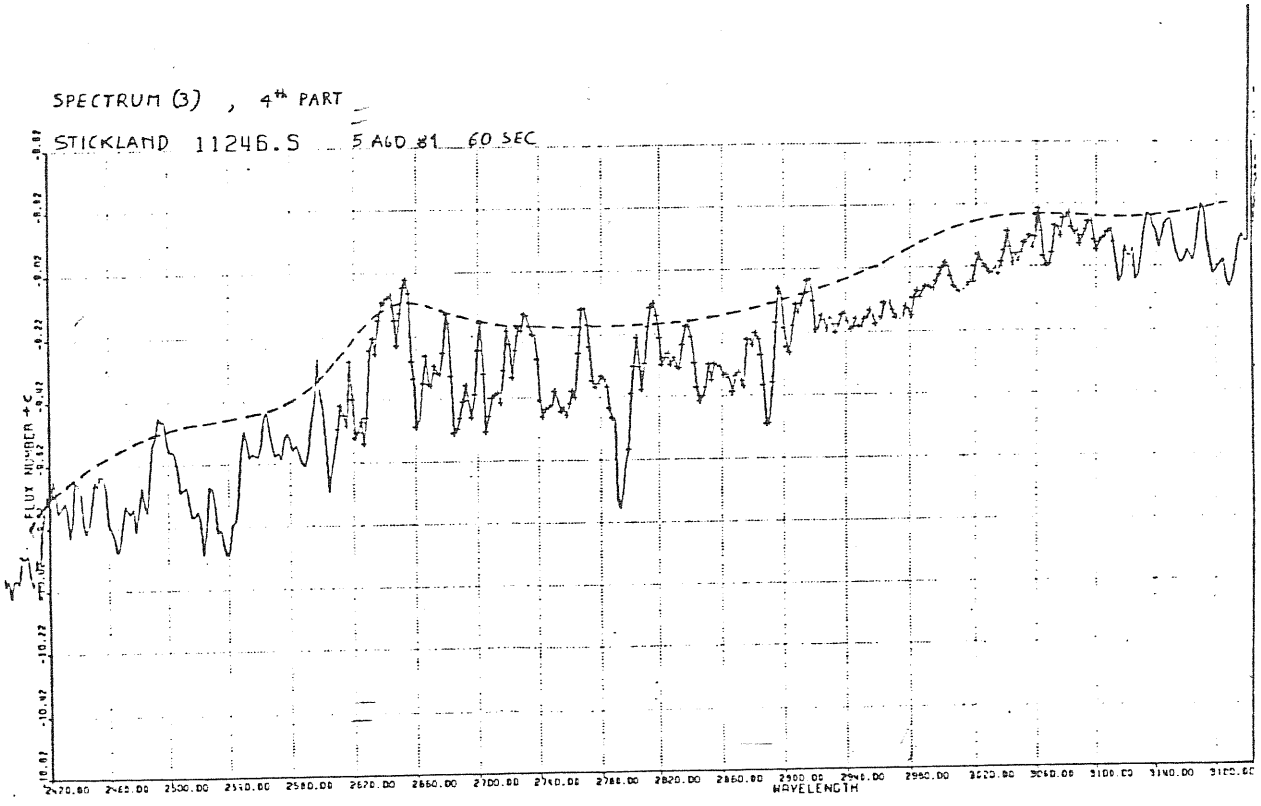

Fig. A3bis – Spectrum (3), taken from IUE data bank of VILSPA (continued)

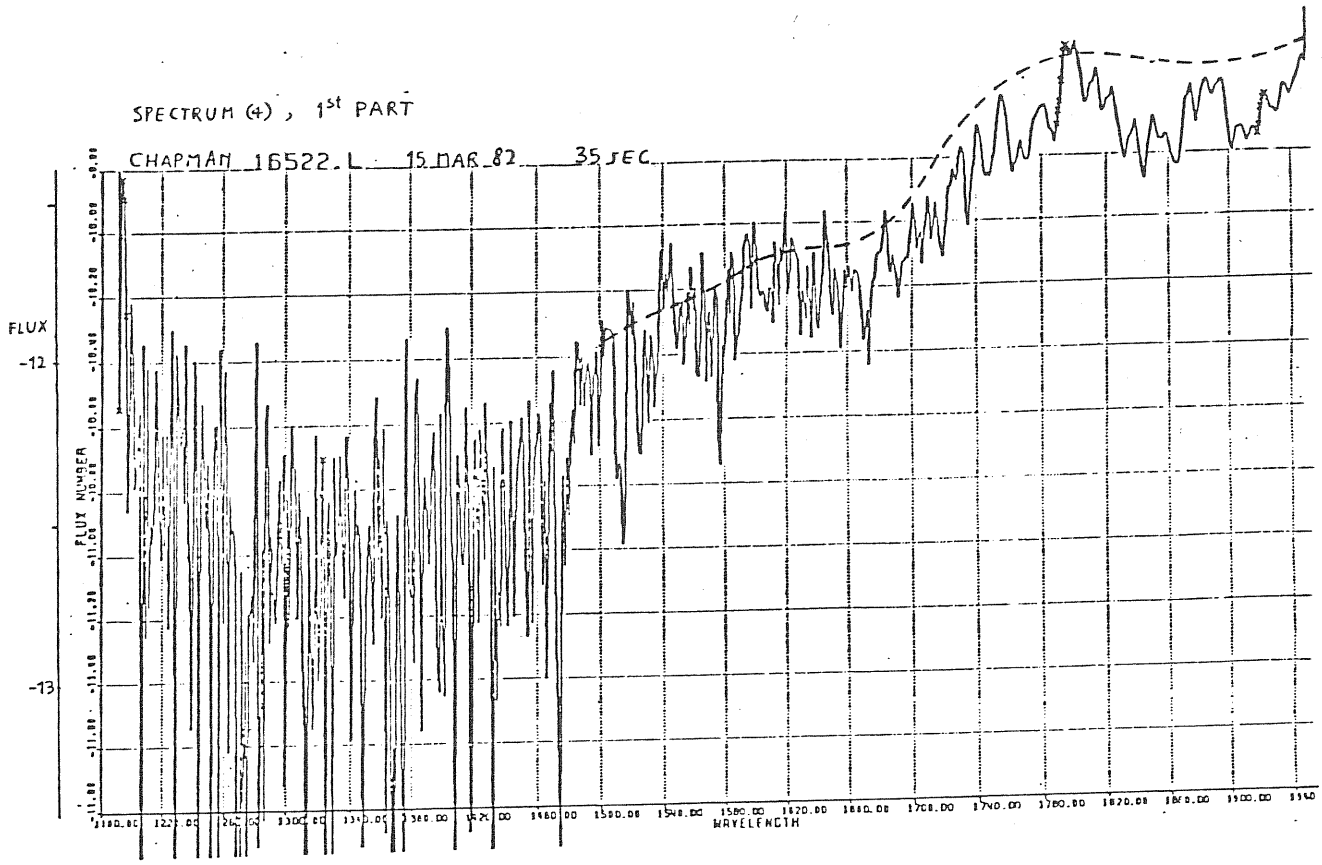

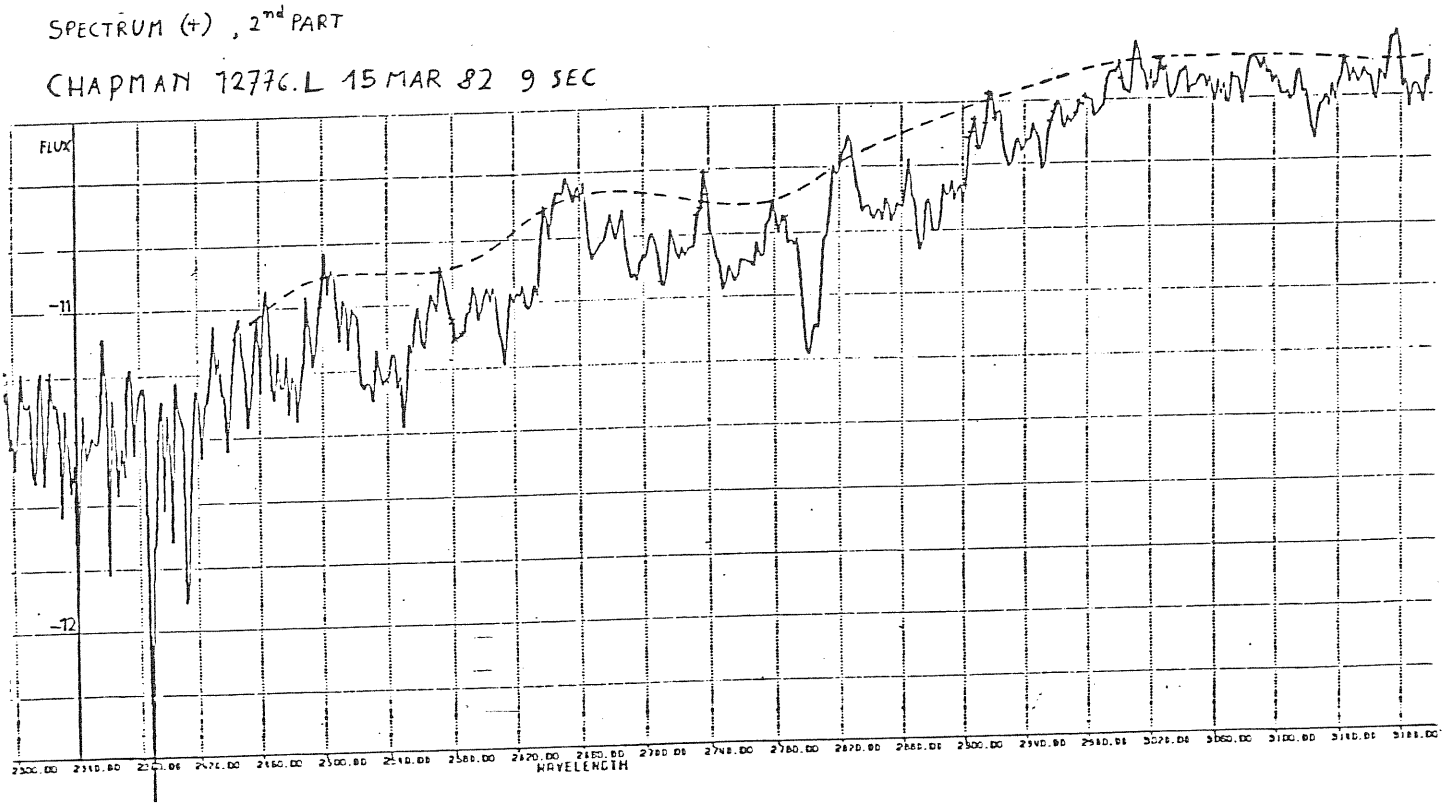

Fig. A4 - Spectrum (4), taken from IUE data bank of VILSPA.

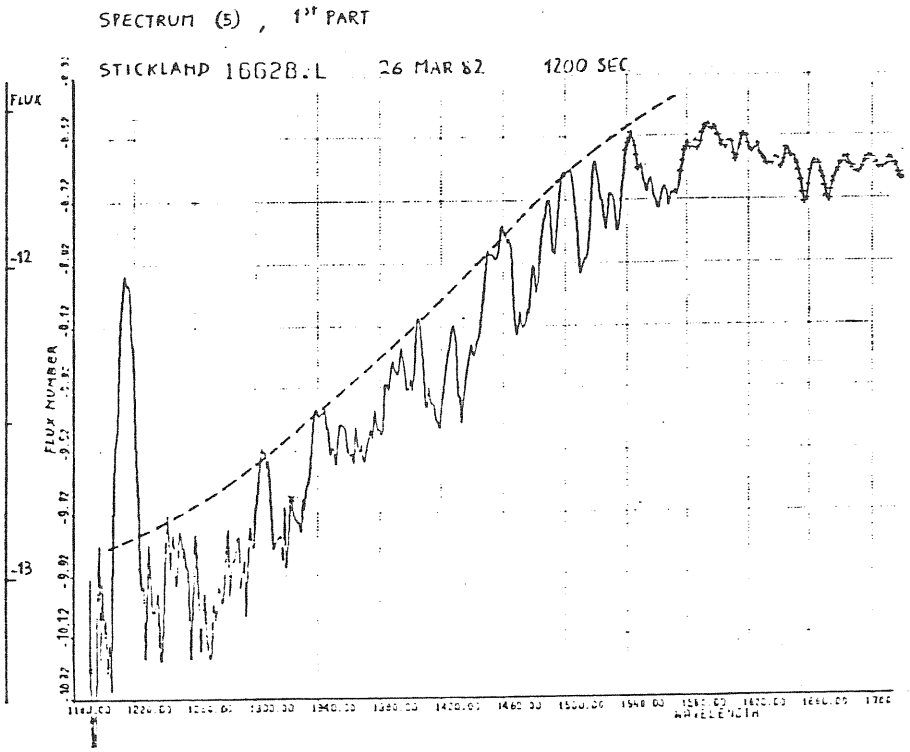

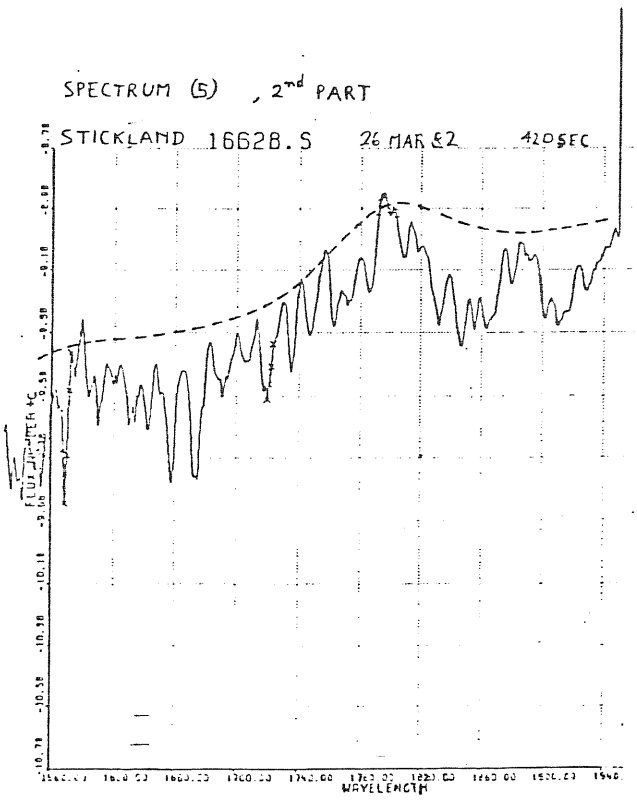

Fig. A5 - Spectrum (5), taken from IUE data bank of VILSPA.

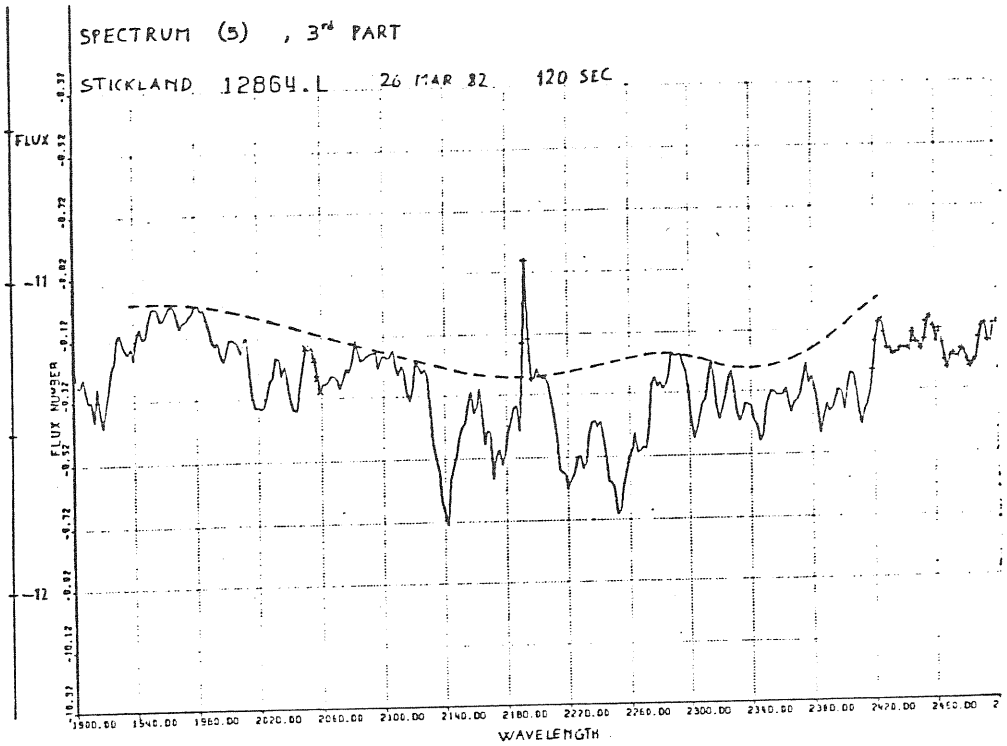

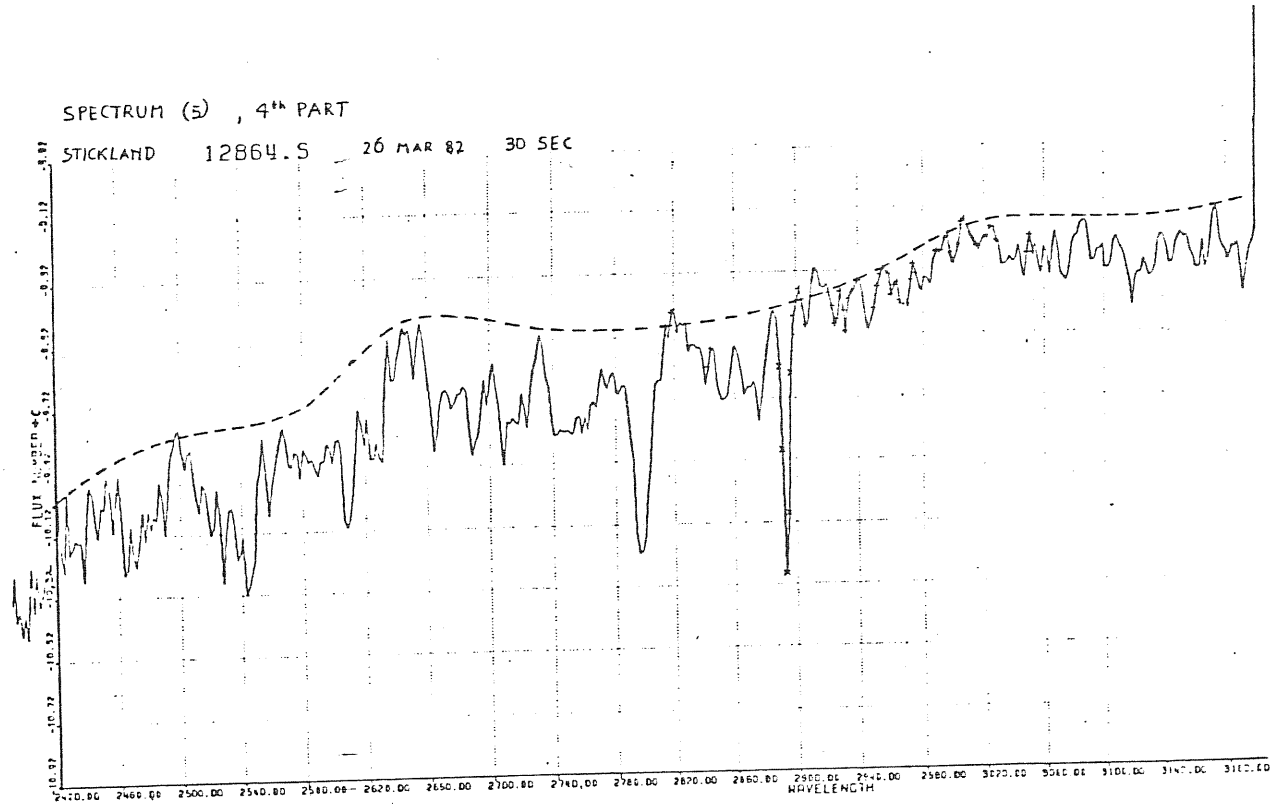

Fig. A5bis – Spectrum (5), taken from IUE data bank of VILSPA (continued)

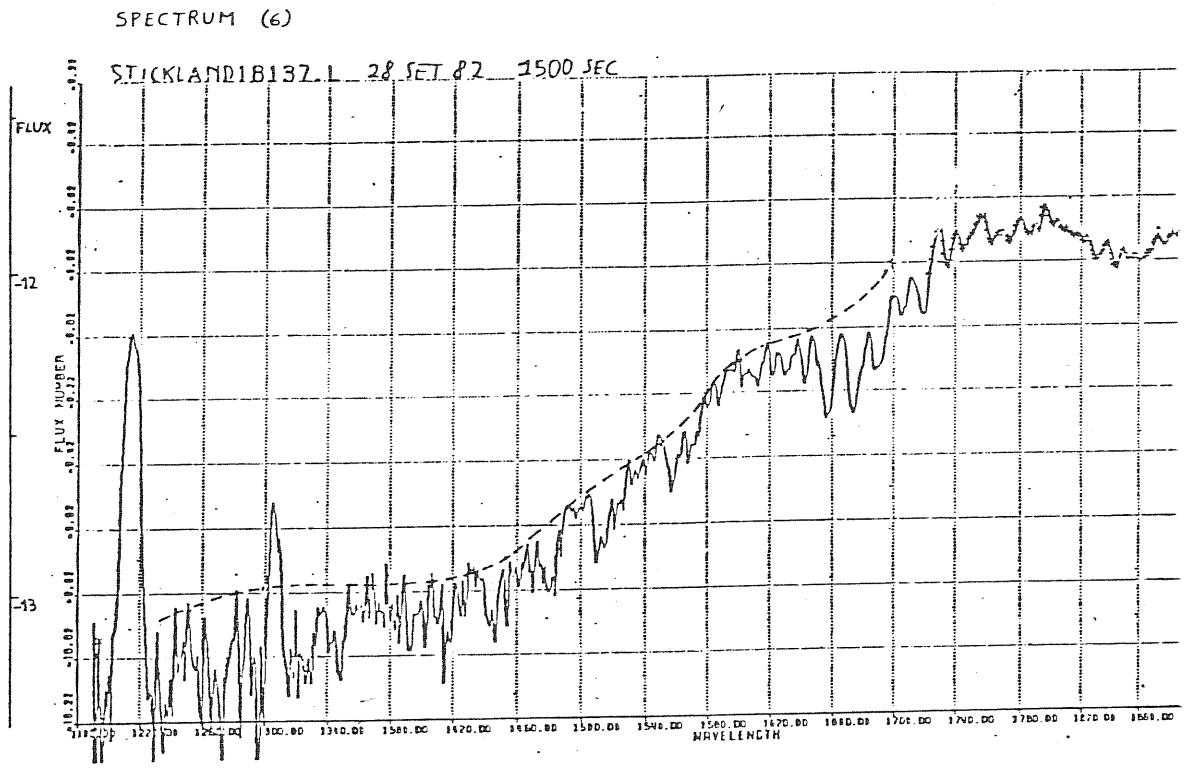

Fig. A6 - Spectrum (6), taken from IUE data bank of VILSPA.

SPECTRUM (7) , 1st PART

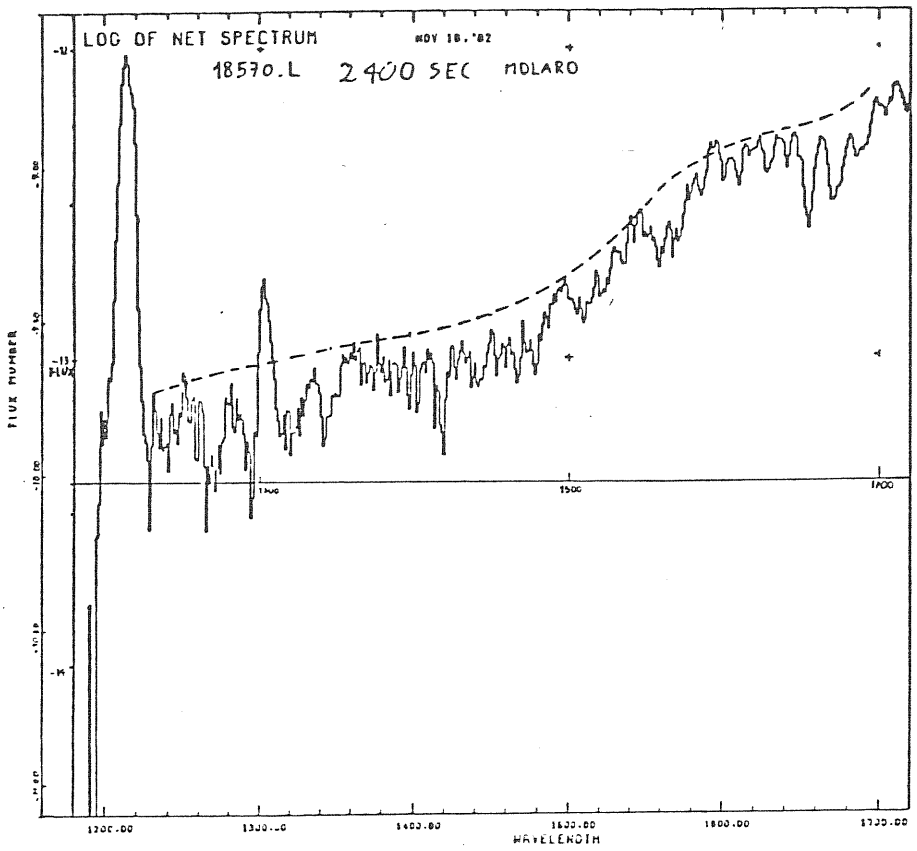

SPECTRUM (7) , 2nd PART

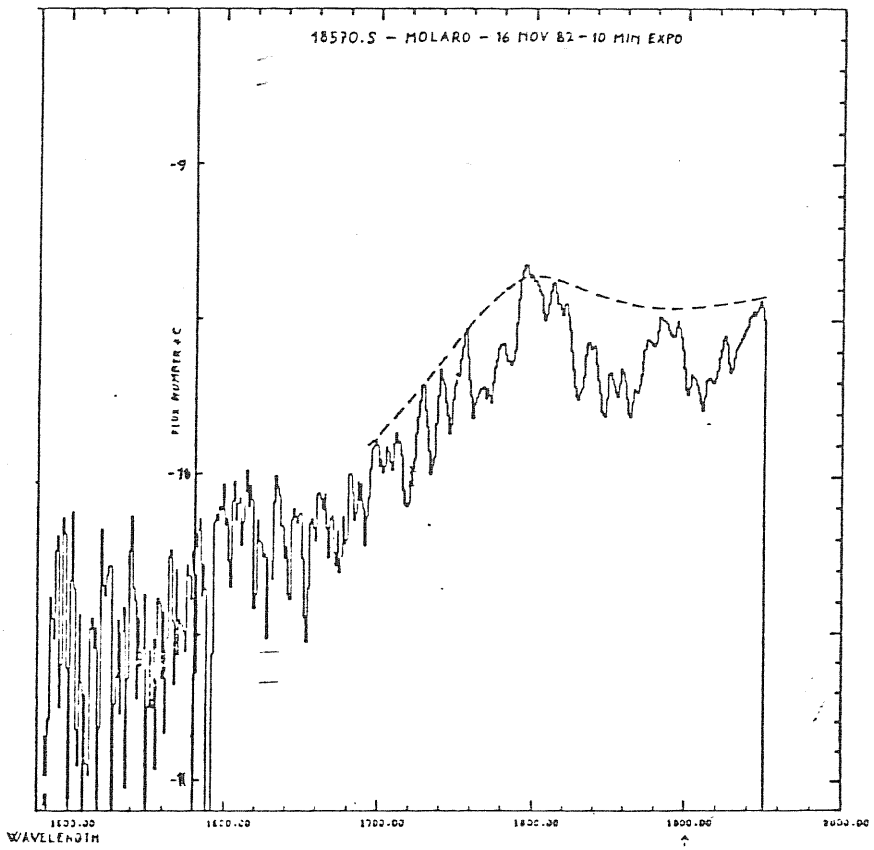

Fig. A7 - Spectrum (7), taken from IUE data archive of OAT.

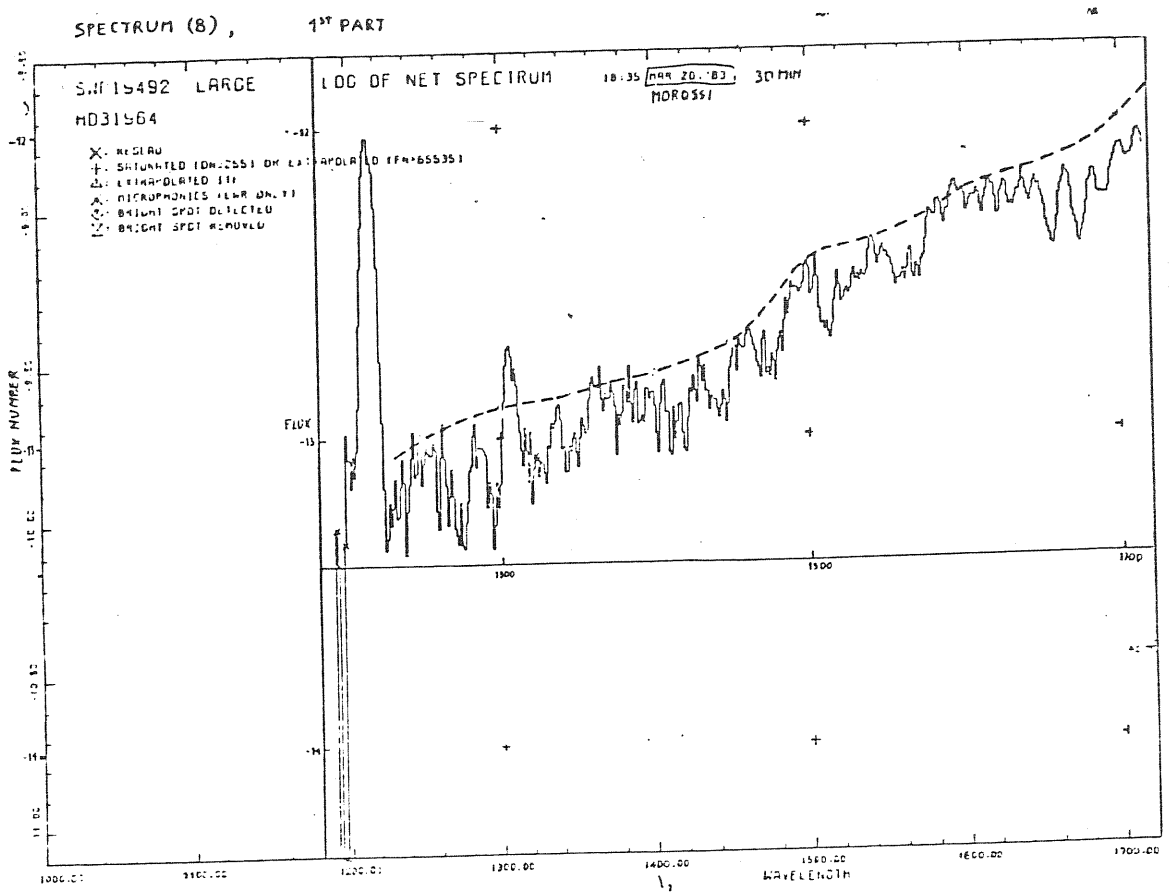

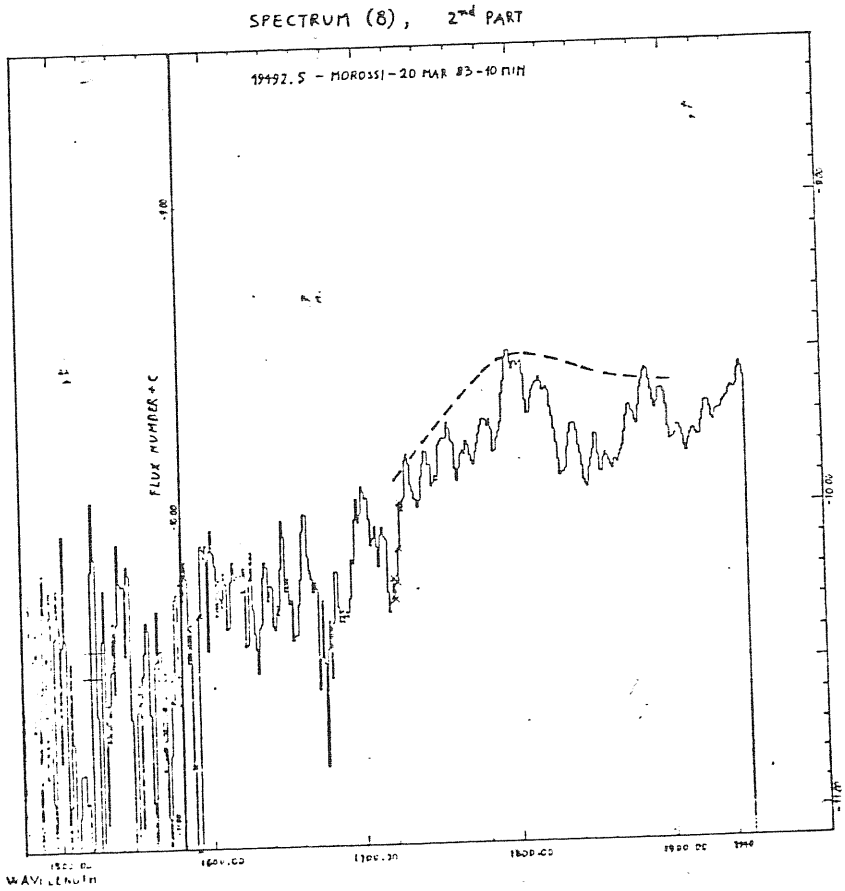

Fig. A8 – Spectrum (8), taken from IUE data archive of OAT.

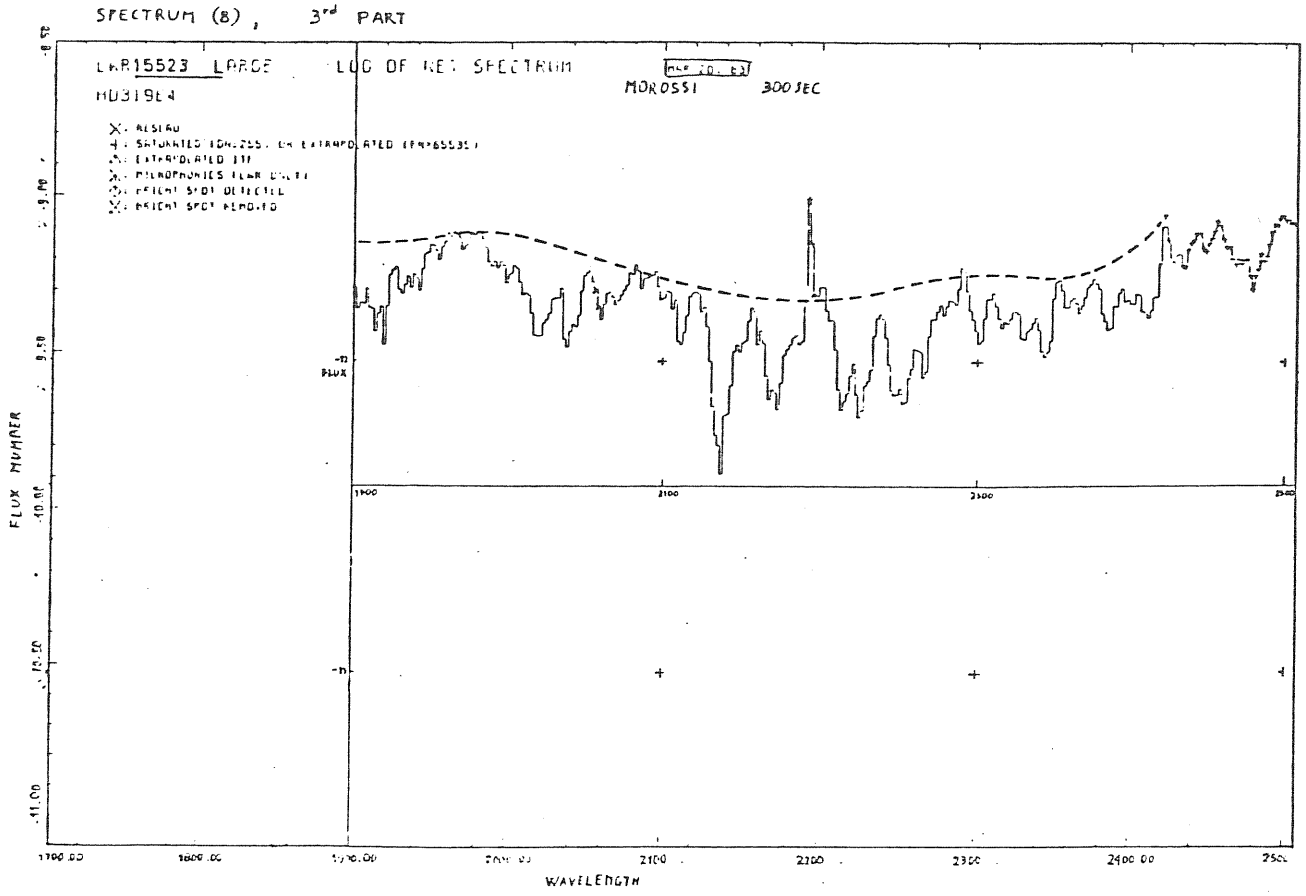

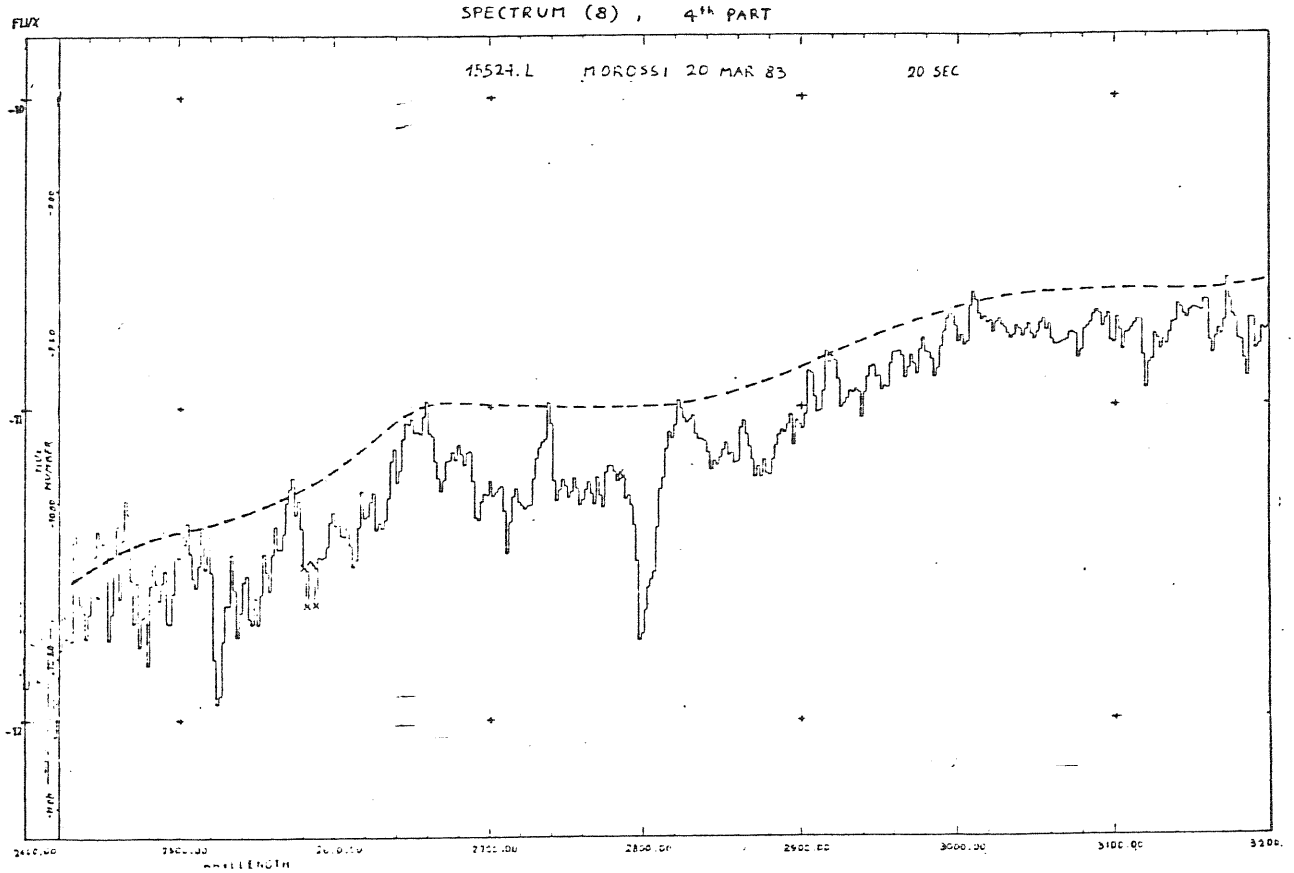

Fig. A8bis – Spectrum (8), taken from IUE data archive of OAT (continued)

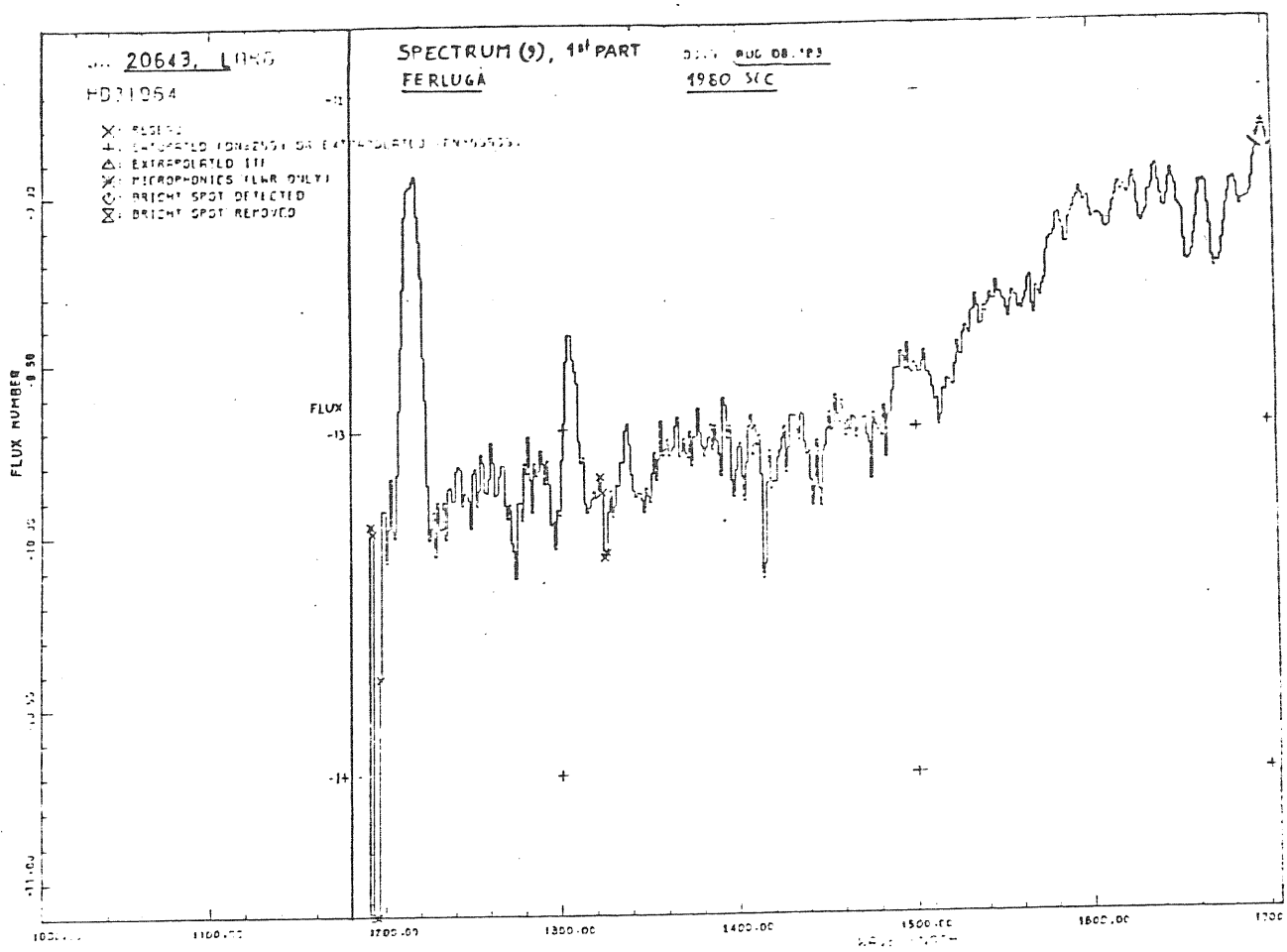

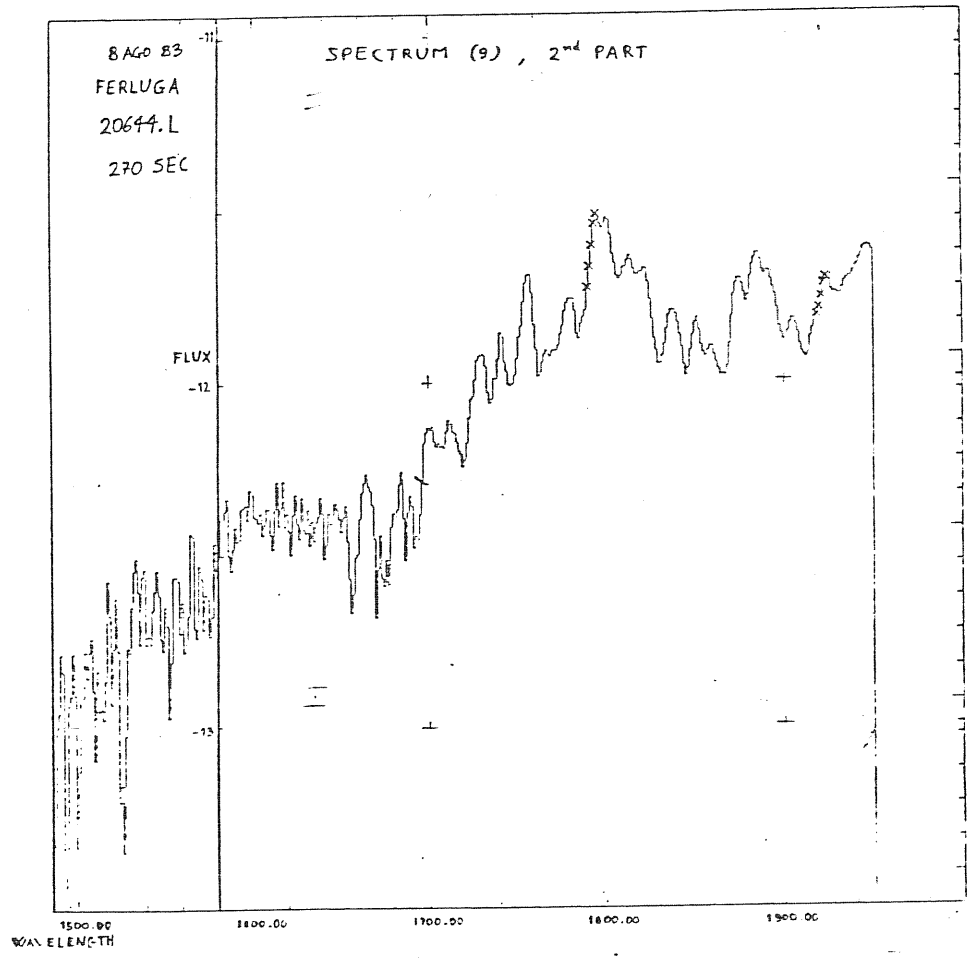

Fig. A9 - Spectrum (9), taken by the author with IUE.

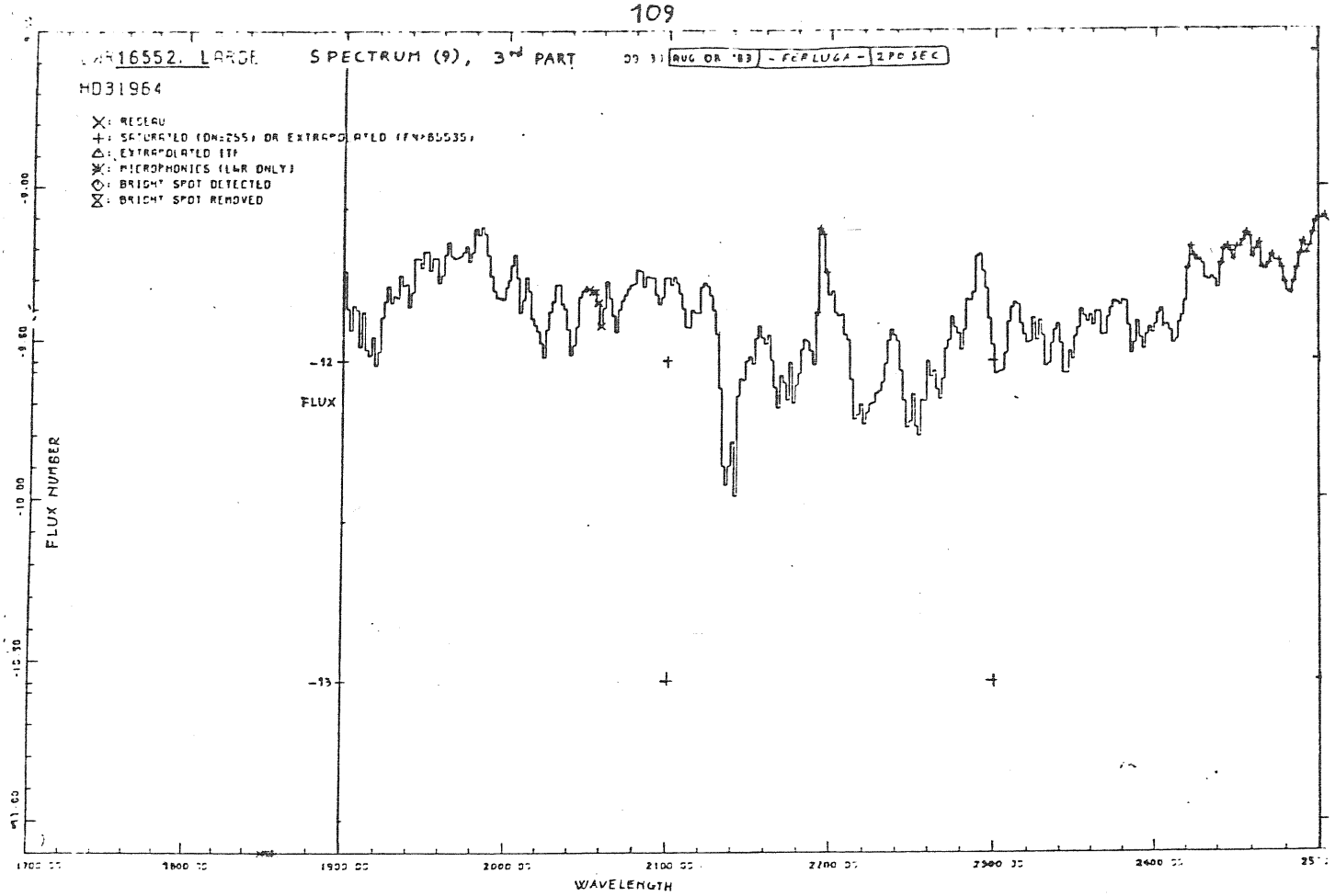

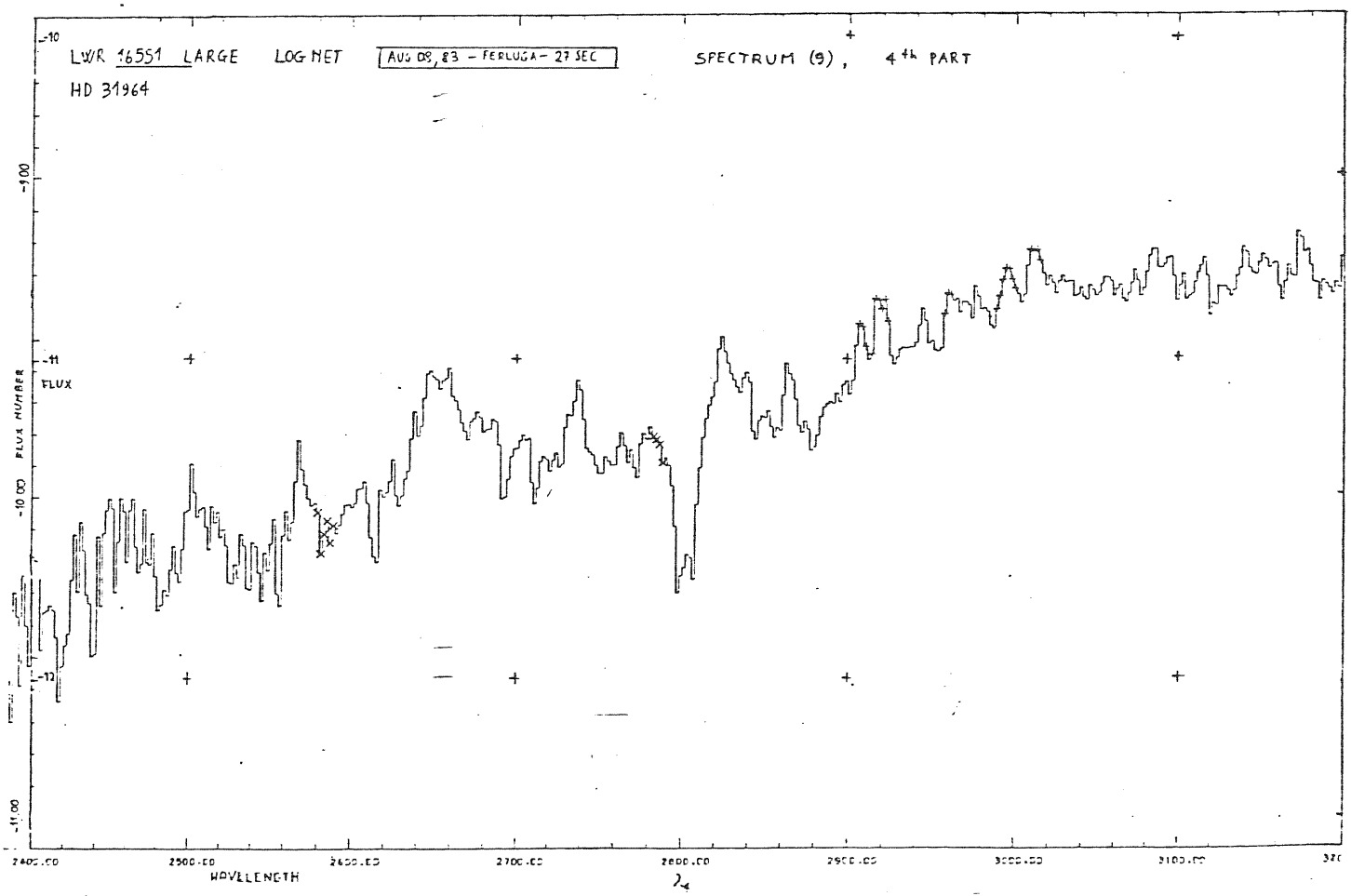

Fig. A9bis – Spectrum (9), taken by the author with IUE

(continued)

APPENDIX B)

THE MID UV SPECTRUM:

PECULIAR LINES IN ECLIPSE

TABLE B1. — *Peculiar lines in the mid-UV spectrum of ε Aurigae.* (Castelli et al., 1982)

element	mult.	λ(Å)	Int.	E.P.	Out-of-eclipse shortward-shift IUE	shortward-shift BUSS	shortward comp. IUE	shortward comp. BUSS
Mg I	1 UV	2852.12	300	0.00	0.2	0.2		
Mg II	1 UV	2795.52	50	0.00	0.3	0.3		
		2802.69	50	0.00	0.3	0.3		
Ti II	5 V	3088.02	75	0.05				0.2
		3078.64	50	0.03				0.2
		3075.22	40	0.01				0.2
		3072.97	40	0.00				0.2
		3072.10	30	0.03				0.2
		3066.22	30	0.01				0.2
		3066.35	20	0.00				0.2
V II	10 UV	2924.02	300	0.39				+
		2924.63	250	0.37				?
		2930.79	150	0.35				?
		2941.48	100	0.33				+
		2950.34	80	0.32				+
		2941.37	200	0.39			?	+
		2952.07	150	0.35				?
		2957.52	100	0.33				?
		2911.05	160	0.35			–	?
	1 V	3093.10	2500	0.39				+
		3110.70	1500	0.35				?
		3125.28	600	0.32				?
		3126.21	150	0.37				+
		3133.32	150	0.33				+
Cr II	5 UV	2835.63	200	1.54			–	+
		2843.24	100	1.52				+
		2849.83	100	1.50	0.2	0.3		
		2855.67	100	1.49				+
		2860.92	85	1.48	0.2			+
		2858.91	75	1.54				?
		2862.57	125	1.52	0.2			+
		2865.10	150	1.50			+	+
		2867.65	100	1.48			?	?
	6 UV	2766.65	150	1.54	–	0.2		
		2762.58	140	1.52		0.2		
		2757.72	80	1.50		0.2		
	5 UV	3132.05	125	2.47				+
Mn II	1 UV	2576.10	400	0.00			+	–
		2593.73	300	0.00	0.2	–		
	5 UV	2949.20	1000	1.17			–	+
		2939.30	800	1.17				+
		2933.05	500	1.17				+
Fe II	1 UV	2599.39	14	0.00	0.2	–		
		2621.67	10	0.12			0.3 em	–
		2598.37	14	0.05			0.3 em	–
		2607.08	13	0.08			? em	–
		2625.66	13	0.05			0.3?em	–
		2631.32	13	0.05				–
		2631.04	13	0.11	0.2	–		
		2628.29	13	0.12			0.3?em	–
	62 UV	2755.73	15	0.98			0.4 em	0.4 em
		2749.32	14	1.04			0.4 em	0.5 em
		2746.49	14	1.07			0.4 em	0.5 em
		2743.19	14	1.09		–	–	
		2716.68	2	0.98		–		–
		2724.88	9	1.04			?	?
		2730.73	11	1.07		0.2		
	63 UV	2739.54	15	0.98	–		–	0.5
		2746.98	14	1.04			0.4 em	0.5 em
		2749.18	13	1.07			? em	? em
		2749.48	12	1.09			? em	? em
		2714.41	13	1.04	0.2	–		
		2727.54	13	1.04	0.2	0.2		
		2736.97	12	1.07			–	0.4
		2768.94	8	1.07			–	?
		2761.81	9	1.09	0.2	0.3?		

Notes: Int = central intensity, E.P. = excitation potential.

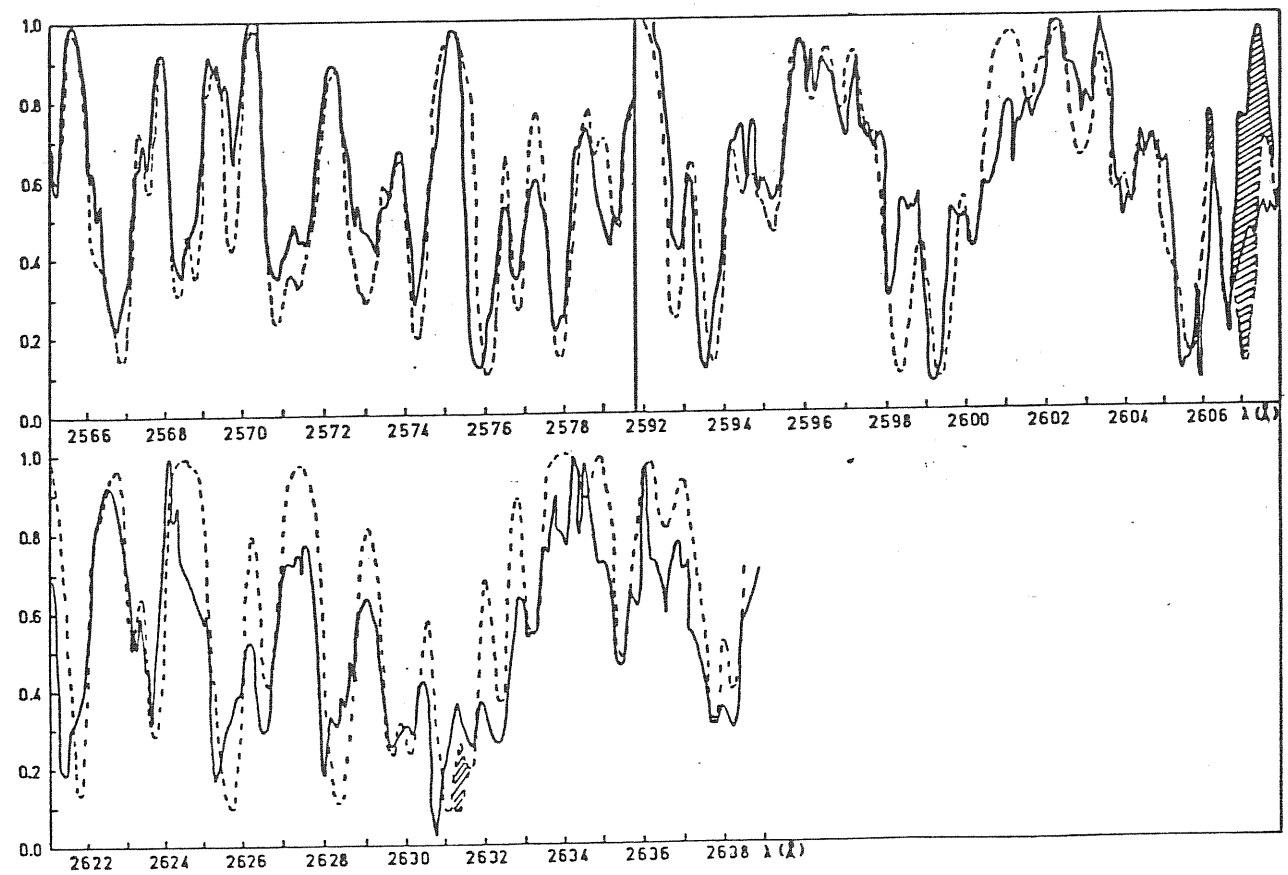

a)

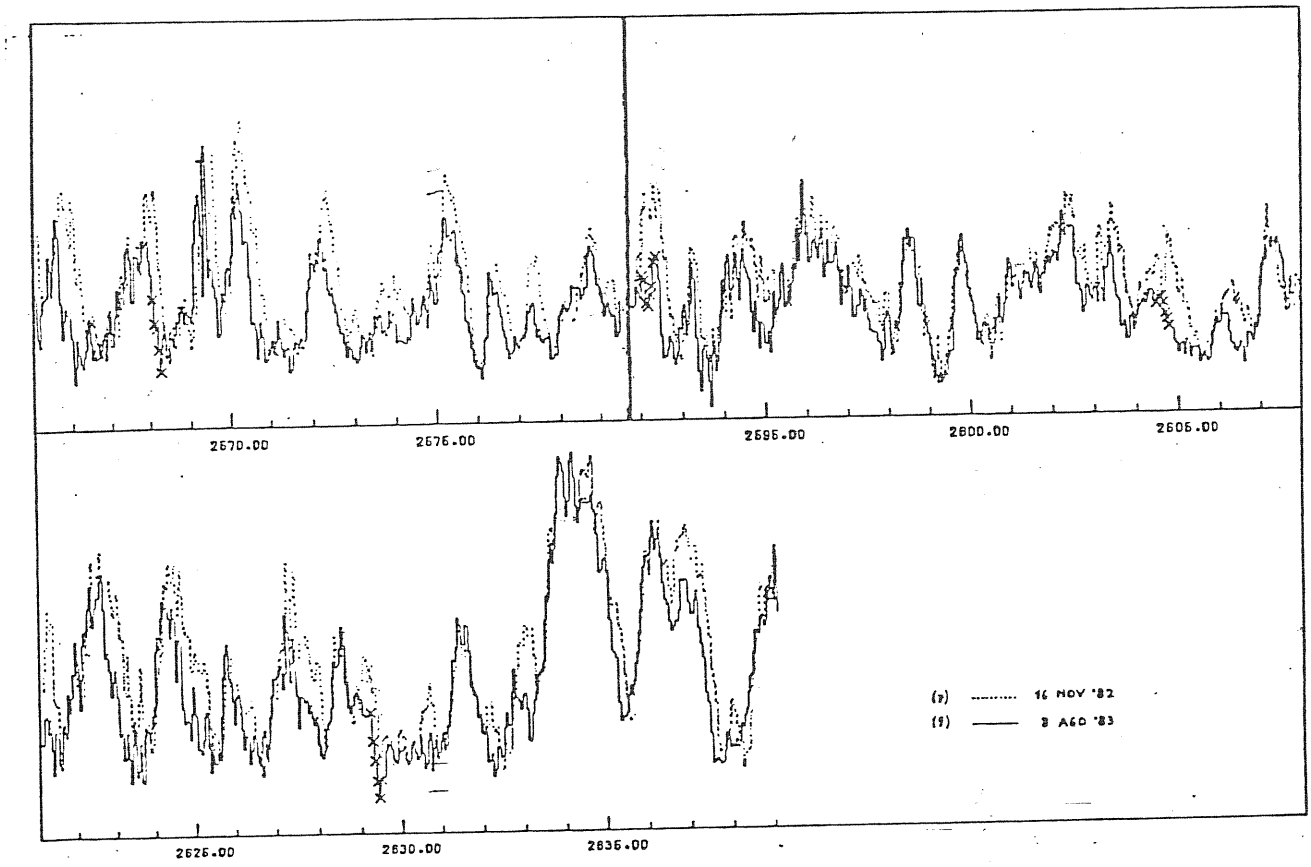

b)

Fig. B1 - Behaviour of peculiar UV lines (for identification, v. Tab B1).
a) Out of eclipse (Castelli '82): model (----) compared with IUE observations (——); normalized intensity scale.
b) Eclipse observations: end ingress (.....) compared with mid totality ( ); linear intensity scale.

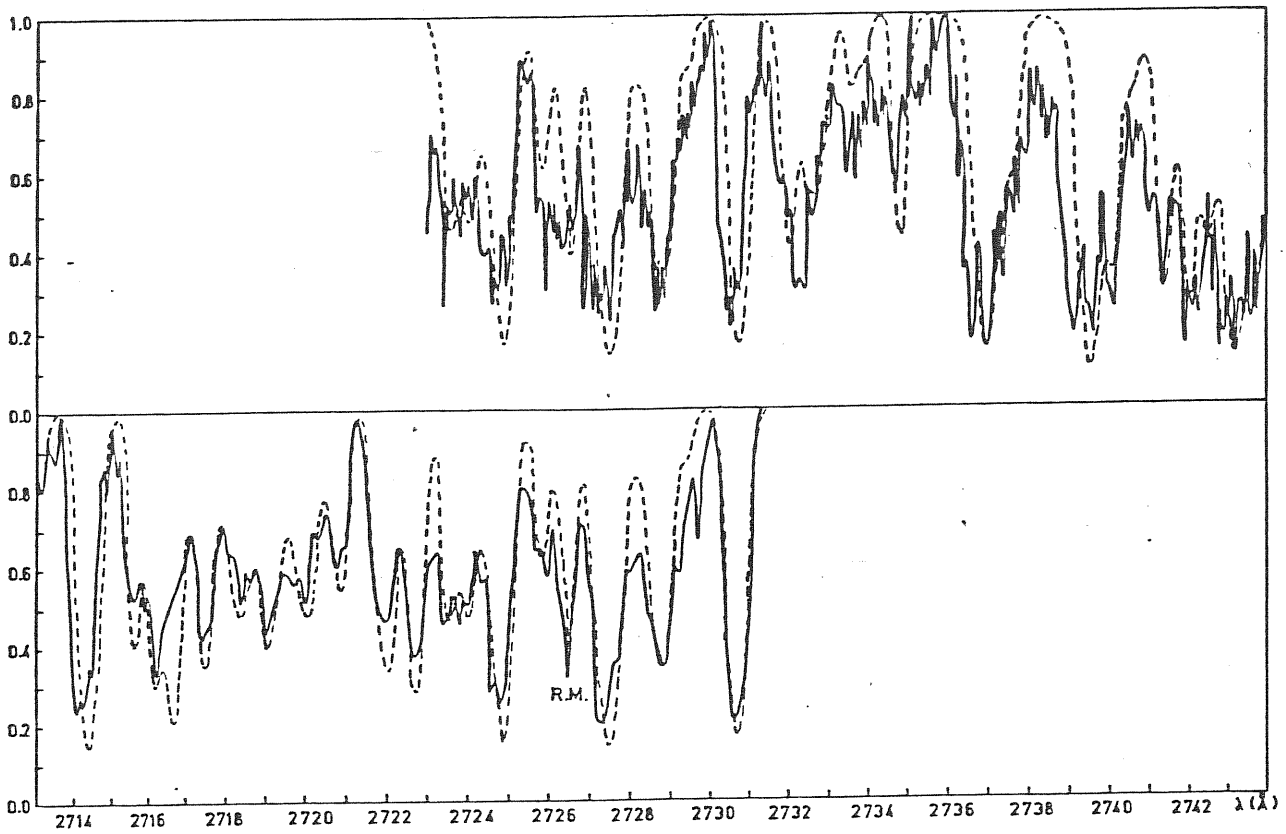

a)

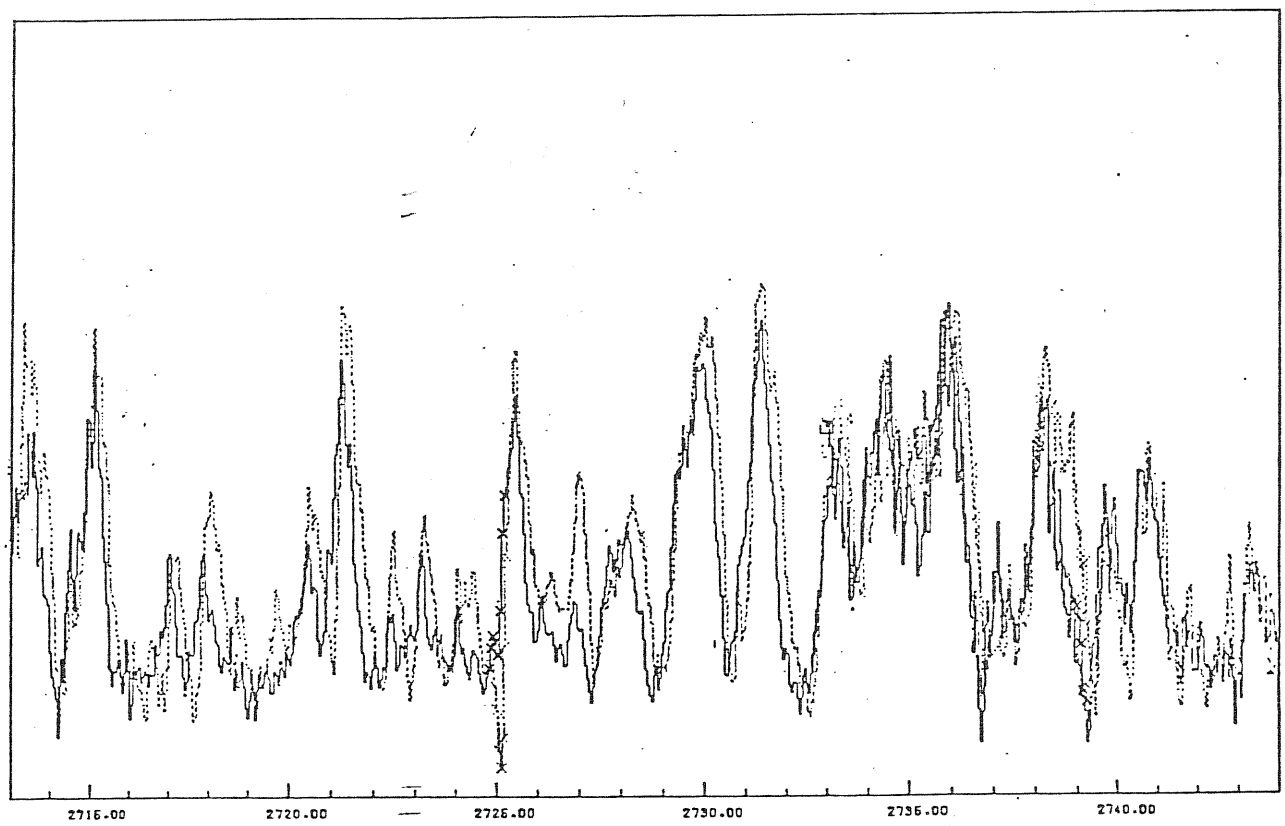

b)

Fig. B2 - Behaviour of peculiar UV lines (for identification, v. Tab B1).

a) Out of eclipse (Castelli, '82): model (- - - -) compared with observations (——) by BUSS (upper) and IUE (lower); normalized intensity scale.

b) Eclipse observations: end ingress (- - - -) compared with mid totality (——); linear intensity scale.

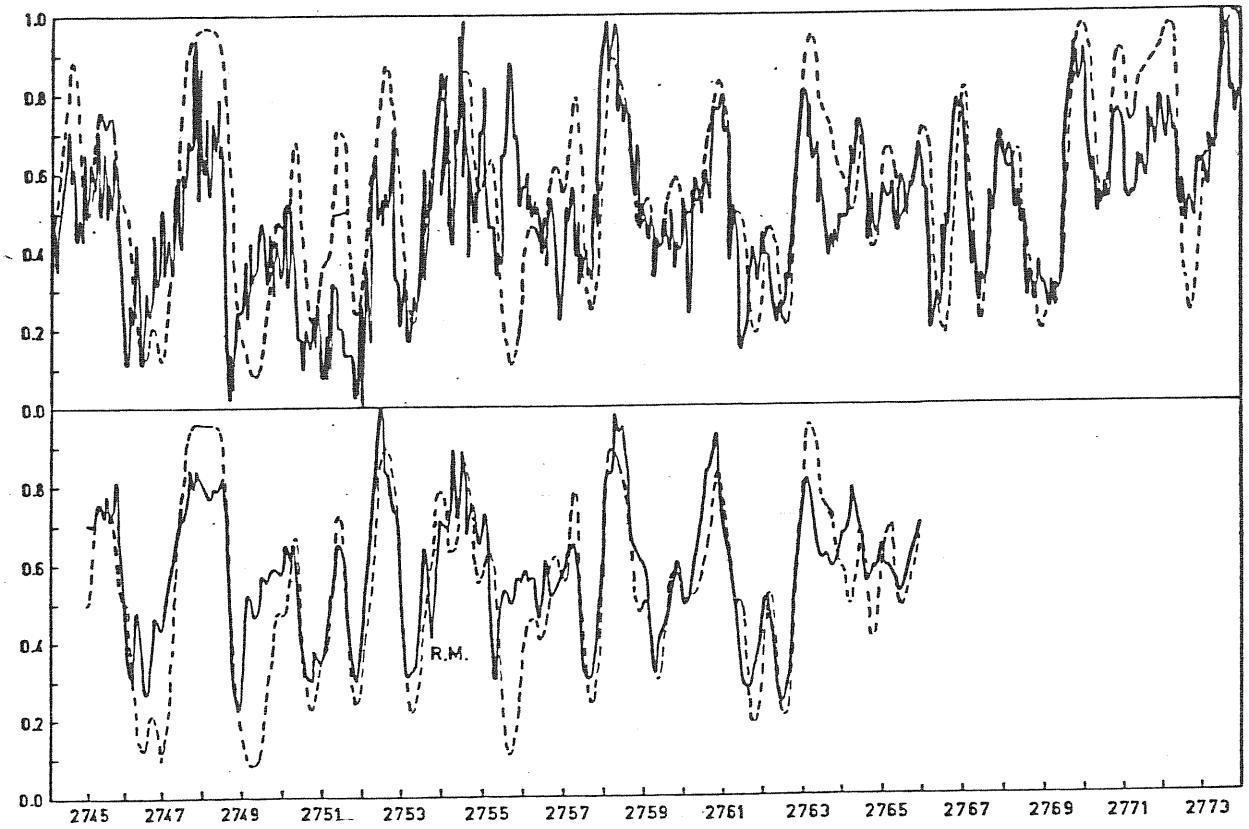

a)

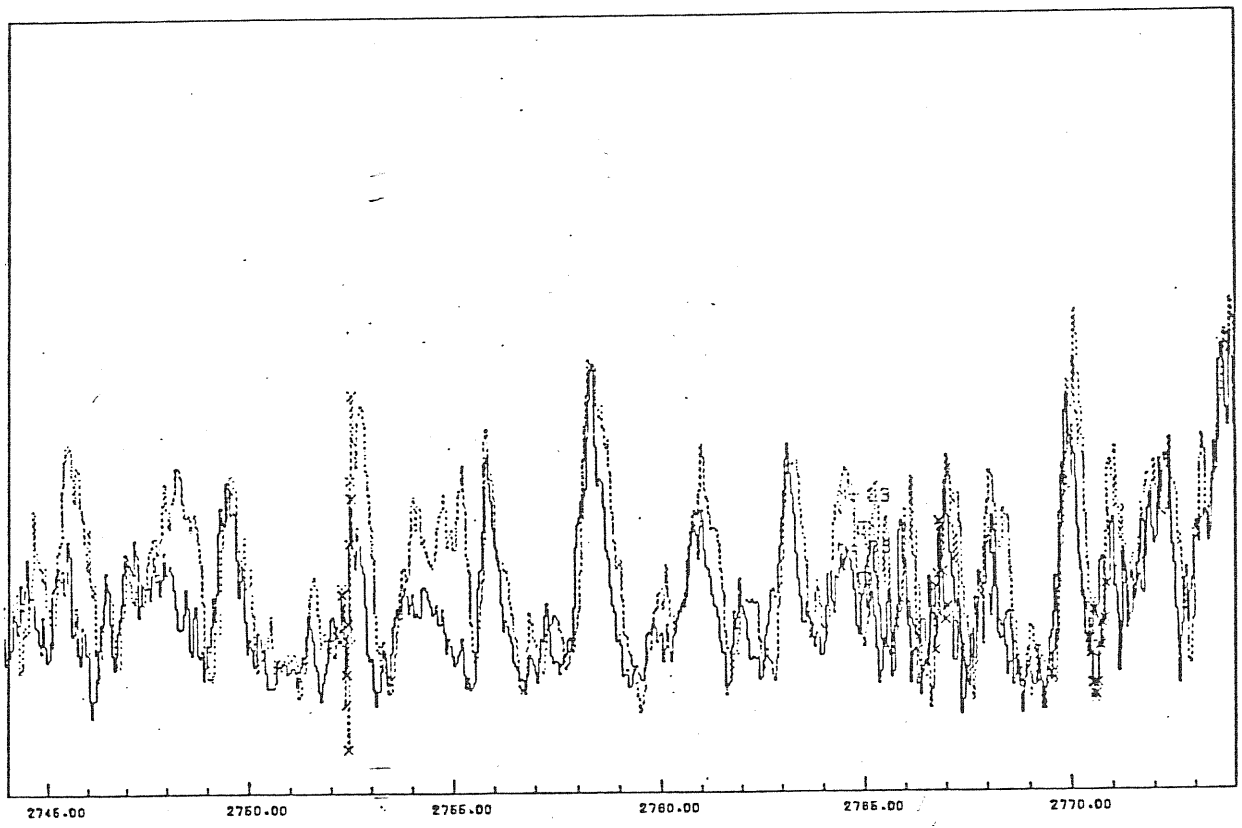

b)

Fig. B3 - Same as fig. B2

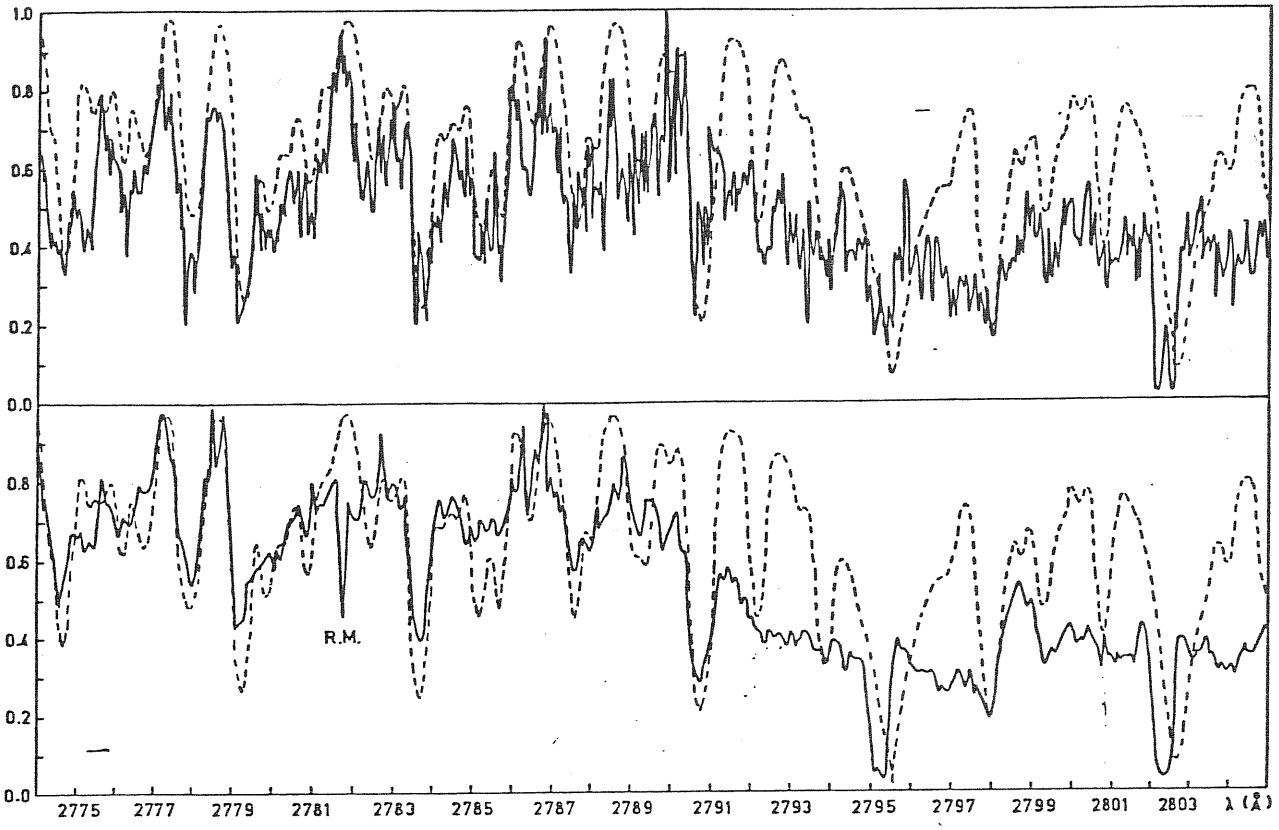

a)

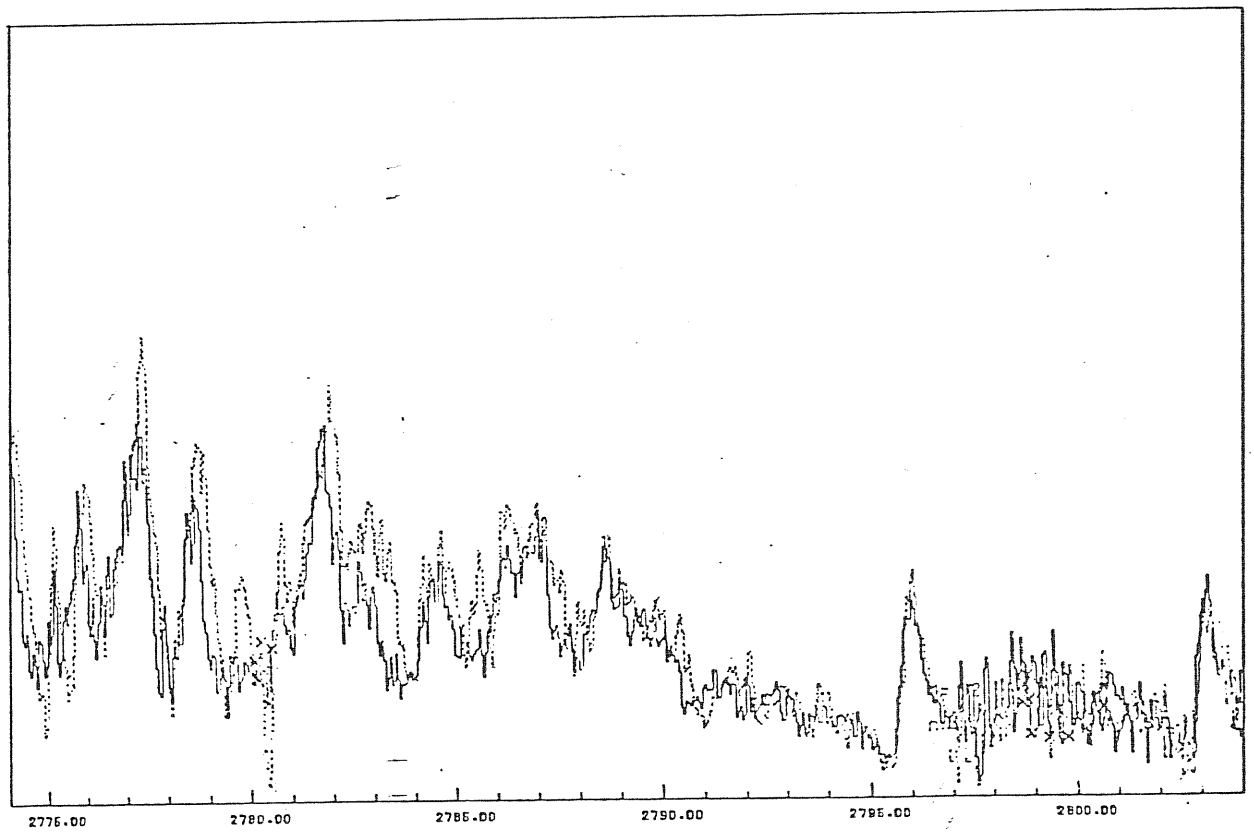

b)

Fig. B4 - Same as fig. B2

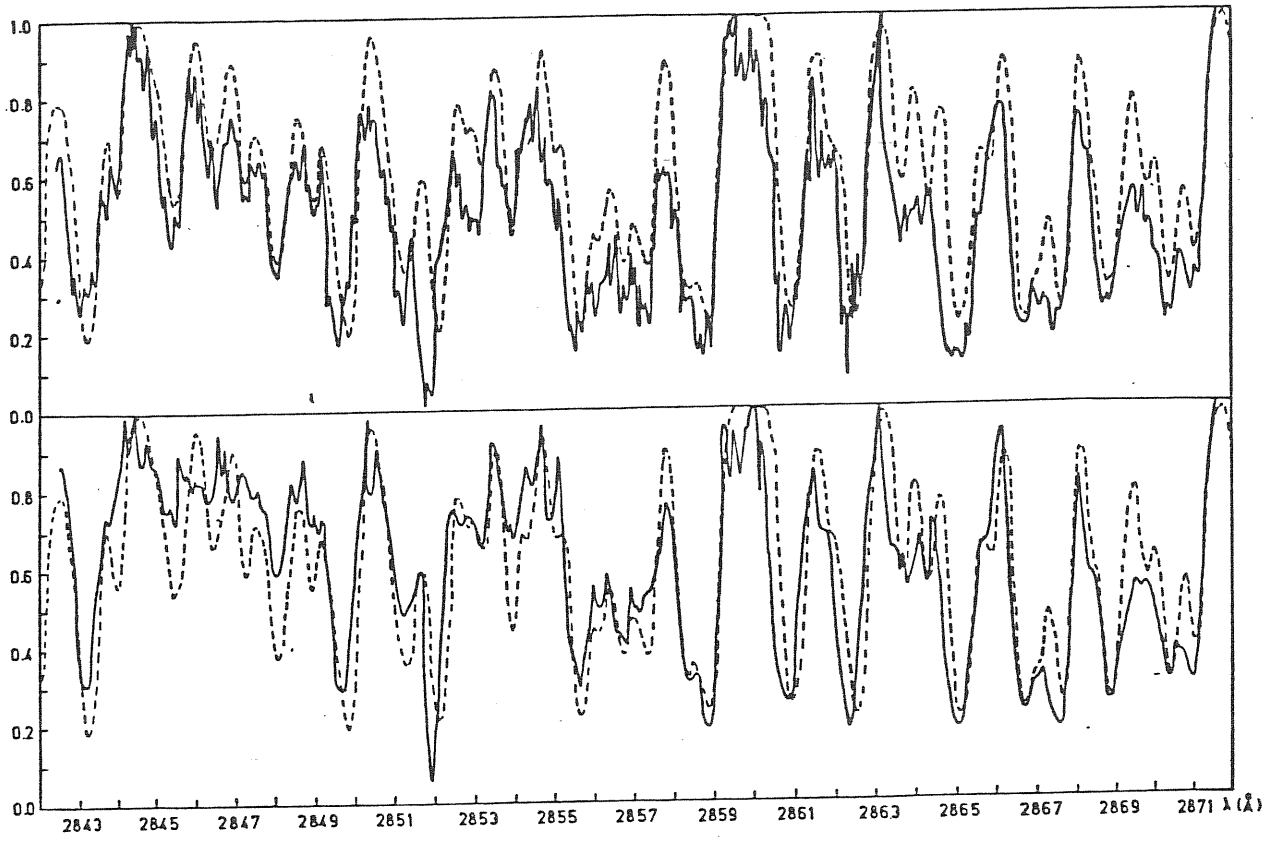

a)

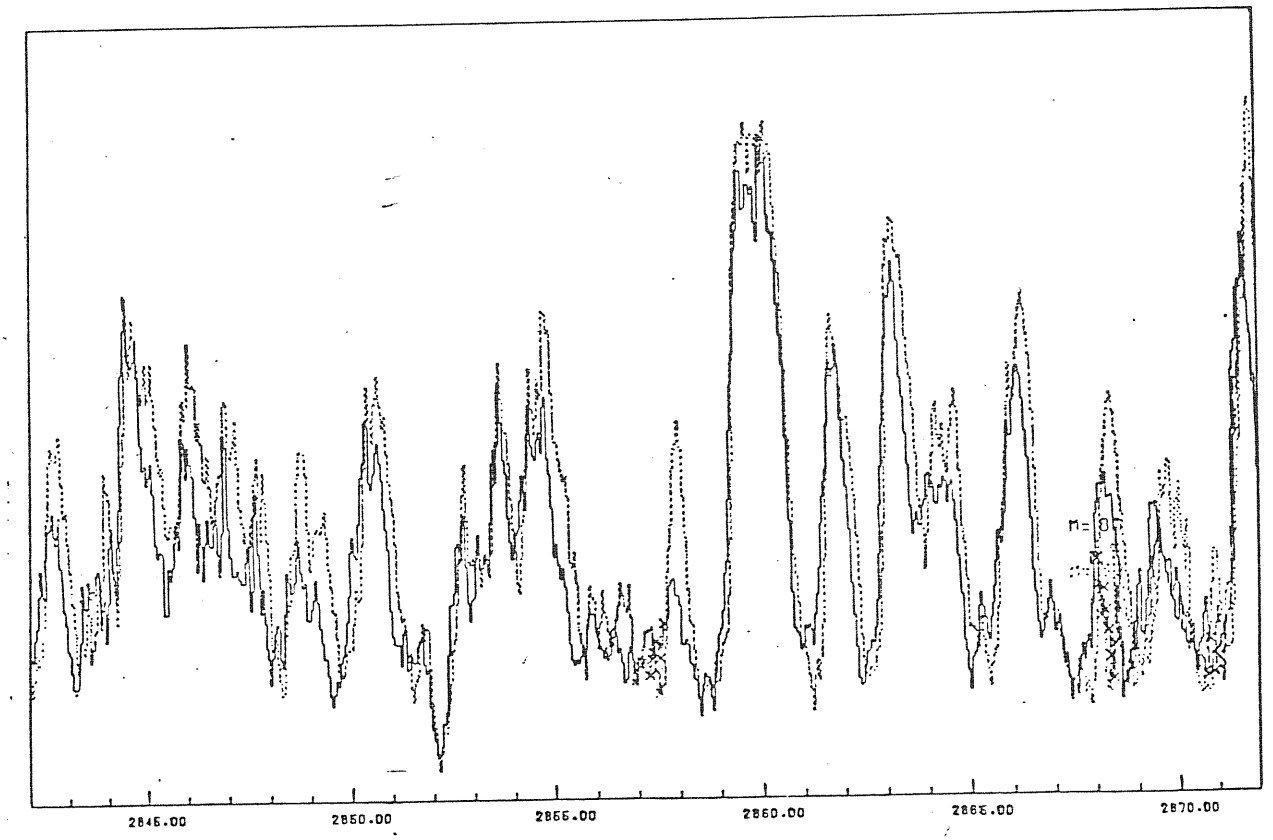

b)

Fig. B5 - Same as fig. B2

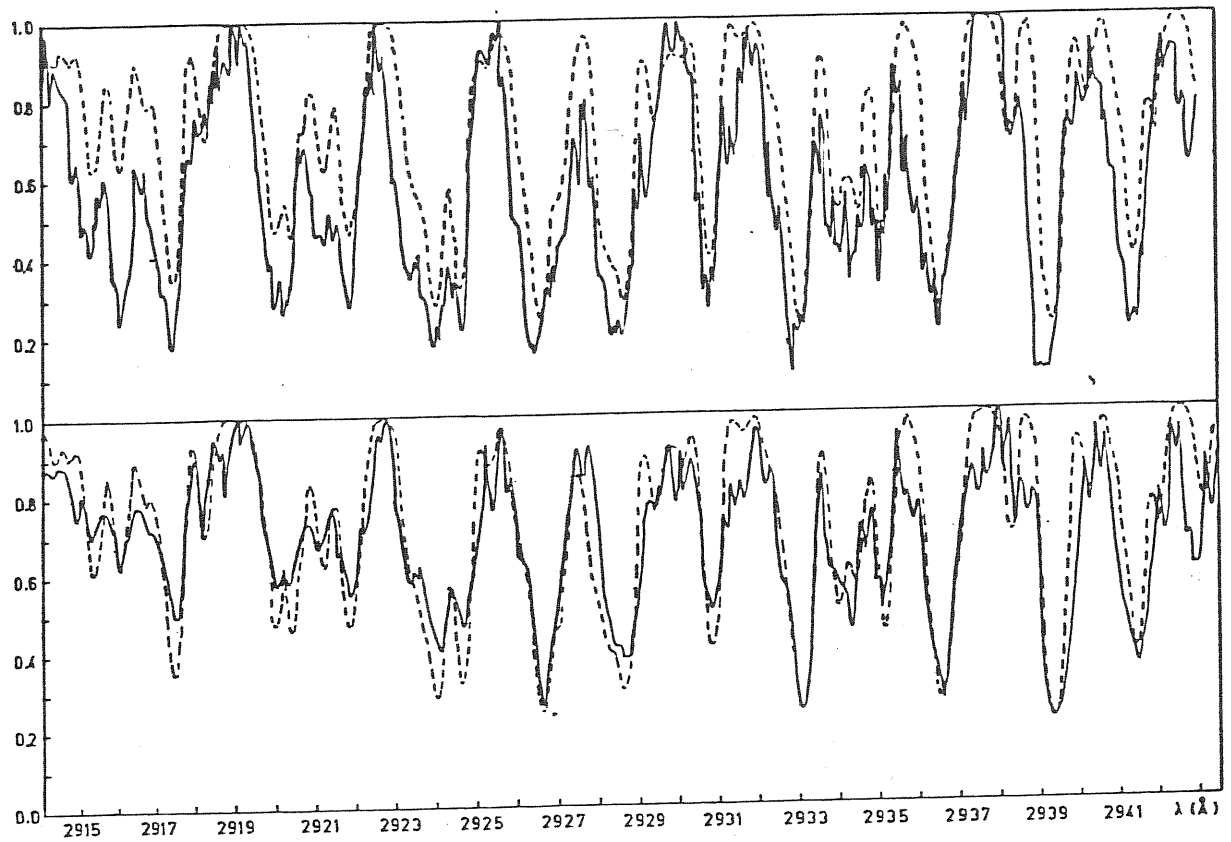

a)

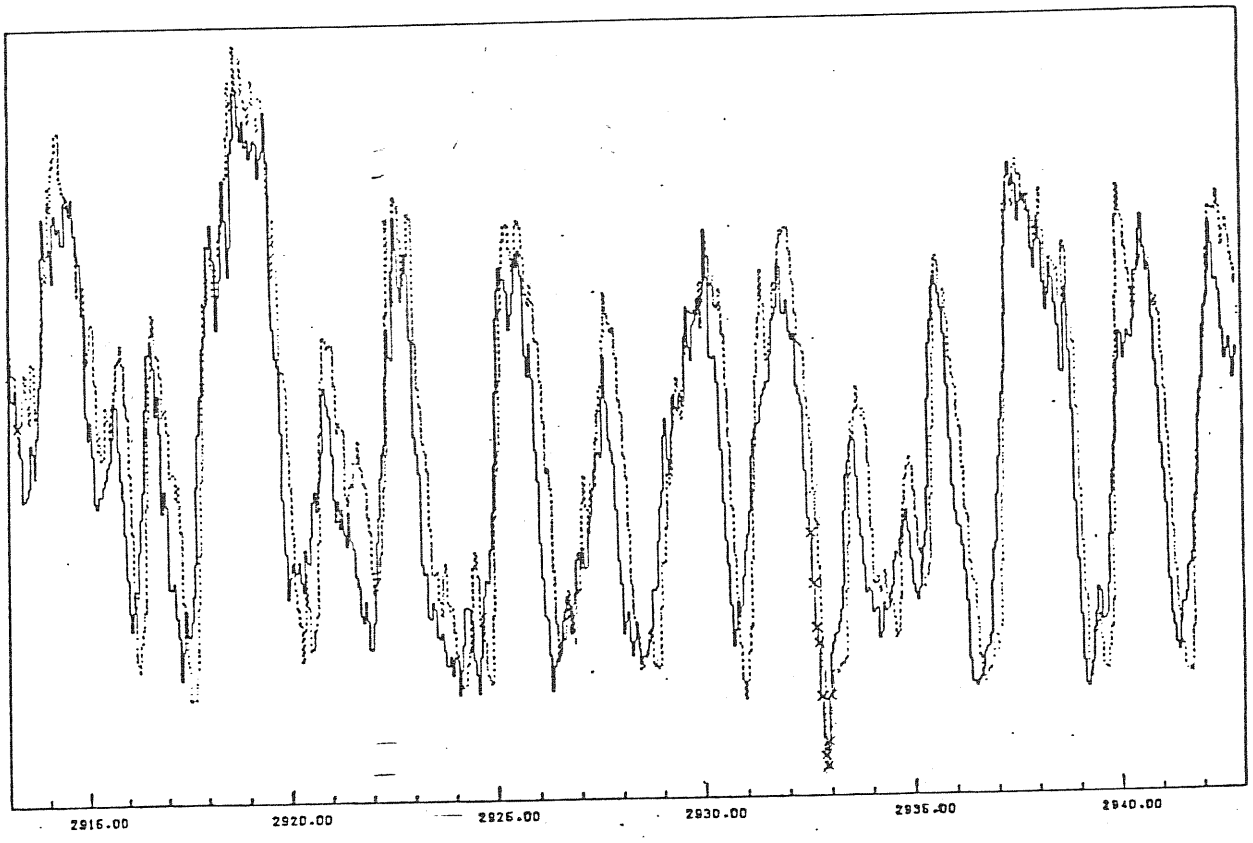

b)

Fig. B6 - Same as fig. B2

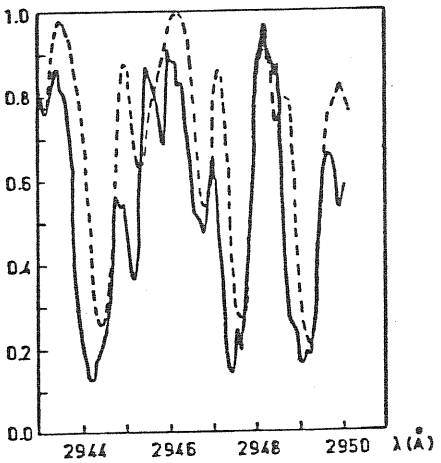

a)

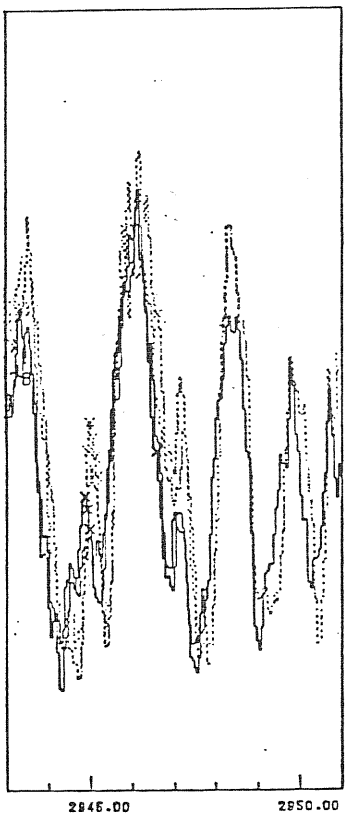

b)

Fig. B7 - Same as fig. B1

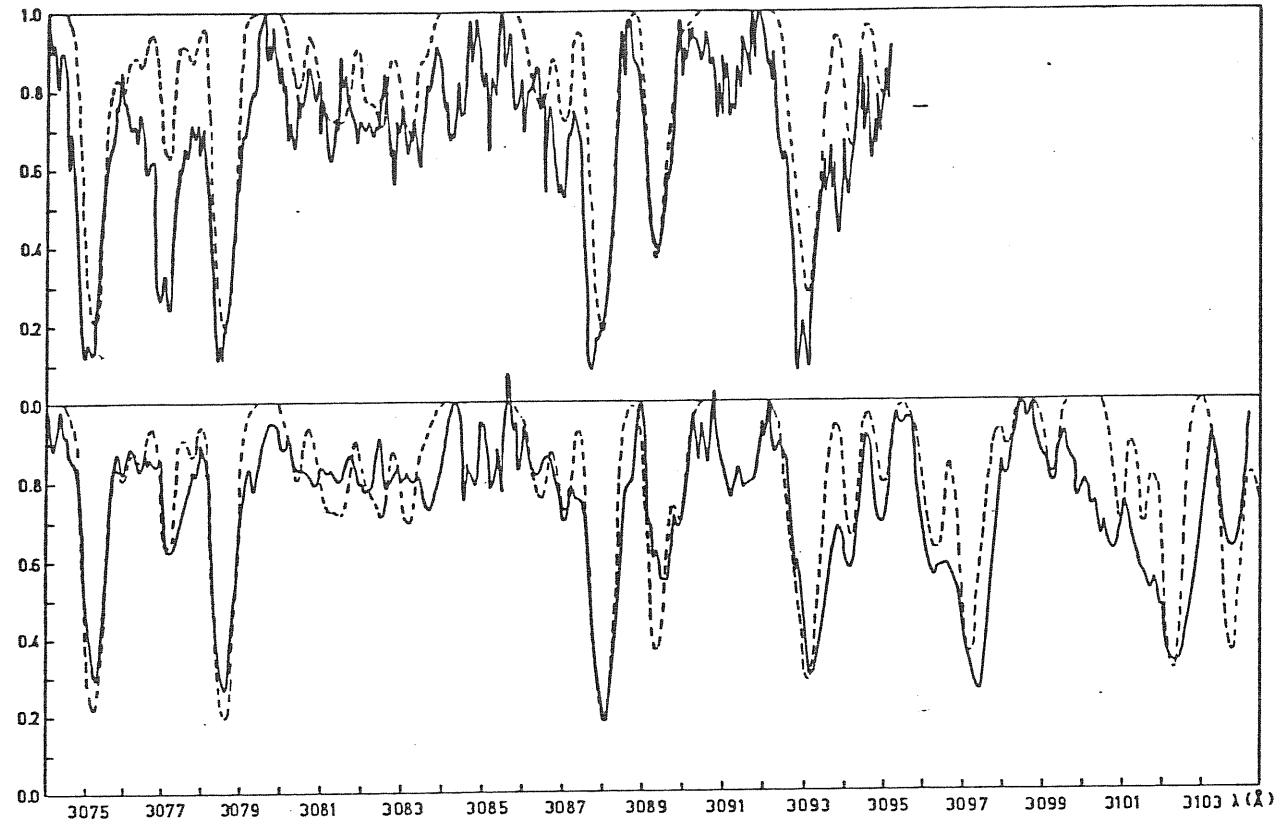

a)

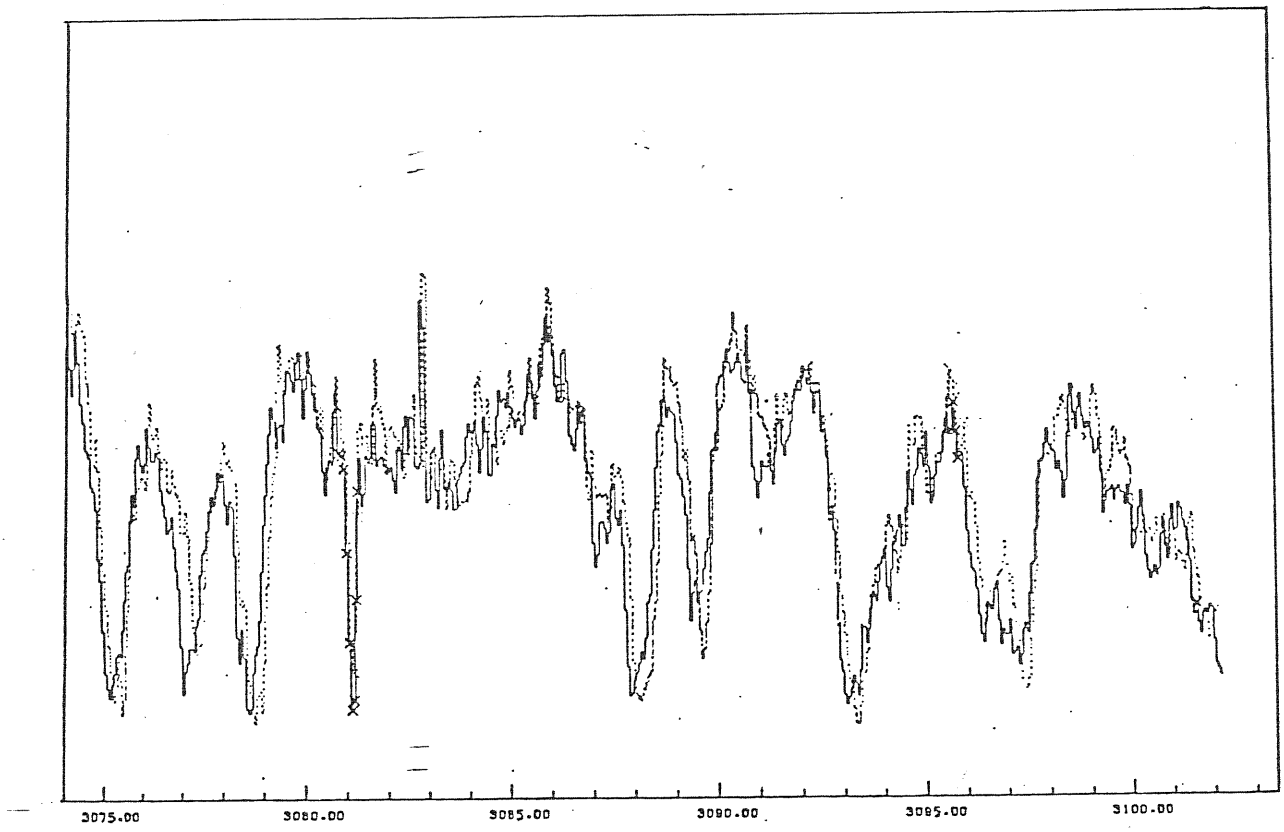

b)

Fig. B8 - Same as fig. B2

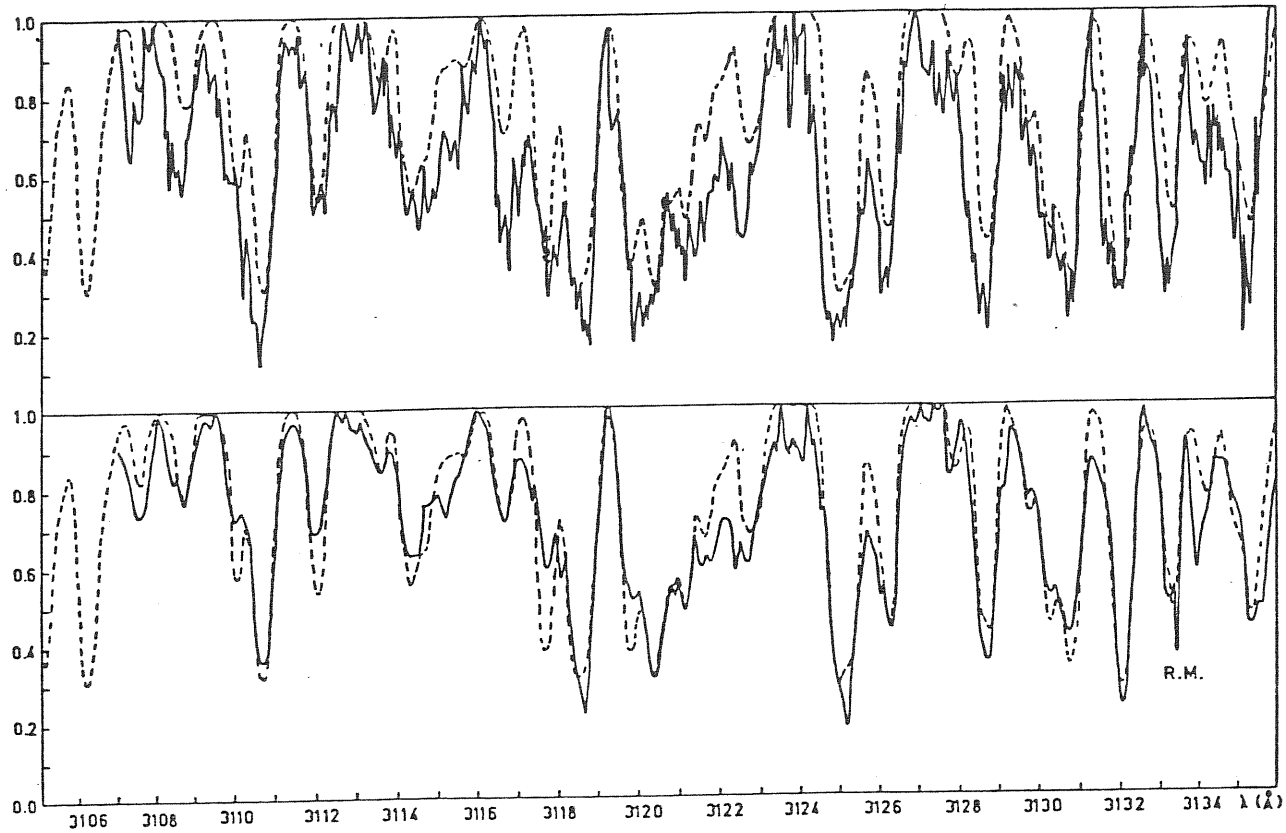

a)

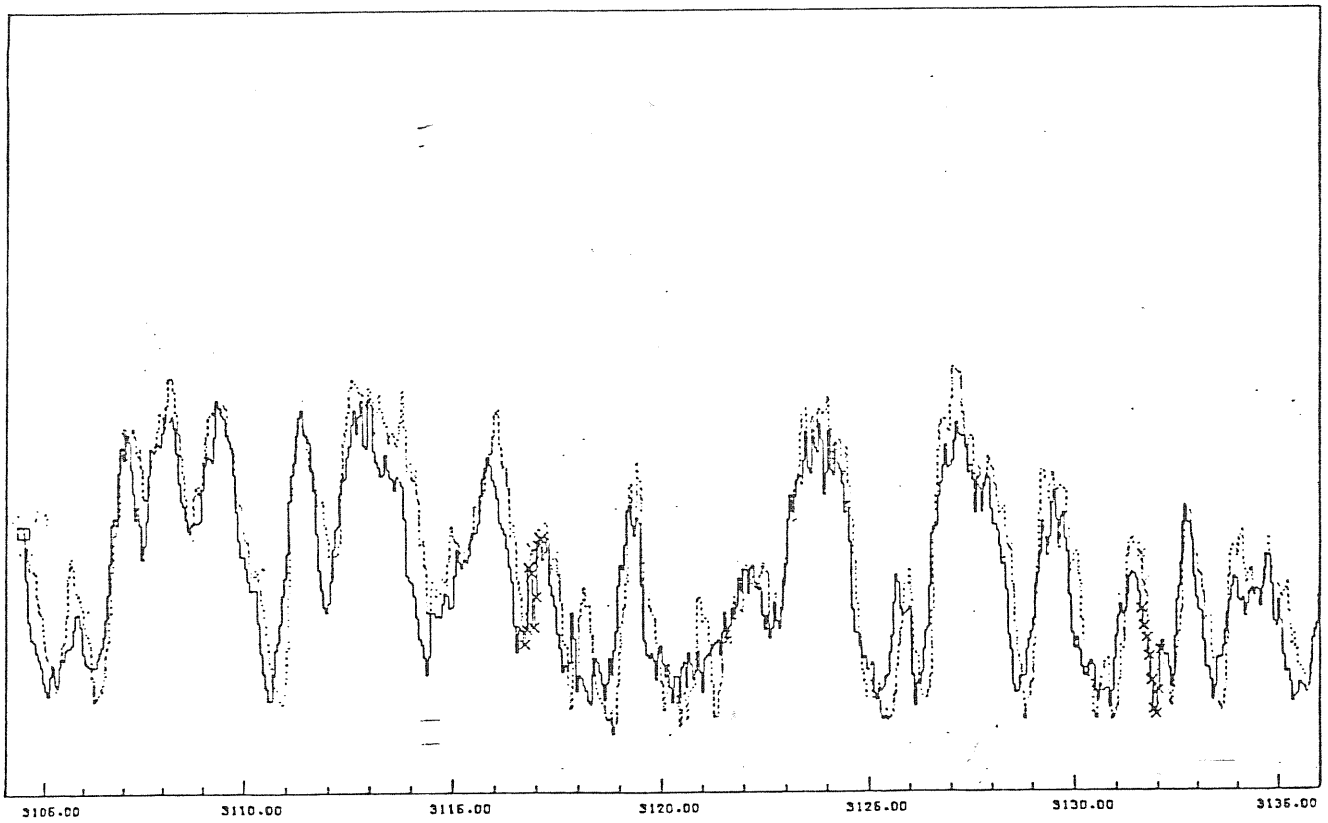

b)

Fig. B9 - Same as fig. B2

APPENDIX C)

DETERMINATION OF

VARIABLE UV EXCESS

(Work in Progress)

Table C.1) Variable UV excess

λ	I.S. (mag)	19.4.78 r_0	4.8.81 r_2	5.8.81 r_3	12.3.82 r_4	26.3.82 r_5	27.9.82 r_6	16.11.82 r_7	20.3.83 r_8	R_2	R_3	R_4	R_5	R_6	R_7	R_8
1250	13.5	(o)														
1300	12.9	53	78	78		128	80	107	150	1.34	1.34		1.72	1.34	1.57	1.84
1350	11.9															
1400	11.2	8.5(-)	10(-)	10(-)		33	7.7(-)	12(-)	18(-)	1.20	1.20		2.27	0.98	1.33	1.66
1450	10.8	7.8	9.2	9.2		39	5.9	9.3	15	1.21	1.21		2.60	0.93	1.22	1.58
1500	10.4	7.9	7.8	7.8	19(-)	35	4.2	6.7	7.2	1.09	1.09	1.78	2.44	0.75	1.00	1.35
1550	10.3	2.6	3.3	3.3	6.6	14	1.8	2.8	4.5	1.32	1.32	1.61	3.14	0.78	1.17	1.63
1600	10.2	2.0		2.8	4.9	(o)7.6	1.5	1.9	2.7		1.48	1.94	2.83	0.78	1.04	1.43
1650	10.2	1.4		2.2	2.9	(o)5.4	1.2	1.5	2.1		1.91	2.40	3.65	0.78	1.23	1.82
1700	10.2	0.6		0.9	1.7	(o)1.9	0.6	0.7	0.8	1.23	1.36	1.93	2.66	0.91	1.22	1.67
1750	10.1	1.0		(o)0.9	1.6	(o)1.8		(o)0.8	(o)0.9	0.10	0.27	0.34	0.62	0.21	0.19	0.14
1800	10.1	0.7		(o)1.0	1.4	(o)1.7		(o)0.9	(o)1.0	8.95	8.73	7.97	7.28	9.60	8.97	8.29
1850	10.1	0.7		(o)0.9	1.3	(o)1.6		(o)0.8	(o)1.0							
1988	11.9	1.6	0.9	0.9		1.1			0.8	4.8.81	5.8.81	12.3.82	26.3.82	27.9.82	16.11.82	20.3.83
2122	12.2	1.5	0.9	0.7		1.0			0.7	(2)	(3)	(4)	(5)	(6)	(7)	(8)
2309	12.7	1.2	0.7	0.7		0.8			0.6							
2450	6.1	1.3	0.7(-)	0.9(o)	0.9(-)	1.1(o)			0.8							
2654	6.7	1.4		(s)	1.5	2.1(o)			1.5							
2720	7.2	1.5			1.6	2.1(o)			1.7							
2832	5.8	1.3			1.6	1.6(o)			1.2							
2938	5.4	1.2			1.7				1.5							
2973	5.3	1.3			1.8				1.6							
3017	5.2	1.4			1.6				1.5							
3051	5.1	1.4			1.7				1.5							
3068	4.9	1.6			1.6	1.7(o)			1.5							
3123	4.7	1.3	(+)		1.4	1.7(o)			1.4							
3167	4.7	1.8	1.2	1.6(o)	1.3	1.6(o)			1.4							
3205	4.6	2.2	1.3	1.7(o)	1.3	1.7(o)			1.3							
		(o)														

Radius (10^{11} cm): $R_t = 1.1 \cdot 10^{11} \cdot \sqrt{\frac{r_t - 1}{r_0 - 1}}$

Visual mag: $V_t = 64.4 - 5 \log \bar{R}_t$

Parameters of B star

	4.8.81	5.8.81	12.3.82	26.3.82	27.9.82	16.11.82	20.3.83
R_B	1.2 ±.1	1.3 ±.2	2.0 ±.3	2.8 ±.5	0.8 ±.1	1.2 ±.1	1.6 ±.1
	1.21	1.26	1.93	2.82	0.83	1.17	1.65
	0.09	0.15	0.34	0.51	0.10	0.12	0.14
V_B	8.99	8.95	7.97	7.15	9.80	9.06	8.31
→	9.0	9.0	8.0	7.2	9.8	9.1	8.3

Note to table C.1). Method by Hack and Selvelli (1978) is applied (hereafter HS).

I.S.: interstellar correction

$r = \frac{F_{corrected\ (I.S.)}}{F_{predicted\ (HS)}}$. Symbols are those by HS; index $i = 0, \ldots 8$ is the number of spectrum in tab III.1).

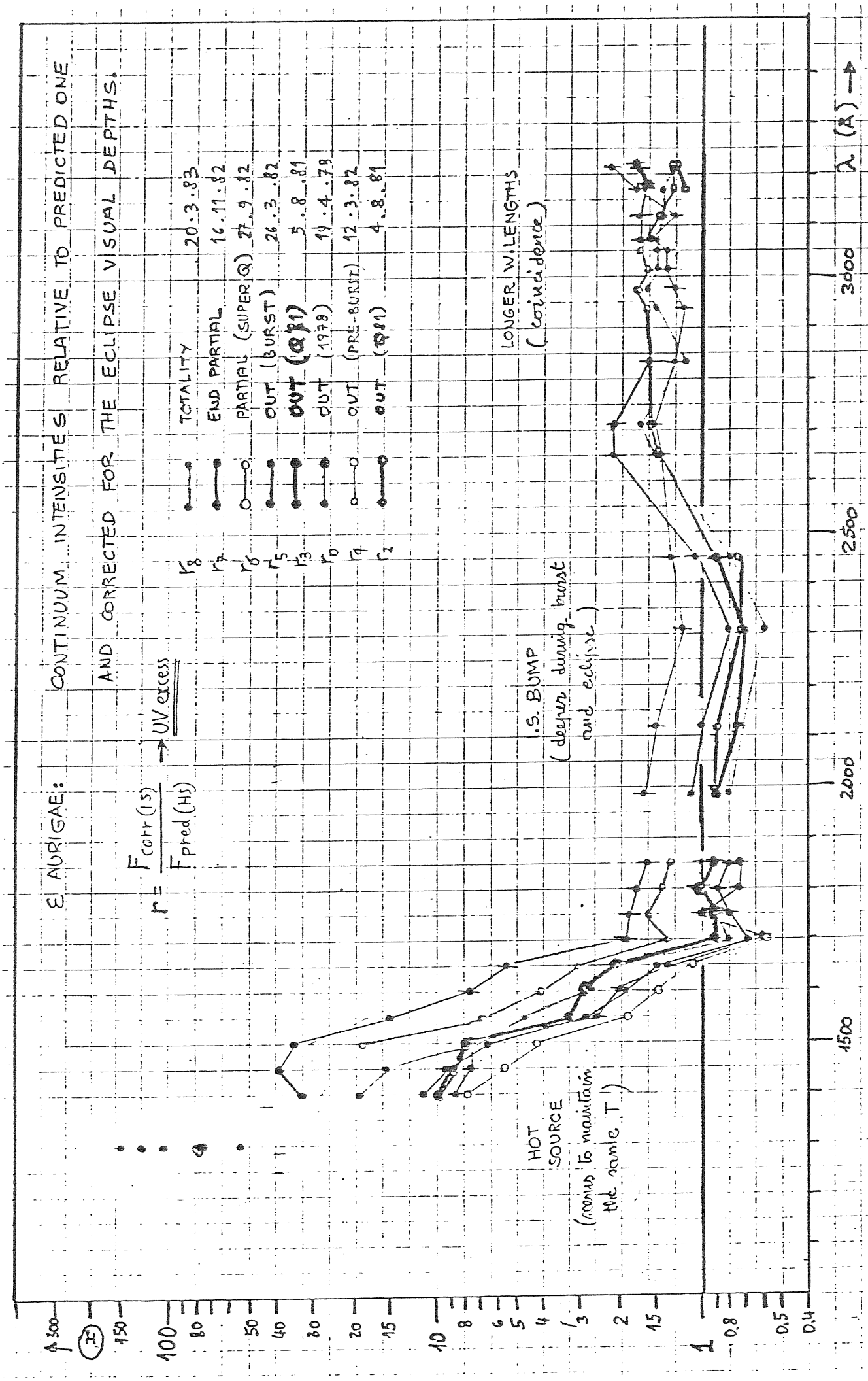

Fig C.1)- Variable UV excess. Parallelism of curves shortward 1700 Å, if real, should indicate that variations are Temperature-independent. (dem. follows)

Note. If UV-excess curves in fig. C1), shortward 1700 Å, are really parallel as the figure seems to suggest (parallelism might be due, however, to a compression of the scale), this could mean that B component's variability occurs at constant effective temperature T_B.

In fact, assuming with HS : $T_A = 7800\,°K$, $R_A = 4 \cdot 10^{12}$ cm , one has, for the UV excess :

$$r-1 \equiv \frac{R_B^2\, F_{\lambda B}}{R_A^2\, F_{\lambda A}} \simeq \frac{R_B^2}{R_A^2}\, \frac{e^{1.44/T_A\lambda}-1}{e^{1.44/T_B\lambda}-1} ,$$

hence :

$$\log (r-1) = 2 \log \frac{R_B}{R_A} + \log \frac{e^{1.44/T_A\lambda}-1}{e^{1.44/T_B\lambda}-1} . \qquad (c1)$$

"Parallelism" in fig. C1) means nothing but :

$$\log (r-1) \equiv f(\lambda, t) = h(t) + g(\lambda), \qquad (c2)$$

where $g(\lambda)$ does not depend on time t, and $h(t)$ does not depend on wavelength λ.

Clearly, eq. (C1) assumes the form (C2), for :

$$h(t) \equiv 2 \log \frac{R_B}{R_A} \quad , \quad g(\lambda) \equiv \log \frac{e^{1.44/T_A\lambda}-1}{e^{1.44/T_B\lambda}-1} .$$

This means $R_B = R_B(t)$, that is (effective) radial "pulsation"; while, from $g(\lambda)$, one must have $T_B =$ constant with time.

Acknowledgments

Observations were made with the support of S.I.S.S.A., and of the "Osservatorio Astronomico di Trieste".

References

Aller, L.H., 1953: "Astrophysics: the Atmospheres of the Sun and Stars". (New York: Ronald Press).

Batten, A.H. Fletcher, J.M. and Mann, P.J., 1978: Publ. Dom.Obs. of Victoria 15, nº 5.

Cameron, A.G.W., 1971: Nature 229, 178.

Chapman, R.D., Kondo, Y. and Stencel, R.E., 1983: Ap.J. Letters 269, 17.

Castelli, F., 1977: Ap. and Space Sci. 49, 179.

Castelli, F., 1978: Astron. Astroph. 69, 23.

Castelli, F., Hoekstra, R. and Kondo, Y., 1982: Astron. Astroph.Suppl.Ser. 50, 233.

Ferluga S. and Hack M., 1983: 7th. IAU Reg.Meeting, Florence.

Ferluga S., Hack M. and Boehm C., 1983: Astron.Astroph., in press.

Ferluga S. and Boehm C., 1983: IBVS nº 2326, p. 11.

Fritsch, J.H., 1824: Berl. Jahrb., p. 252.

Frost, E.B., Struve, O. and Elvey, C.T. 1932, Pub.Yerkes Obs. 7, part 2.

Gyldenkerne, K., 1970: Vistas in Astron. 12, 199.

Hack, M., 1959: Ap.J. 129, 291.

Hack, M., 1961: Mem.S.A.I.t. 32, 351.

Hack, M., and Selvelli, P.L., 1979: A.A. 75, 316.

Handbury, M.J. and Williams, I.P., 1976: Ap and Space Sci. 45, 439.

Hoffleit, D., 1982: "the Bright Star Catalogue".

Holm.A. and Rice, G., 1981: IUE Newslett. 15, 74.

Huang, S., 1965: Ap.J. 141, 976.

Huffer, C.M., 1932: Ap.J. 76, 1.

van de Kamp, P., 1978 a: A.J. 83, 975.

van de Kamp, P., 1978 b: Sky and Tel., nov. '78, p. 397.

Kopal, Z., 1971: Ap. and Space Sci. 10, 332.

Kraft, R.P., 1954: Ap. J. 120, 391.

Kuiper, G.P., Struve, O. and Strömgreen, B., 1937: Ap. J. 86, 570.

Larsson-Leander, G., 1958: Arch.Astr. 3, 17.

Low, F.J. and Mitchell, R.I., 1965: Ap.J. 141, 327.

Ludendorff, H., 1903: Astr.Nachr. 104, 81.

Ludendorff, H., 1924: Sitz.Der Preuss.Akad.Wiss. (Math.--Naturwiss.Kl.) 9, 49.

Morris, S.C., 1962: J.R.A.S. Can 56, 210.

Morris, S.C., 1963: Ph.D.Thesis, Univ.of.Toronto.

Paczynski, 1975: quoted in "Interacting Binary Stars" (Sahade and Wood, 1978), p. 157.

Plavec, M., 1982: in "Advances in UV Astronomy: 4 years of IUE Research", NASA C.P. 2238, p. 526.

Stencel, R.E., 1983: Epsilon-Aur Campaign Newsletter n° 6.

Struve, O. and Elvey, C.T., 1930: Ap.J. 71, 136

Struve, O., 1951: P.A.S.P. 63, 138.

Struve, O., 1956: P.A.S.P. 68, 27.

Wilson, R.E., 1971: Ap.J. 170, 529.

Woolf, N.J., 1973: Ap.J. 185, 229.

Wright, K.O. and Kushwaha, R.S., 1957: VIII Coll. de Liège, p. 421.

Wright, K.O., 1970: Vistas in Astron. 12, 150.